

REPUBLIQUE DE COTE D'IVOIRE  
*Union-Discipline-Travail*

Ministère de l'Enseignement supérieur  
et de la Recherche Scientifique



UNIVERSITE FELIX HOUPOUËT BOIGNY



DOCTORAL SCHOOL: CLIMATE CHANGE AND BIODIVERSITY

**Year : 2015-2016**

## **THESIS**

**Submitted for the Degree of Doctor of Philosophy  
at Félix Houphouët Boigny University**

**Speciality: Climate Change & Biodiversity**

**BOAKYE Emmanuel Amoah**

**Effect of Climatic Variation and Agricultural Landuse on  
Woody Plant Diversity and Growth of Riparian Forests in the  
Volta Basin of Ghana**

Public defence on 29 September 2016

### **Members of Jury**

Mr. TANO Yao	Full Professor	Université Nangui Abrogoua	President
Mr. KONE Daouda	Full Professor	Université Félix Houphouët-Boigny	Supervisor
Mr. ASSOGBADJO Achille Ephrem	Associate Professor	Université d'Abomey-Calavi	Referee
Mr. SAVANE Issiaka	Full Professor	Université Nangui Abrogoua	Referee
Mr. KOUAME Koffi Fernand	Full Professor	Université Félix Houphouët-Boigny	Examiner

**Number : 01**

## **DEDICATION**

**To my wife, Comfort Badu Asare and daughter, Afua Serwaah Boakye for their love, patience and prayers.**

## **ACKNOWLEDGEMENTS**

This research was made possible through the financial support of the West African Science Service Center on Climate Change and Adapted Land Use programme (WASCAL) of the German Federal Ministry for Education and Research. I also want to thank Prof. Daouda Kone and Dr. François Kouamé of the WASCAL Graduate Research Program, Climate Change and Biodiversity for organizing all the resources to enable me undertake this research.

I am very grateful to the Remote Sensing Unit of the Forestry Commission of Ghana for providing me with the high resolution ALOS satellite imagery.

Special thanks to the Institute of Geography of the Friedrich-Alexander University of Erlangen-Nurnberg (FAU), Germany and Faculty of Renewable Natural Resources of the Kwame Nkrumah University of Science and Technology (KNUST), Ghana for providing me with support to enable me complete the laboratory works respectively on dendro-isotope and soil analyses.

I am grateful to Prof. Stefan Porembski of the University of Rostock (Germany) for advising me on riparian ecology. I am also grateful to Prof. Achim Brauning and Dr. Aster Gebrekirstos of FAU (Germany) and World Agroforestry Centre (Kenya) respectively for supervising the component of my research dealing with riparian dendrochronology. Dr. Michael Thiel of the University of Wuerzburg (Germany) provided a huge intellectual support on riparian remote sensing for which I am very grateful. Finally, I want to thank Dr. Dibi N. Hyppolite and Dr. Victor R. Barnes of the Universite Felix Houphouet Boigny (Cote d'Ivoire) and KNUST (Ghana) respectively for supervising the entire research.

Lastly, I would like to thank my parents, Papa Thomas and Mama Victoria for being there for me since the beginning of my educational career. Without them I would not have gotten to this far.

## **PREFACE**

Climate simulations have predicted decrease in precipitation in the West African sub-region within this 21<sup>st</sup> Century. The fulfilling predictions could have serious consequences on the survival of species and climate sensitive ecosystems such as riparian forests in the savanna landscapes of the world. Within the water limiting savannas, however, the readily availability of water and rich soil nutrients have attracted agricultural activities into riparian areas. The intensification of this activity could cause modification to the riparian forests to result in the loss of biodiversity and ecosystem functioning. Understanding the response of riparian forests to climate and agricultural land use change is therefore a crucial step in the development of strategies for conservation and management. This research was conducted in the Afram and Tankwidi riparian catchments in the humid (Guinean savanna) and dry savanna (Sudanian savanna) zones of the Volta basin of Ghana. The Volta basin is an agricultural watershed and falls within the savanna matrix, hence the effect of climate and agricultural land use is worth investigating. The research was conducted within the framework of the West African Science Service Center on Climate Change and Adapted Land Use programme with funding support from the Federal Ministry of Education and Research in Germany.

## TABLE OF CONTENTS

<b>INTRODUCTION .....</b>	<b>1</b>
<b>I. LITERATURE REVIEW .....</b>	<b>8</b>
1.1 Global climate change.....	9
1.2 Drivers of climate change .....	9
1.3 Projections on climate change.....	12
1.4 Impacts of climate change.....	14
1.5 Delineating riparian zones .....	14
1.6 Physical and ecological functions of riparian zones .....	15
1.7 Threats to riparian forests .....	17
1.8 Mapping of riparian forests.....	18
1.9 Dendrochronology .....	20
<b>II. MATERIALS AND METHODS .....</b>	<b>22</b>
2.1 Study area.....	23
2.1.1 Summary description.....	23
2.1.2 Climate .....	28
2.1.3 Hydrology, surface waters and relief .....	30
2.1.4 Soil.....	33
2.1.5 Geology .....	33
2.1.6 Vegetation and land use .....	34
2.1.7 Demographic trends .....	34
2.2 Methods.....	38

2.2.1 Assessment of forest cover dynamics in the Afram and Tankwidi riparian catchments between 1986 to 2014 .....	38
2.2.2 Assessment of woody plant diversity and structure and soil properties of riparian forests between protected area and farmland in the humid and dry savanna zones .....	43
2.2.3 Assessment of the growth of riparian wood species in the humid and dry savanna zones ....	51
2.2.4 Assessment of Carbon-13 ( $\delta^{13}\text{C}$ ) isotope in riparian wood species in the humid and dry savanna zones .....	55
<b>III. RESULTS .....</b>	<b>60</b>
3.1 Trends in forest cover dynamics in the Afram and Tankwidi riparian catchments from 1986, 2000 to 2014 .....	61
3.2 Comparison of woody plant diversity and structure of riparian forests between protected area and farmland in the humid and dry savanna zones.....	67
3.2.1 Density, basal area and size-class distribution of woody species .....	67
3.2.2 Woody species composition, diversity and similarity.....	71
3.2.3 Soil physical properties in protected area and farmlands and between the humid and dry savanna zones.....	73
3.2.4 Soil chemical properties in protected area and farmlands and between the humid and dry savanna zones.....	73
3.2.5 Relationship between woody plant density, and soil properties .....	74
3.3 Long-term growth patterns and the relationship between radial growth of riparian woody species and climatic parameters in the humid and dry savanna zones.....	82
3.3.1 Characteristics of trees growth rings .....	82
3.3.2 Cross-dating of growth rings of riparian trees.....	84
3.3.3 Radial growth of trees .....	87
3.3.4 Relationships between growth rings of trees in the humid and dry savanna zones .....	87

3.3.5 Relationships between growth rings of trees species and climatic parameters .....	90
3.3.6 Cyclicity in the growth of riparian trees.....	93
3.4 Inter-annual variability of carbon isotope ratios of riparian trees in the humid and dry savanna zones to climatic parameters.....	95
3.4.1 Patterns of Carbon-13 of whole wood and cellulose.....	95
3.4.2 Patterns of Carbon-13 in tree rings using whole wood .....	95
3.4.3 Patterns of Carbon-13 in whole wood of trees in the humid and dry savanna zones.....	99
3.4.4 Relationship between Carbon-13 in whole wood of trees and climatic parameters .....	102
<b>IV. DISCUSSION .....</b>	<b>104</b>
4.1 Forest cover loss in Afram and Tankwidi riparian catchments .....	105
4.1.1 Map accuracies .....	105
4.1.2 Forest cover change.....	105
4.2 Woody species diversity and structure in protected area and farmlands in the humid and dry savanna zones .....	107
4.2.1 Plant density, basal area and size-class distribution.....	107
4.2.2 Plant diversity and similarity in protected areas and farmlands.....	107
4.2.3 Relationships between woody plant density and soil properties .....	108
4.3 Relationship between radial growth of riparian woody species and climatic parameters in the humid and dry savanna zones .....	111
4.3.1 Wood anatomical features .....	111
4.3.2 Cross-dating of growth rings .....	111
4.3.3 Radial growth .....	112
4.3.4 Climate-growth relationships .....	114

4.3.5 Cyclicality of growth fluctuation .....	115
4.4 Climatic signals in carbon isotope ratios of riparian trees in the humid and dry savanna zones	116
4.4.1 Patterns of Carbon-13 of whole wood and cellulose.....	116
4.4.2 Patterns of Carbon-13 in tree rings using whole wood .....	116
4.4.3 Variation in Carbon-13 of whole wood between tree species .....	117
4.4.4 Relationship between carbon-13 of whole wood of trees and climatic parameters .....	118
<b>CONCLUSION, RECOMMENDATIONS AND PERSPECTIVES .....</b>	<b>119</b>
<b>REFERENCES .....</b>	<b>122</b>
<b>ANNEXES .....</b>	<b>138</b>

## LIST OF ABBREVIATION

ALOS-AVNIR	Advanced Land Observing Satellite-Advanced Visible & Near-infrared Radiometer
AVG	Average
DBH	Diameter at breast height
DplR	dendrochronology program library in R statistical software
DS	Dry savanna zone
EPS	Express Population Signal
FA	Farmland
GLK	Gleichlaeufigkeit
GLOWA-Volta	Global Change and the Hydrological Cycle
GPS	Global Positioning System
HadISST1	Hadley Centre Sea Ice and Sea Surface Temperature
HS	Humid savanna zone
ITCZ	Inter-tropical convergence zone
KNUST	Kwame Nkrumah University of Science and Technology
LANDSAT	Land satellite
PA	Protected area
PPM	Parts per million
RF	Riparian forests
RWI	Ring width index
SeD	Species Density
SR	Species richness
SST	Sea Surface Temperature
SWI	Shannon-Wiener Index
TV-BP	T-value of Baillie-Pilcher
TSAP	Time Series Analysis and Presentation

## LIST OF FIGURES

<b>Figure 1:</b> Schematic overview of energy flows within the climate system .....	10
<b>Figure 2:</b> Map showing distribution of the average temperature change between 1901 and 2012 and graph showing temperature dynamics in relation to CO <sub>2</sub> changes. ....	10
<b>Figure 3:</b> Carbon cycling in the earth systems .....	11
<b>Figure 4:</b> Model depiction of earth temperature change based on human and natural changes.....	13
<b>Figure 5:</b> Study sites in two main ecological zones of the Volta basin in Ghana (West Africa) .....	25
<b>Figure 6:</b> Temperature and precipitation patterns of the dry and humid savannas from averaged per month from 1961 to 2012 .....	27
<b>Figure 7:</b> Potential evapotranspiration rates per annum in Ghana indicating the study sites .....	29
<b>Figure 8:</b> Volta Riparian Basin sub-catchments .....	31
<b>Figure 9:</b> Relief of the Volta basin .....	32
<b>Figure 10:</b> Landcover types in the Afram and Tankwidi riparian catchments .....	41
<b>Figure 11:</b> Sampling sites in the Afram and Tankwidi riparian catchments .....	44
<b>Figure 12:</b> Plot layout for vegetation survey .....	48
<b>Figure 13:</b> Landcover in the Afram river catchment for the studied years (1986-2014).....	63
<b>Figure 14:</b> Landcover in the Tankwidi river catchment for the studied years (1986-2014).....	66
<b>Figure 15:</b> Diameter and height class distribution of individuals' $\geq 5\text{cm}$ DBH in riparian forests in protected area (PA) and farmland (FA) along the Afram river .....	69
<b>Figure 16:</b> Diameter and height class distribution of individuals' $\geq 5\text{cm}$ DBH in riparian forests in protected area (PA) and farmland (FA) along the Tankwidi river .....	70
<b>Figure 17:</b> Transverse sections of <i>Afzelia africana</i> and <i>Anogeissus leiocarpus</i> in the humid and dry savanna zones of Ghana.....	83
<b>Figure 18:</b> Records of ring widths of the five best cross-dated individuals of <i>Afzelia africana</i> and <i>Anogeissus leiocarpus</i> in the dry (DS) and humid (HS) savanna zones of Ghana.....	85
<b>Figure 19:</b> Comparison of ring widths of <i>Afzelia africana</i> and <i>Anogeissus leiocarpus</i> in the dry and humid savanna zones of Ghana .....	88
<b>Figure 20:</b> Correlation of detrended time series of <i>Afzelia africana</i> and <i>Anogeissus leiocarpus</i> in the dry and humid savanna zones of Ghana .....	89
<b>Figure 21:</b> Correlation of <i>Afzelia africana</i> and <i>Anogeissus leiocarpus</i> individual chronologies from the dry and humid savanna to monthly and yearly average precipitation (Avg) data of climatic stations of each savanna types .....	91

<b>Figure 22:</b> Correlation of <i>Afzelia africana</i> and <i>Anogeissus leiocarpus</i> individual chronologies from the dry and humid savanna to maximum mean monthly temperature (January to December) and yearly average (Avg) data of climatic stations of each savanna types .....	91
<b>Figure 23:</b> Spatial correlation of growth rings of <i>Afzelia africana</i> and <i>Anogeissus leiocarpus</i> to Sea Surface Temperatures (SST).....	92
<b>Figure 24:</b> Ring Width Index (RWI) series and wavelet spectra with cone of influence (shaded area) for <i>Afzelia africana</i> and <i>Anogeissus leiocarpus</i> in the humid and dry savanna zones. Black contours show frequencies significant on the 0.05 confidence level. ....	94
<b>Figure 25:</b> Correlation of the pattern of Carbon-13 ( $\delta^{13}\text{C}$ ) time series in whole wood and cellulose of <i>Afzelia africana</i> and <i>Anogeissus leiocarpus</i> in the dry (DS) and humid (HS) savanna zones of Ghana.....	96
<b>Figure 26:</b> Time series of individuals of species-specific Carbon-13 ( $\delta^{13}\text{C}$ ) of <i>Afzelia africana</i> and <i>Anogeissus leiocarpus</i> in the dry and humid savanna zones of Ghana .....	97
<b>Figure 27:</b> Comparison of Carbon-13 ( $\delta^{13}\text{C}$ ) of <i>Afzelia africana</i> and <i>Anogeissus leiocarpus</i> in both the humid and dry savanna zones.....	100
<b>Figure 28:</b> Correlation of <i>Afzelia africana</i> and <i>Anogeissus leiocarpus</i> individual chronologies from the dry and humid savanna to temperature .....	103
<b>Figure 29:</b> Correlation analysis of <i>Afzelia africana</i> and <i>Anogeissus leiocarpus</i> in both the humid and dry savanna zones with precipitation.....	103

## LIST OF TABLES

<b>Table 1:</b> Description of Afram and Tankwidi river catchments .....	26
<b>Table 2:</b> Population data (2008) for countries in the Volta Basin and projections for 2025 .....	37
<b>Table 3:</b> Attributes of the Landsat TM, ETM+ and OLI imagery used in the study .....	39
<b>Table 4:</b> Confusion matrix of Landcover map of Afram and Tankwidi riparian catchments using ALOS AVNIR imagery (2011) .....	45
<b>Table 5:</b> List of studied species with summary of their habit and annual growth increments.....	56
<b>Table 6:</b> Confusion matrix of Landcover map using Landsat 2000 (Afram catchment) .....	62
<b>Table 7:</b> Confusion matrix of Landcover map using Landsat 2014 (Afram catchment) .....	62
<b>Table 8:</b> Landcover proportions from 1986-2014 at the Afram catchment .....	62
<b>Table 9:</b> Confusion matrix of Landcover map using Landsat 2000 (Tankwidi catchment) .....	65
<b>Table 10:</b> Confusion matrix of Landcover map using Landsat 2014 (Tankwidi catchment) .....	65
<b>Table 11:</b> Landcover proportions from 1986-2014 at the Tankwidi catchment .....	65
<b>Table 12:</b> Stand structural characteristics of riparian buffer in protected area (PA) and farmland (FA) along the Afram river (Humid savanna) and Tankwidi river (Dry savanna) .....	68
<b>Table 13:</b> Soil texture in protected area (PA) and farmland (FA) along Afram (Humid savanna) and Tankwidi (Dry savanna) rivers.....	75
<b>Table 14:</b> Soil bulk density and moisture content in Protected Area (PA) and Farmland (FA) in the humid and dry savanna zones.....	75
<b>Table 15:</b> Soil moisture content in Protected Area (PA) and Farmland (FA) in the humid and dry savanna zones.....	76
<b>Table 16:</b> Riparian buffer soil in top and bottom layers of protected area and farmland along Afram (Humid savanna) and Tankwidi rivers (Dry savanna) .....	77
<b>Table 17:</b> Riparian buffer soil in protected area and farmland .....	78
<b>Table 18:</b> Riparian buffer soil in the humid and dry savanna zones.....	79
<b>Table 19:</b> Two-way Anova of the effect of savanna and land use types on riparian buffer soil chemical properties .....	80
<b>Table 20:</b> Regression analysis between riparian woody density and soil properties in Protected Areas and Farmlands in the humid and dry savanna zones.....	81
<b>Table 21:</b> Characteristics of tree ring series of <i>Afzelia africana</i> and <i>Anogeissus leiocarpus</i> in the dry and humid savanna zones of Ghana .....	86

<b>Table 22:</b> Statistical characteristics of Carbon-13 ( $\delta^{13}\text{C}$ ) series of <i>Afzelia africana</i> and <i>Anogeissus leiocarpus</i> in the dry and humid savanna zones of Ghana.....	98
<b>Table 23:</b> Comparison of Carbon-13 values of the <i>Afzelia africana</i> and <i>Anogeissus leiocarpus</i> in both the humid and dry savanna zones.....	101

## LIST OF ANNEXES

Annex 1: Lists of woody plants in Afram and Tankwidi riparian forests.....	139
Annex 2: Publications.....	146

# **INTRODUCTION**

Global mean annual temperature increased by 0.72°C during the 20<sup>th</sup> Century (**IPCC, 2007 & Hartmann *et al.*, 2013**). The temperature increase was attributed to anthropogenic greenhouse gases emissions such as carbon dioxide (CO<sub>2</sub>), methane (CH<sub>4</sub>) and nitrous oxide (N<sub>2</sub>O) (**IPCC, 2007**). Current predictions indicate that over this 21<sup>st</sup> Century, the concentrations of the greenhouse gases will result in a rise of 1.4-5.8°C in global mean annual temperature (**IPCC, 2007, 2013**). This temperature rise will also influence other global climatic factors such as precipitation and evapo-transpiration patterns (**IPCC, 2013**). For tropical and sub-tropical regions, the most important climate change factor is the spatial and temporal patterns of precipitation (**IPCC, 2013**). In the case of the African continent, climate simulations have shown that there will be modest increases in mean annual precipitation over equatorial Africa, particularly in the eastern region and a decrease in precipitation in the northern, southern and western Africa (**IPCC, 2007; Hartmann *et al.*, 2013**). The fulfilment of these projections will have serious consequences on the survival of species and climate sensitive ecosystems such as riparian forests in the savanna landscapes of the world (**Warren *et al.*, 2011; Kayranli *et al.*, 2012**). It is worth mentioning that the threat of climate change on ecosystems have been worsened by the intense human activities which causes modification to natural habitats, nutrient cycling as well as temperature and moisture states of the forests (**Jetz *et al.*, 2007**). **IPCC (2013)** indicates that the future will witness simultaneous changes in climatic and human impacts and therefore, there is a need to study riparian ecosystems in the light of these changes.

Savannas are spatial mosaics of herbaceous and woody plant-dominated patches (**Goetze *et. al.*, 2006; Azihou *et al.*, 2013**). They are formed from long period of interaction of biotic and abiotic factors such as herbivory, soil moisture, soil nutrients and fire (**Goetze *et. al.*, 2006; Azihou *et al.*, 2013**). Savannas occur under rainfall regimes, varying greatly in terms of patterns, frequency and intensity (**Ford, 2002; Sambare *et al.*, 2011**). This rainfall differences influence the structure of vegetation and the diversity of species (**Ford, 2002**). One characteristic of savanna landscapes is that they are interspersed with riparian forests, which are composed of dense strips of woody vegetation growing along waterways (**Azihou *et al.*, 2013**). Riparian forests vary with the size of water feature and geomorphology of a landscape. They are wider downstream, where flooding and river channel migration affects a much wider area (**Naiman & Decamps, 1997**). Many studies have described riparian forests as anywhere from 1m to 1 km from the waterbody. The size of riparian forest is normally dependent on the width of the river channel (**Naiman *et al.*, 1993; Rykken *et al.*, 2007**).

As riparian forests form a transition between savanna terrestrial landscape and aquatic ecosystem, they receive continuous supplies of moisture from the waterbody to sustain their composition, structure and functions (**Naiman *et al.*, 1993; Sambare *et al.*, 2011**). The functions are considered disproportionately large given that they occupy less than 10% of the earth's terrestrial surface area (**Naiman *et al.*, 1993**). Riparian forests provide a large variety of habitats for biodiversity and the many rare ones that depend on water (**Sambare *et al.*, 2011; Azihou *et al.*, 2013**). They provide shade and moderate stream temperatures for aquatic life. Their litter production from trees is important for the river foodweb (**Naiman *et al.*, 1993; Rykken *et al.*, 2007**). Further, the forest cover reduces erosion and stabilises river banks. Riparian forests trap seeds and process water, sediment and nutrients transported from adjacent land areas. This makes the riparian forests to support high plant productivity and biomass growth compared to non-riparian areas in a landscape (**Arroyo *et al.*, 2010; Azihou *et al.*, 2013**). Riparian forests have social benefits including opportunities for tourism, medicines, nutrition, firewood, and raw material for different crafts and construction (**Ceperley *et al.*, 2010; Gray *et al.*, 2014**). Culturally, riparian forests are sometimes designated as sacred groove (**Ceperley *et al.*, 2010**). Due to these functions and many others, some riparian forests are protected by Ramsar convention and others by national regulations (**McCracken *et al.*, 2012; Gray *et al.*, 2014**).

A number of physical and environmental factors control the growth and diversity of riparian forests. They include soil physical and chemical properties, size of riparian forests, width of river channel, and topography (**Natta *et al.*, 2002; Natta & Porembski, 2003; Azihou *et al.*, 2013**). For instance, soils found in riparian forests have pronounced spatial variability in terms of structure and particle size distribution which influence the ability of the soils to retain moisture and nutrient for plant utilization and distribution in the riverine area. Knowledge of species diversity patterns and growth in relation to their physical and environmental determinants in riparian forests is still limited (**Naiman *et al.*, 1993; Rykken *et al.*, 2007**). Understanding this is crucial for the management and rehabilitation of degraded riparian forests.

Riparian forests are highly vulnerable to the effects of climate change (**IPCC, 2007; 2013**). This is because changes in meteorological variables such as precipitation, air temperature, wind speed and solar radiation have effect on the hydrology of rivers which riparian forests is dependent for sustenance (**IPCC, 2007; Sambare *et al.*, 2011; Azihou *et al.*, 2013**). **Mantyka-Pringle *et al.* (2012)** reported that a higher mean temperature and a lower mean precipitation had resulted in a global loss of species and habitats moisture conditions of riparian forests. These processes have also had negative effects on

photosynthesis and consequently, the growth of riparian tree species (**Krepkowski *et al.*, 2010**). Since the tropics experience erratic climatic conditions, it is highly probable that riparian forests in this region will become vulnerable to future constraints in precipitations and temperature patterns (**Sambare *et al.*, 2011**). The projections on the future decline in precipitation in tropical areas (**IPCC, 2007; Warren *et al.*, 2011**) have raised concerns on the potential effects on riparian diversity value and growth of the trees.

**Millennium Ecosystem Assessment (2005)** report showed that the growth of agriculture is the primary driver of habitat loss in all human-dominated landscapes. Within riparian landscape in particular, agricultural land use intensification (e.g. cropland expansion, increased use of agrochemicals, increased input of pesticides and fertilizers) and landscape simplification is a key threat to riparian forests. This is because prolonged periods of water availability and relatively fertile soil attract agricultural activities within the riparian areas (**Callo-Concha *et al.*, 2012**). The expansion of the agricultural activities results in habitat conversion, loss of landscape structural diversity, biodiversity loss and changes ecological processes of riparian areas (**Vieilledent *et al.*, 2012; Azihou *et al.*, 2013**). Furthermore, habitat conversion causes changes in energy and nutrient cycling as well as emissions of carbon. Fertilizer and herbicide applications on farmlands also pollute waterways (**Rykken *et al.*, 2007; Surasinghe & Baldwin, 2015**). Projection shows future increase of human population of about 8-10 billion in the next century. This will invariably increase the demand for food resources (**Gray, 2014**) and results in more conversions of natural vegetation to agricultural lands. Balancing the need to increase yields against the negative ecological impacts of agriculture is therefore, one of the greatest challenges of this century. Already, the intensification of agricultural activities has resulted in the conversion of 70% of grassland, 50% of the savanna, 45% of the temperate deciduous forest, and 27% of the tropical forest biome (**Gray, 2014**). Since the last 30 years, majority of agricultural expansion has occurred in tropical regions, with about 80% of new croplands replacing forests (**Gray, 2014**). The increasing agricultural lands as against protected natural reserve areas have attracted interest in ensuring that biodiversity is also maintained on farmlands (**Traore *et al.*, 2012; Gray *et al.*, 2014**). With appropriate management, agricultural landscapes can contribute to the preservation of biodiversity and delivery of ecosystem services as evidence has been found in heterogeneous farmlands (**Morelli, 2013**). Documenting riparian changes as a result of agricultural activities will deepen the understanding on the link between human welfare and riparian ecosystem for sustainable use. This is important in savanna landscape where human need for fertile lands compete with riparian forests conservation.

A number of approaches such as Remote Sensing and Dendrochronology have evolved rapidly over the years as effective tools for studying forest ecosystems and their responses to climate and land cover changes. Remote sensing involves collecting information about an object using tools such as satellite and aerial camera which are not directly in contact with the object (**Lillesand *et al.*, 2004**). In forestry, Remote Sensing has the potential for assessing the spatial structure and long term trends of forest cover dynamics in relation to agricultural activities. This principally form an important starting point for assessing deforestation patterns in any ecosystem (**Chai *et al.*, 2009; Johansen *et al.*, 2010; Salifu & Agyare, 2012**). The assessment of the deforestation is made possible through the use of satellite remote sensing imageries from Landsat, SPOT, ASTER, Quickbird, IKONOS and ALOS (**Chai *et al.*, 2009; Johansen *et al.*, 2010; Bagan *et al.*, 2012**). Many studies have utilized remote sensing for large scale assessment of forest management. However, its use in riparian forest assessment has been under-utilized, especially in sub-Saharan Africa. The problem was attributed to the lack of high spatial resolution satellite imagery (<10m) for mapping the narrow strips of riparian forests (**Natta, 2003; Johansen *et al.*, 2010**). It is anticipated that the use of this technology will enhance the assessment of riparian forests in this study.

Dendrochronology is the discipline of dating tree rings to the year of their formation and using exactly dated tree rings for detecting environmental signals that are common for a population of trees (**Gebre Kirstos *et al.*, 2014**). The rings are formed from the periodic cessation of growth caused by extreme fluctuations in environmental condition (**Schongart *et al.*, 2006**). Studies have shown that trees hold greater potential for studying climate and past environmental conditions as the pattern of their rings width is a reflection of changes that occur in their environment (**Krepkowski *et al.*, 2010; Gebre Kirstos, *et al.*, 2011**). In recent times, carbon, hydrogen and oxygen components of wood extracted from growth rings have also been known to contain environmental and climatic information (**McCarroll & Loader, 2004; Singer *et al.*, 2013**). This is because air and water sampled by a tree are subtly modified by the tree as it responds to the varying environments in which it lives, and these small changes, expressed as variations in isotopic ratios, provide an archive for reconstructing past environments. The use of both ring widths and isotopic ratios are possible because they can exactly be dated on an annual scale (**Fichtler *et al.*, 2004; Gebre Kirstos, *et al.*, 2011**).

Compared to natural archives such as ocean and lake sediments, peat bogs and ice cores, trees hold the greatest advantage for climatic and environmental studies (**McCarroll & Loader, 2004; Gebre Kirstos *et al.*, 2011**). This is because trees are widespread so that it is possible to examine geographical

variations in the environmental conditions. It is also possible to create chronologies of several overlapping trees, and analyze the variability within the measurements (**McCarroll & Loader, 2004; Gebrekirstos *et al.*, 2008**). The isotope ratios in the tree rings have the added advantage of providing information on the tree physiology (**McCarroll & Loader, 2004**). Dendrochronology has been utilized in many forest ecosystems in temperate regions (**McCarroll & Loader, 2004**), but under-researched in the tropics. This is because it was initially perceived that tropical trees do not form annual rings. Recent studies in Benin, Burkina Faso, Cote d'Ivoire, Ethiopia and Namibia have however, demonstrated that growth rings of tropical trees can be dated on an annual scale (**Fichtler *et al.*, 2004; Schongart *et al.*, 2006; Gebrekirstos *et al.*, 2008; Gebrekirstos *et al.*, 2011**). In Ghana, the potential of dendrochronology has not been tested and this research will assess its capability in the country.

Because riparian forests influence a range of ecological and hydrological processes, they are protected in many countries (**McCracken *et al.*, 2012; Gray *et al.*, 2014**). In Ghana, riparian forests are protected by the Ghana buffer zone policy for freshwater management and other regulatory requirements in the natural resource and environment sector (**Government of Ghana, 2011**). It is however unclear if the regulatory tools have been effective in preserving the ecological integrity of riparian forests in the country. It is against the background that this study is being conducted in riparian forests in the tropical savannas of the Volta basin in Ghana. The Volta basin is located in West Africa between latitudes 5° 30"N and 14° 30"N and longitudes 2° 00"E and 5° 30"W. It is the 9th largest river basin in sub-Saharan Africa and covers approximately 400,000 km<sup>2</sup>. Its resources are shared by six countries: Benin, Burkina Faso, Côte d'Ivoire, Ghana, Mali and Togo. Approximately, 42% of the basin is in Ghana (**UNEP-GEEF, 2012**). The Volta Basin is defined as an agricultural watershed and the intensification of the farming activities possess a threat to woody plant diversity and ecosystem functions of riparian forests. The farming activities could also alter the habitat conditions of the riparian forests to increase climate change impacts on the growth of woody species (**Callo-Concha *et al.*, 2012**). Understanding the response of riparian forests to climate and agricultural land use impact is important in order to develop management strategies for their conservation.

The objective of the study is to contribute to a better understanding of the response of riparian forest in the humid and dry savanna zones of the Volta basin of Ghana to climate and agricultural land use impacts.

The specific objectives are following:

- To assess historical changes (1986-2014) in forest cover of Afram and Tawkwidi riparian catchments within the Volta basin.
- To compare woody plant diversity and structure, and soil properties of riparian forests between protected area and farmland in the humid and dry savanna zones.
- To evaluate the relationship between the radial growth of riparian woody species and climatic parameters in the humid and dry savanna zones.
- To examine inter-annual variability of carbon isotope ratios of riparian woody species in the humid and dry savanna zones with climatic parameters.

The study pursued the following research questions:

- What is the trend of forest cover change in the Afram (humid) and Tawkwidi (dry) riparian catchments (1986-2014) within the Volta basin of Ghana?
- Are there significant differences in woody plant diversity, structure and soil properties of riparian forests between protected areas and farmlands, and in the humid and dry savanna zones?
- What is the relationship between radial growth of riparian woody species and climatic parameters in the humid and dry savanna zones?
- Are there climatic signals in carbon isotope ratios of riparian woody species in the humid and dry savanna zones?

# **I. LITERATURE REVIEW**

## 1.1 Global climate change

Climate is defined as the statistical description of weather, where weather consists of precipitation, temperature and wind (**IPCC, 2007**). Climate change on the other hand refers to a change in the state of the climate that can be determined by changes in the mean and/or the variability of its properties and that persists for an extended period of time (typically decades or longer). Climate is generally as a result of the interaction of the sun's energy with the earth (Figure 1): atmosphere, oceans, land surfaces and ice sheets (**IPCC, 2013**). The rates at which energy enters the Earth system from the Sun, and leaves the system, approximately balance on average globally. As the solar radiation passes through the Earth's atmosphere, the processes of scattering, absorption, and reflection of the constituents reduce the intensity of the shortwave beam. The shortwave energy received by the Earth is balanced by a similar quantity of longwave radiation leaving back to space. Energy absorbed at the surface is transferred to the atmosphere through infrared radiation, conduction of sensible heat, and evaporation of water whose latent heat is released later when the water condenses again (**Hartmann *et al.*, 2013**).

## 1.2 Drivers of climate change

Climate change can occur through both natural and human-induced causes. The natural variations can originate in two ways: from internal fluctuations that exchange energy, water and carbon between the atmosphere, oceans, land and ice, and from external influences on the climate system, including variations in the energy received from the sun and the effects of volcanic eruptions (**IPCC, 2007**). Human activities influence climate by changing the concentrations of (CO<sub>2</sub>) and other greenhouse gases in the atmosphere (Figure 2), altering the concentrations of aerosols and altering the reflectivity of Earth's surface by changing land cover (**Hartmann *et al.*, 2013**). Figure 2 depicts the surface temperature adapted from **IPCC (2013)**, Fifth Assessment Report.

Atmospheric concentrations of CO<sub>2</sub>, methane and nitrous oxide began to rise around two hundred years ago. The concentration of CO<sub>2</sub> has increased from 280 parts per million (ppm) before 1800, to 396 ppm in 2013. This history of greenhouse gas concentrations has been established by a combination of modern measurements and analysis of ancient air bubbles in polar ice. Since the 19th century, human-induced CO<sub>2</sub> emissions from fossil fuel combustion, cement manufacture and deforestation have disturbed the balance, adding CO<sub>2</sub> to the atmosphere faster than it can be taken up by the land biosphere and the oceans (Figure 3).

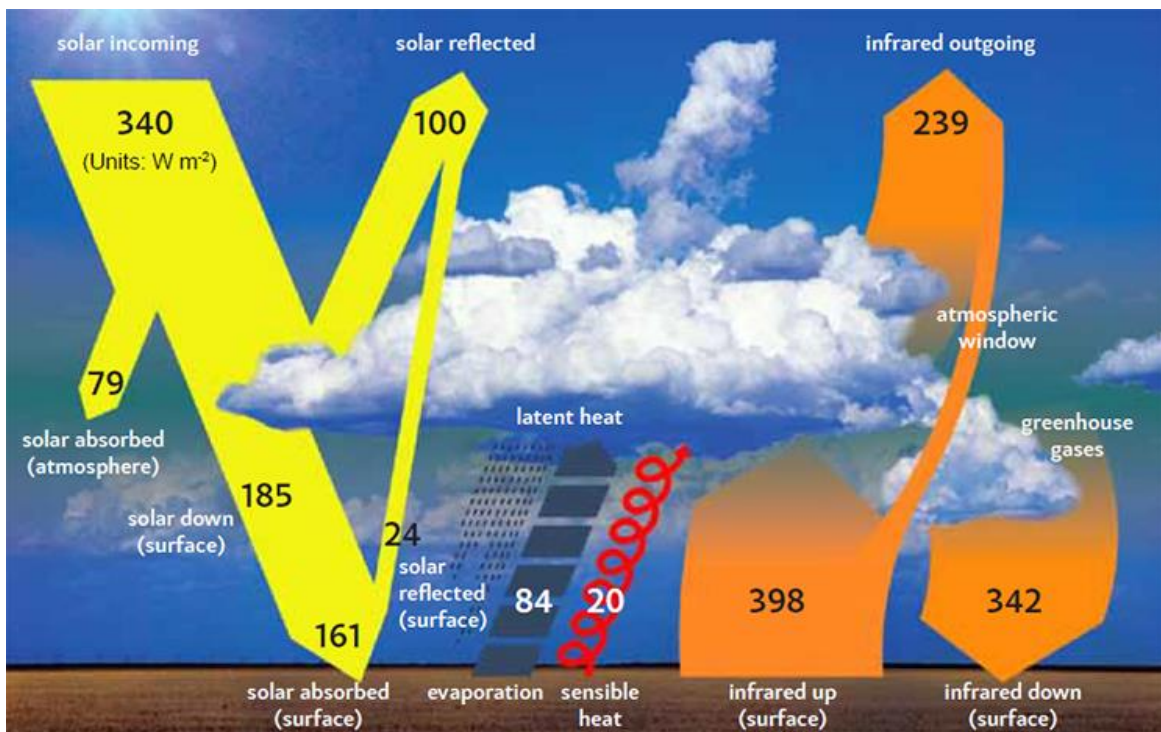


Figure 1: Schematic overview of energy flows within the climate system

The arrows show global average energy transfer rates in units of Watts per square metre

(Source: **IPCC (2013)**, Fifth Assessment Report)

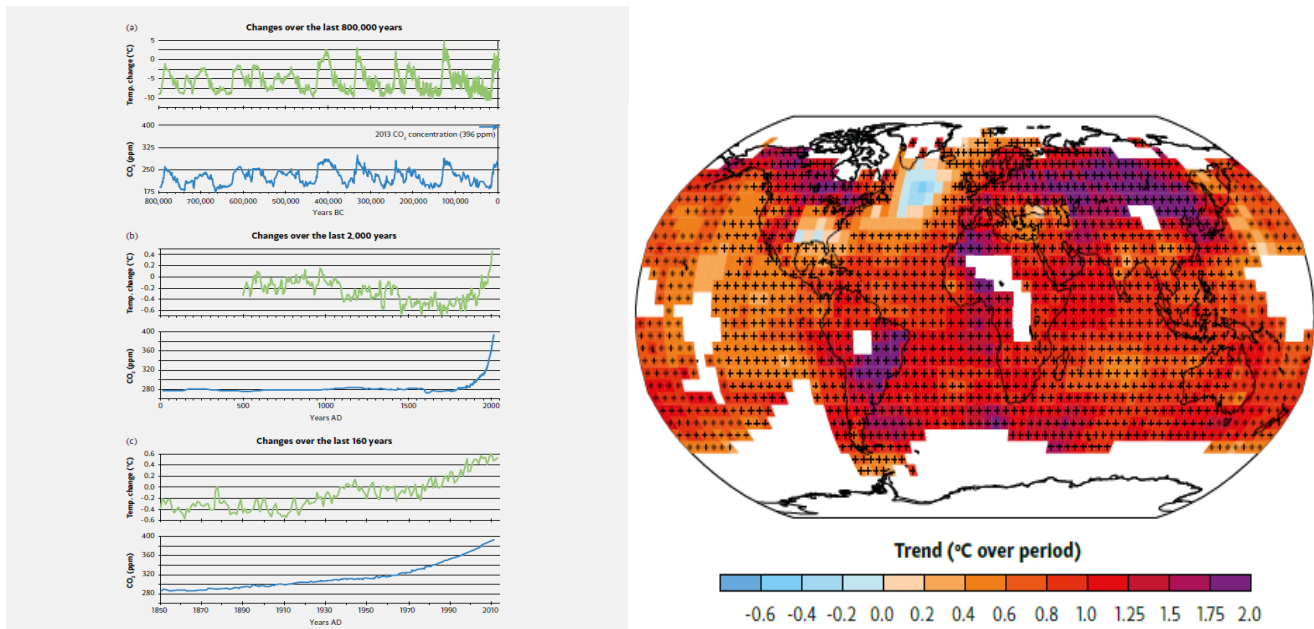


Figure 2: Map showing distribution of the average temperature change between 1901 and 2012 and graph showing temperature dynamics in relation to CO<sub>2</sub> changes.

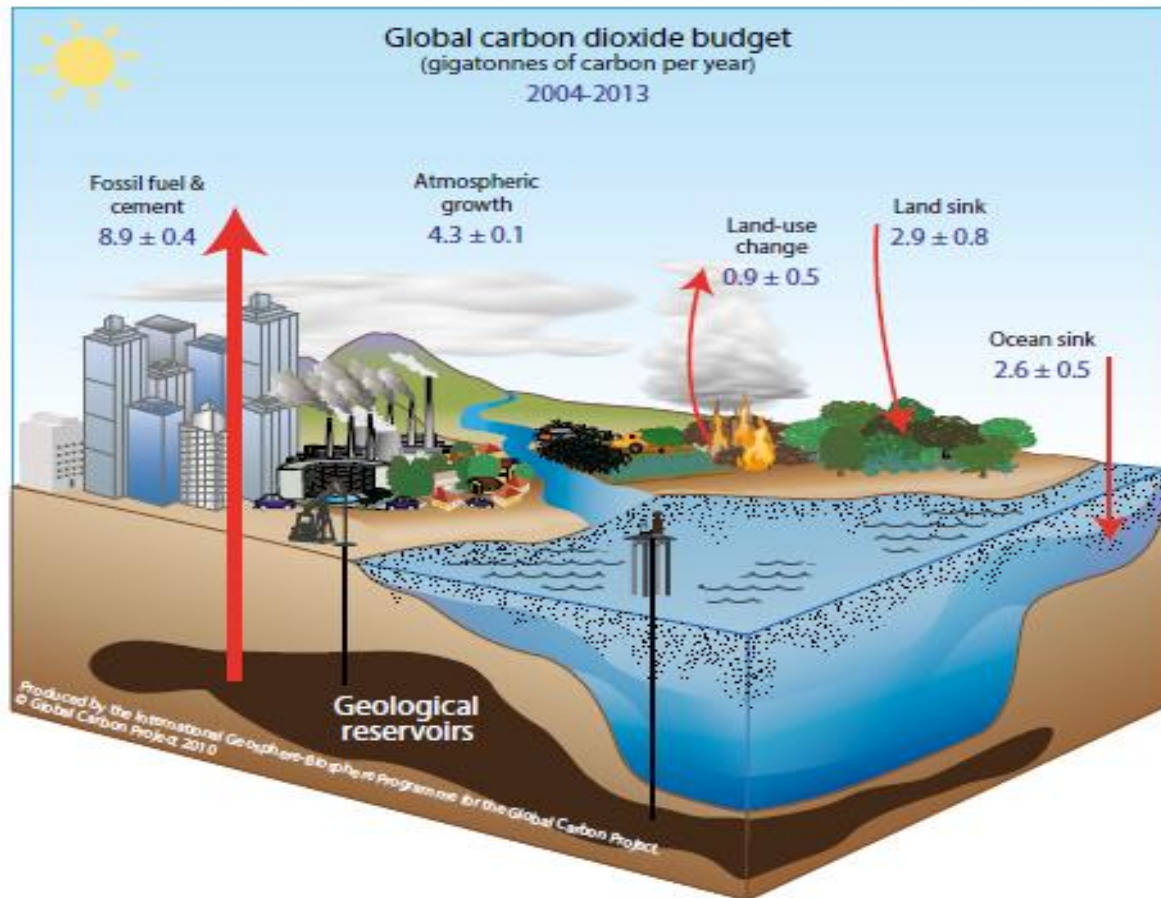


Figure 3: Carbon cycling in the earth systems

In the diagram of the global carbon cycle, numbers on arrows represent carbon flows averaged over 2004–2013, in gigatonnes (billion tonnes) of carbon per year. It depicts the natural carbon cycle, in which CO<sub>2</sub> circulates between the atmosphere, land and oceans, has been changed by emissions of CO<sub>2</sub> from human activities (**Global Carbon Project, 2015**).

### **1.3 Projections on climate change**

In comparison with other influences, the effects of solar variations on present global warming are small (**IPCC, 2007**). Indirect estimates suggest that changes in the brightness of the Sun have contributed only a few percent of the global warming since 1750 (**IPCC, 2007**). Direct measurements show a decreasing solar intensity over recent decades, opposite to what would be required to explain the observed warming (**IPCC, 2007 & 2013**). Solar activity has declined significantly over the last few years, and some estimates suggest that weak activity will continue for another few decades, in contrast with strong activity through the 20th century (**IPCC, 2007**). Nevertheless, the possible effects on warming are modest compared with anthropogenic influences (**IPCC, 2013**).

Through climate models, **IPCC (2013)** has separated the effects of the natural and human-induced influences on climate. The models were successful in reproducing the observed warming over the last 150 years when both natural and human influences are included, but not when natural influences act alone. This is both an important test of the climate models against observations and also a demonstration that recent observed global warming results largely from human rather than natural influences on climate (Figure 4).

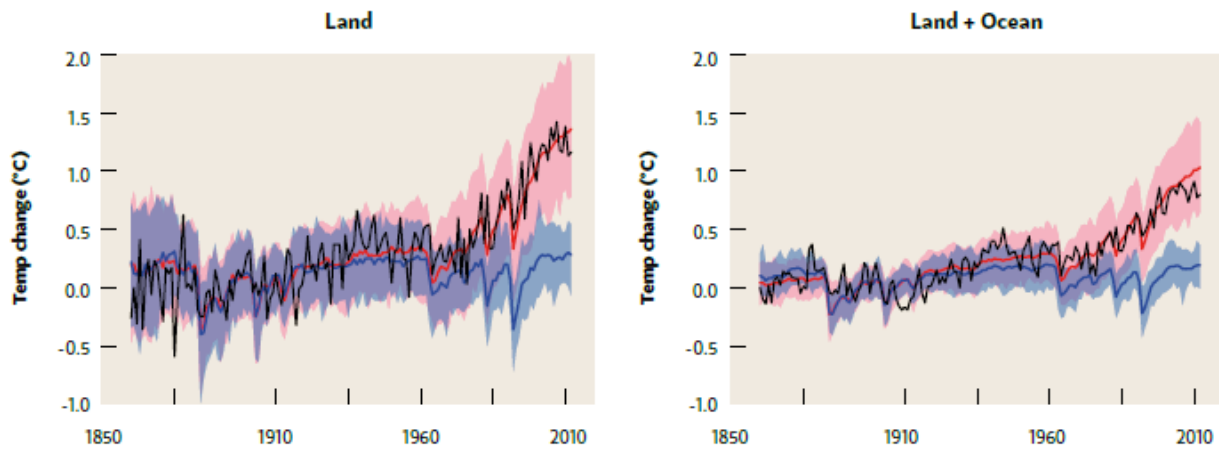


Figure 4: Model depiction of earth temperature change based on human and natural changes

The figure makes comparison of observed changes (black lines) in global temperatures (°C) over land (left) and land plus ocean (right) with model projections including both natural plus human influences (red lines) and natural influences only (blue lines). Shadings around model results indicate 5-95% confidence bands. Adapted from **IPCC (2013)**, Fifth Assessment Report.

## 1.4 Impacts of climate change

Current climate changes are expected to continue and intensify in the future (**Jetz *et al.*, 2007; Kayranli *et al.*, 2012**). The impacts of future climate change and related sea-level rise will be experienced in many areas, from the natural environment to food security and human environment (**Seavy *et al.*, 2009**). Some of the most vulnerable terrestrial ecosystems to climate change are (1) tropical rainforests due to warming temperatures (moderated or intensified by rainfall changes) (**Jetz *et al.*, 2007**); (2) coastal wetlands affected by sea-level rise and saline intrusion; (3) inland ecosystems dependent on freshwater and groundwater that are affected by changed rainfall patterns (**Seavy *et al.*, 2009**) and (4) tropical savannas affected by changes in the frequency and severity of bushfires (**Goetze *et al.*, 2006; Azihou *et al.*, 2013**).

Climate warming cause's land and ocean life to migrate away from areas that have become too warm, and towards areas that previously were too cool (**Naiman & Decamps, 1997**). In many places, climate change is likely to lead to invasion by new species and extinctions of some existing species that will have nowhere to migrate, for example because they are located on mountain tops. Seemingly small changes, such as the loss of a key pollinating species, may potentially have large impacts (**Warren *et al.*, 2010**).

## 1.5 Delineating riparian zones

The term riparian refers to biotic communities living on the shores of streams, rivers, ponds and lakes (**Naiman & Decamps, 1997; Meyer *et al.*, 2007**). Due to their interaction with the aquatic system, riparian areas have peculiar ecological features; thus, their boundaries can be delineated by changes in soil conditions, vegetation, and other factors that reflect this aquatic terrestrial interaction (**Natta *et al.*, 2003**). The spatial extent of the riparian zone is difficult to delineate precisely because its physical heterogeneity is expressed in an array of plant life history strategies and successional patterns, while the functional attributes depend not only on community composition but also on the environmental setting (**Gray *et al.*, 2014**).

The wider used definition of riparian zone is the area that encompasses the stream channel towards the uplands where vegetation may be influenced by elevated water tables or flooding. The width of the riparian zone, the level of control that the streambed vegetation has on the stream environment, and the

diversity of functional attributes are related to the size of the stream, the position of the stream within the drainage network, the hydrologic regime, and the local geomorphology (**Naiman & Decamps, 1997**). Riparian vegetation (forests) on the other hand refers to floodplain vegetation or vegetation directly adjacent to rivers and streams. Vegetation outside the zone that is not directly influenced by hydrologic conditions may be considered part of riparian zones, since contribute to the river dynamics by providing organic matter (e.g. leaves, wood, dissolved materials) to the floodplain or channel, or influencing the physical regime of the floodplain or channel by shading (**Naiman & Decamps, 1997; Gray *et al.*, 2012**).

### **1.6 Physical and ecological functions of riparian zones**

Plants influence many properties of riparian ecosystems. Through the process of evapotranspiration, riparian plants affect stream flow rates, ground water levels, and local climates (**Meyer *et al.*, 2007; Artigas *et al.*, 2013**). Riparian forests reduce solar heating of stream water by shading, thus controlling microclimate. Rates of evapotranspiration and of groundwater use vary widely between plant species depending on factors such as rooting depth, leaf area, and ability to regulate stomatal conductance (**Naiman & Decamps, 1997**).

With respect to stream geomorphology, plants influence rates of sedimentation and resistance of soils to erosion during flood events. Increased friction with the soil surface can cause reduced velocity and consequent sedimentation of particulates (**Naiman & Decamps, 1997**). This process modifies sediment transport either by physically entrapping materials, which appears to be most important in relatively low gradient environments, or by altering channel hydraulics. Alteration of channel hydraulics is accomplished either by roots or by large woody debris in the channel. All provide physical structure that slows water, decreases stream power, and holds materials in place. Plants also influence the vertical patterns of moisture throughout the soil profile, with root architecture being one of the factors that influences zones of water uptake and patterns of ‘hydraulic redistribution’ of soil water (**Meyer *et al.*, 2007; Artigas *et al.*, 2013**).

Riparian zones, as networks distributed over large areas, are key landscape components in maintaining biological connections along extended and dynamic environmental gradients. The riparian corridor can be viewed as a major vector propagating matter, energy and organisms longitudinally (**Naiman & Decamps, 1997**). Ecological investigations of riparian corridors have demonstrated them to be a

crucial landscape feature with important regulatory controls on environmental vitality (**Naiman & Decamps, 1997; Meyer *et al.*, 2007**).

Plants influence many properties of soils, such as salinity, organic matter, and C:N ratios, depending on their rate of litter production and on the chemical composition of the litter, and directly and indirectly mediate many nutrient cycling processes, as reducing levels of nitrogen and other minerals from stream or ground water (**Naiman & Decamps, 1997; Artigas *et al.*, 2013**). Organic matter from riparian vegetation becomes also a source of nourishment for aquatic organisms. One of the most important role played by riparian vegetation is the control and the movement reduction of nonpoint sources of pollution by sediment and nutrients in agricultural watersheds, particularly inorganic nitrogen and phosphorus. Further, due to nitrogen saturation, phosphorus may become the limiting factor for tree growth, particularly in wetlands, making vegetation an effective phosphorus sink (**Naiman & Decamps, 1997**).

Riparian forests are one of the biosphere's most complex ecological systems but also one of the most important for maintaining the vitality of landscape and its rivers. As interfaces between terrestrial and aquatic systems, riparian forests encompass sharp gradients in environmental and community processes, and are diverse mosaic of landforms in the large landscape (**Naiman & Decamps, 1997**). Their natural disturbances such as floods are responsible for structuring spatial heterogeneity. Consequently, plant species richness varies considerably in space and time along stream margins. According to **Naiman *et al.* (1993)**, the reasons for the high diversity of plants on riparian areas are related to: (1) the intensity and frequency of floods, (2) the small scale variation in topography and soils as a result of lateral migration of river channel, (3) variation in climate following the altitudinal gradient, and (4) disturbance regime created by upland environment. Also the migration capacity of plants along the riparian corridor is an important factor explaining this high biodiversity.

Further, the presence of a mosaic of habitats allows the overlap of different niches and thus the co-existence of a wide variety of species (**Naiman *et al.*, 1993**). Riparian zones exhibit high diversity of wildlife species because of habitat they provide for obligate riparian species, species seeking edge habitat, and species associated with early successional plant communities. They sustain high trophic levels and provide sources of food for granivores and herbivorous/detrital insects, birds, and mammals. Riparian zones covered with a variety of woody vegetation (from shrubs to trees) are extremely

important as refuges for small mammals, offering nesting and perching sites for birds, acting also as corridors for migration and dispersal (**Naiman & Decamps, 1997; Artigas *et al.*, 2013**).

### **1.7 Threats to riparian forests**

Nearly all rivers in the tropical environment are threatened by land use change, power generation, or flood control (**Natta *et al.*, 2002; Mantyka-pringle *et al.*, 2012**). For many rivers, land use activities, including timber harvest, livestock grazing, agriculture and urbanization are the primary causes of altered riparian areas. Particularly, river systems in arid climates often have relatively pristine upper catchments, but have been heavily transformed by anthropogenic activities (**McCracken *et al.*, 2012**). These are seasonally water-stressed environments (with climatic harshness and interrupted hydrological regime) are highly affected by human interferences in the flow regime, particularly water abstraction. Consequently, they are the most threatened habitats in agricultural environments of tropical environment as a result of the intense competition between humans and nature for limited supplies of fresh water (**McCracken *et al.*, 2012**).

Converting forest to agricultural lands generally decreases soil infiltration and result in increased overland flow, channel incision, floodplain isolation. This reduces retention of water in watersheds and, instead, routes it quickly downstream, increasing the size and frequency of floods and reducing base flow levels during dry periods. Similarly, urbanization creates impermeable surfaces that directs water away from subsurface pathways to overland flow (**Meyer *et al.*, 2007**). Consequently, floods increase in frequency and intensity, bank erode, and base flow declines during dry periods. Further, river ecosystems are highly prone to invasion by alien plants, largely because of their dynamic hydrology and because rivers act as conduits for the efficient dispersal of propagule (**Artigas *et al.*, 2013**). The same factors supporting high plant species richness in riparian habitats may also increase susceptibility to invasion by exotic species (**Naiman *et al.*, 1993**). Disturbance is thought to facilitate successful invasions by exotic species for some of the same reasons that it maintains native species diversity. Relations between invasion and disturbance are complex and depend on the type and frequency of disturbance, the environmental constraints and the biology of the particular species concerned (**Naiman & Decamps, 1997; Artigas *et al.*, 2013**).

Conventional river engineering operations produce major anthropogenic impacts on the fluvial ecosystem (**Gray *et al.*, 2014**). Channelization generally reduces the physical heterogeneity of

riverbeds and banks, accelerates erosional processes, changes flow and sediment load patterns, and consequently, at ecosystem level, the river system experiences a reduction of habitat heterogeneity, niche potential, and frequently ecological diversity as well. Regulation and fragmentation by dams also modify river flow, blocking the movement of organisms, and preventing the downstream flow of mineral sediment and organic material (**Naiman *et al.*, 1993; Artigas *et al.*, 2013**). Dams capture all but the finest sediment moving down a river, with severe downstream consequences for many aquatic species living in or using interstitial spaces among finest sediment. Also species with life stages sensitive to sedimentation, such as the eggs and larvae of many invertebrates and fish, can suffer high mortality rates (**Naiman *et al.*, 1993**). Dams have the potential to affect hydrochory in a number of ways, through modifying the hydrologic regime, influencing how far seeds travel and where they are deposited along channel margins and the availability and suitability of streamside habitat for seed germination and seedling establishment. Moreover, they serve as a physical barrier to the downstream movement of plant propagules, trapping and storing seeds in reservoirs and resulting in retention and high rates of seed mortality. Considering the critical importance of riparian areas for their ecological functions, there is no doubt that the problem of conservation and adequate management of rivers is of worthwhile importance, and addressing it is urgent because their threats are growing daily, and their impacts are increasingly severe (**Naiman & Decamps, 1997; Artigas *et al.*, 2013**).

### **1.8 Mapping of riparian forests**

Detailed riparian buffer studies over small geographic areas are often performed using airborne digital or film cameras, including manual interpretation and automated analysis of the data (**Lillesand *et al.*, 2004**). However, for coarser assessment over large spatial scales, it is more cost-effective to use satellite imagery. Traditionally, Land Satellite (Landsat) and the French Syst`eme Pour L'Observation de la Terre (SPOT) has been a reliable data sources for land cover mapping (**Chai *et al.*, 2009**). Their 20-30m spatial resolutions have proved effective for mapping wide riparian buffers, land cover, and changes in large watersheds. However, their resolutions are unable to adequately identify smaller hydrological features.

More recently, the availability of high-spatial resolution (<10m) data has significantly improved the capacity for mapping riparian buffers, wetlands, and other ecosystems from space (**Johansen *et al.*, 2010**). High-resolution (0.4–10m) imagery can be readily obtained from satellites, such as Ikonos (1-4m), QuickBird (0.61-2.44m), OrbView (1-4m), Worldview 0.5-2m) and ALOS (5-10) (**Arroyo *et al.*,**

**2010; Bagan *et al.*, 2012).** Their high resolution increases their efficiency for mapping the structural characteristics of riparian vegetation. Compared to temperate regions, high resolution images have been under-utilised in the tropical environment. This is primarily due to the cost of the satellite image and for which ideal data for landscape assessment can be expensive (**Johansen *et al.*, 2010).**

Many image processing and analysis techniques have been developed to aid the interpretation of remote sensing images and to extract as much information as possible from the images. The choice of specific techniques or algorithms to use depends on the goals of each individual project. Prior to data analysis, initial processing on the raw data is usually carried out to correct for any distortion due to the characteristics of the imaging system and imaging conditions (**Lillesand *et. al.*, 2004; Johansen *et al.*, 2010).** Depending on the user's requirement, some standard correction procedures may be carried out by the ground station operators before the data is delivered to the end-user. These procedures include radiometric correction to correct for uneven sensor response over the whole image and geometric correction to correct for geometric distortion due to Earth's rotation and other imaging conditions (such as oblique viewing). The image may also be transformed to conform to a specific map projection system. Furthermore, if accurate geographical location of an area on the image needs to be known, ground control points (GCP's) are used to register the image to a precise map (geo-referencing) (**Lillesand *et. al.*, 2004; Chai *et al.*, 2009; Rawata & Kumarb, 2015).**

Different landcover types in an image can be discriminated using some image classification algorithms using spectral features, i.e. the brightness and "colour" information contained in each pixel. The classification procedures can be "supervised" or "unsupervised" (**Lillesand *et. al.*, 2004).** In supervised classification, the spectral features of some areas of known landcover types are extracted from the image. These areas are known as the "training areas". Every pixel in the whole image is then classified as belonging to one of the classes depending on how close its spectral features are to the spectral features of the training areas. In unsupervised classification, the computer program automatically groups the pixels in the image into separate clusters, depending on their spectral features. Each cluster will then be assigned a landcover type by the analyst. Each class of landcover is referred to as a "theme" and the product of classification is known as a "thematic map" (**Lillesand *et. al.*, 2004; Johansen *et al.*, 2010).** Accuracies of maps are presented in the form of error matrix that indicates overall, producer and user accuracies. Another characteristic used to assess accuracy is the kappa (k)

statistic that determined the extent at which classification result surpass random assignment of pixels (Lillesand *et al.*, 2004).

## 1.9 Dendrochronology

Dendrochronology is the discipline of dating tree rings to the year of their formation and using exactly dated tree rings for detecting environmental signals that are common for a population of trees (Fichtler *et al.*, 2012; Gebrekirstos *et al.*, 2014). The rings are formed from the periodic cessation of growth caused by extreme fluctuations in environmental condition (Schongart *et al.*, 2006; Gebrekirstos *et al.*, 2008). Trees have greater advantage compared to the other natural archives for climatic and environmental studies (Schweingruber *et al.*, 1988; McCarroll & Loader, 2004; Gebrekirstos *et al.*, 2011) since trees are widespread so that it is possible to examine geographical variations in the environmental conditions. It is also possible to create chronologies of trees with overlapping life times and to analyze the variability within the measurements (McCarroll & Loader, 2004; Gebrekirstos *et al.*, 2008).

In the tropics, studies have proven the existence of annual rings in tree species from arid (Fichtler *et al.* 2004; Gebrekirstos *et al.*, 2008; Gebrekirstos *et al.*, 2014) to humid zones (Trouet *et al.*, 2010) and riparian areas (Schongart *et al.*, 2006). Such studies have shown that many tree species from tropical regions characterized by one severe dry season per year form annual rings with anatomical structures similar to growth rings of temperate tree species. Unlike temperate zones, few studies have been conducted for tropical regions (Worbes 2002; Schongart *et al.*, 2006), despite the numerous reports on the potential of tropical trees for climatic and environmental studies (Worbes, 2002; Gebrekirstos *et al.*, 2011). This is generally caused by the limited technical facilities and financial resources in tropical countries. In addition, the difficulty for accessing forest stands and low sampling replication because of the enormous species diversity that comes along with low abundances of individuals of any particular species in most tropical forests have hampered tree ring research (Worbes, 2002). In recent time, the isotope ratios in tree rings cellulose have provided another possibility of studying the physiology of riparian trees (McCarroll & Loader, 2004; Gebrekirstos *et al.*, 2014).

Carbon, hydrogen, nitrogen and oxygen are the chemical elements in wood that have more than one stable (i.e. non-radioactive) isotope. Carbon (C), for example, has two stable isotopes,  $^{12}\text{C}$  and  $^{13}\text{C}$ , each with six protons but with either six or seven neutrons (McCarroll & Loader, 2004). These

isotopes have identical chemical properties but the difference in mass allows physical, chemical and biological processes to discriminate against one of them, resulting in fractionation of carbon isotopes (McCarroll & Loader, 2004; Krepkowski *et al.*, 2013). There are two main processes during which carbon isotopic fractionation occurs during the transition of external air to leaf sugars (McCarroll & Loader, 2004): When air diffuses through the stomata, the carbon dioxide (CO<sub>2</sub>) molecules that include the lighter isotope of carbon (<sup>12</sup>C) bounce off each other furthest and therefore diffuse more easily than those including the heavier isotope (<sup>13</sup>C). The net effect is that internal air of plant leaves is depleted in <sup>13</sup>C relative to the ambient air. The second point of fractionation occurs when internal CO<sub>2</sub> is utilized by the photosynthetic enzyme, Ribulose-1-5-bisphosphat-carboxylase which is a primary CO<sub>2</sub> acceptor in plants. This biological process tends to use <sup>12</sup>C in preference to <sup>13</sup>C (Krepkowski *et al.*, 2013).

Leaf phenology (i.e. seasonal variations in leaf area) of plants influence carbon assimilation (Caldararu *et al.*, 2014). Phenological cycles are highly dependent on climate and the timing and spatial patterns of phenological dates may change significantly in response to changes in climate (Krepkowski *et al.*, 2013). Consequently, <sup>13</sup>C/<sup>12</sup>C ratios of tree-ring cellulose sometimes show high correlations with climate parameters (Fichtler *et al.*, 2010; Brien *et al.*, 2011). A number of studies have successfully applied stable isotope approaches in climate studies (Gebrekirstos *et al.*, 2009; Fichtler *et al.*, 2010; Brien *et al.*, 2011; Gebrekirstos *et al.*, 2012). For instance, a significant negative correlation between annual precipitation and <sup>13</sup>C time series of tree rings was found for several broadleaved tree species in various tropical climates (Fichtler *et al.*, 2010). Gebrekirstos *et al.* (2011 & 2012) found significant negative correlations of annual <sup>13</sup>C variations in West African Sahel woodland species with precipitation and humidity, and positive correlations with temperature. Isotope composition of material or compound is usually expressed using delta notation (δ) as deviations from internationally accepted standard material (Pee Dee Bee) for which the isotopic ratio is known. The measurement of the isotopic ratio is done in the mass spectrometer.

## **II. MATERIALS AND METHODS**

## 2.1 Study area

### 2.1.1 Summary description

The study was conducted within the Volta sub-basin of Ghana along two river catchments: Afram and Tankwidi rivers (Figure 5 and Table 1) respectively located in the Guinean (1°22.00' West, 7° 22.00' North) and Sudanian savannas (0° 57.00' West, 10° 44.00' North). The two research sites were selected because of the following reasons: (1) they are within the core research area of West African Science Service Centre on Climate Change and Adapted Land Use (WASCAL) and the study contributes to its research priorities; (2) Secondary data such as climatic parameters (temperature and precipitation), medium resolution and high resolution satellite images were available for the two study sites; and (3) Conservation areas (forest reserve area) were also available in the two catchments to serve as controls in order to meet the objectives of the study.

Generally, three major agro-climatic zones have been identified within the basin: Guinean, Sudanian and Sudano-Sahelian zones (**de Condappa & Lemoalle, 2009**). In this study the Guinean and Sudanian zones are referred as humid and dry savanna zones respectively due to their differences in annual rainfall levels. The humid savanna receives in excess annual rainfall of 1100mm. The mean annual maximum temperature is 32 °C. In the case of the dry savanna, the mean annual rainfall is 800mm and the mean annual maximum temperature is 36 °C (**de Condappa & Lemoalle, 2009; Callo-Concha et al., 2012**). Both rainfall and temperature are highly variable in the humid and dry savanna zones. The two study sites however, have approximately 4 months of extremely dry period starting from November and ending in February (Figure 6). The width of rivers of both Afram and Tankwidi catchments ranges between 8-12m. The predominant soil type is Luvisol. Luvisols are soils with sub-surface accumulation of clay and organic matter, high activity clay and high base saturation. Flat and gently sloping favourable soil physical structure, well drained, porous and well aerated mostly fertile soils (**Callo-Concha et al., 2012**).

Along the Afram river (humid savanna), the study was conducted in the Kogyae Strict Nature Reserve and surrounding farmlands. Kogyae Strict Nature Reserve was established in 1971 under the Wildlife Reserves Regulations (Legislative instrument 710). The reserve protects the tributaries of the Afram river. Additionally, the reserve protects the wildlife (e.g. *Colobus vellerosus*, *Potamochoerus porcus*, *Syncerus caffer*, *Kobus ellipsiprymnus* and *Tragelaphus scriptus*) in the area (**Kyerematen et al., 2014; Egyir et al., 2015**). In the case of the Tankwidi river (dry savanna), the study was conducted in

the Tankwidi forest reserve and farmlands. The reserve was established in 1956 under the Ghana Forest Ordinance, Cap 157. The main purpose of establishment of the Tankwidi reserve is to protect the Tankwidi river and its tributaries as well as important bird species such as *Bucorvus abyssinicus* and *Eupodotis melanogaster* (**BirdLife, 2014**). Commercial logging is prohibited in the two reserves; however, communities fringing the reserves have traditional use rights to harvest non-timber forest products and for religious festivities. The main land use activity of the communities in the vicinity of the two reserves is farming and along the river, cereals are the widely cultivated food crops. The farmlands are affected by various anthropogenic activities including extensive livestock grazing, bush fires, and various harvestings of timber and non-timber forest products such as wood, leaves, bark, flowers and fruits (**BirdLife, 2014; Kyerematen et al., 2014; Egyir et al., 2015**).

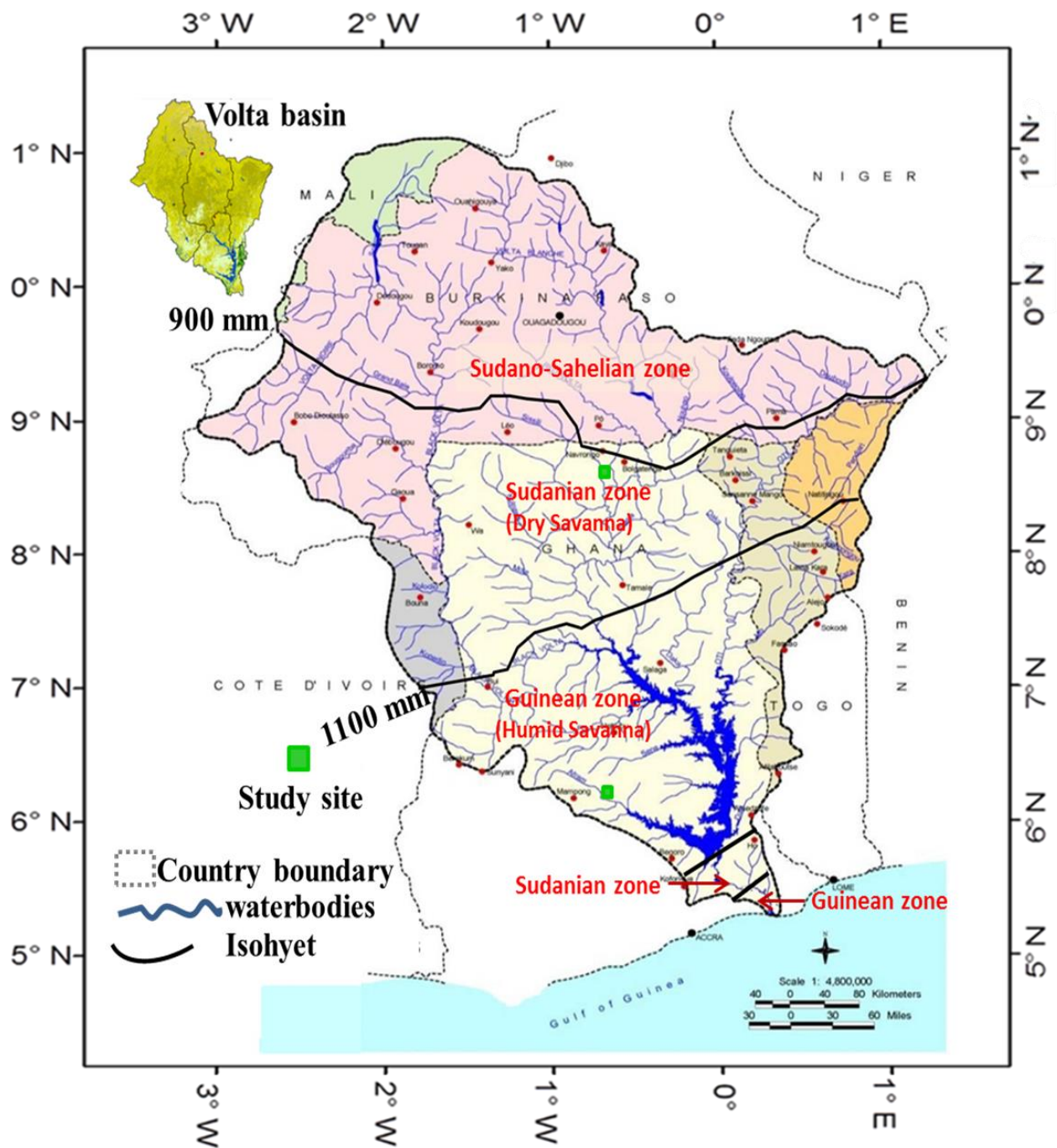
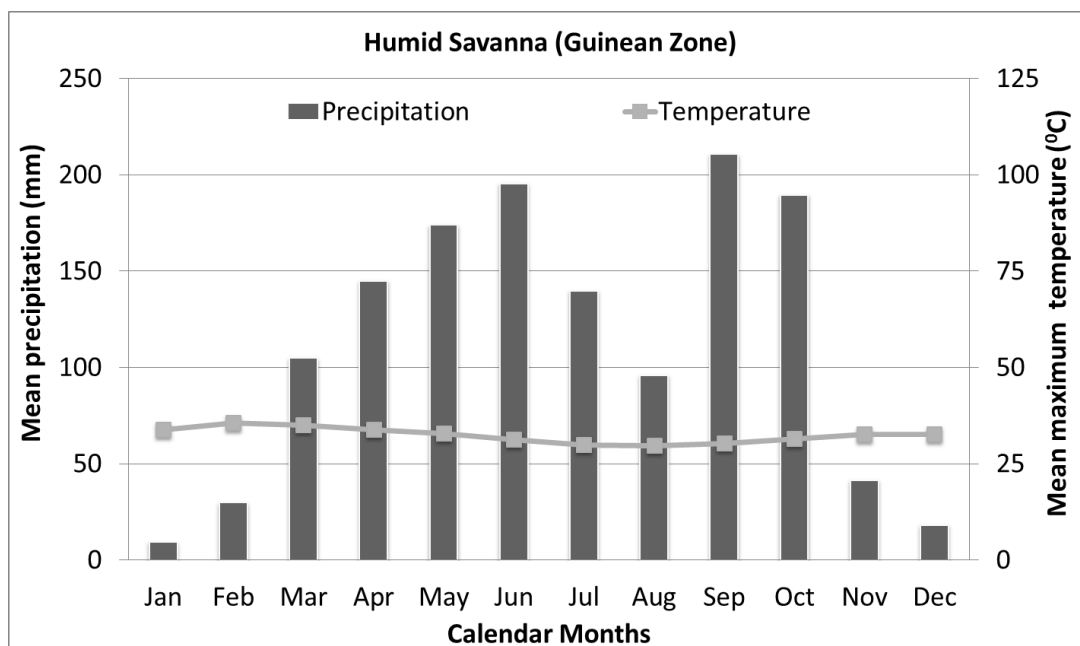
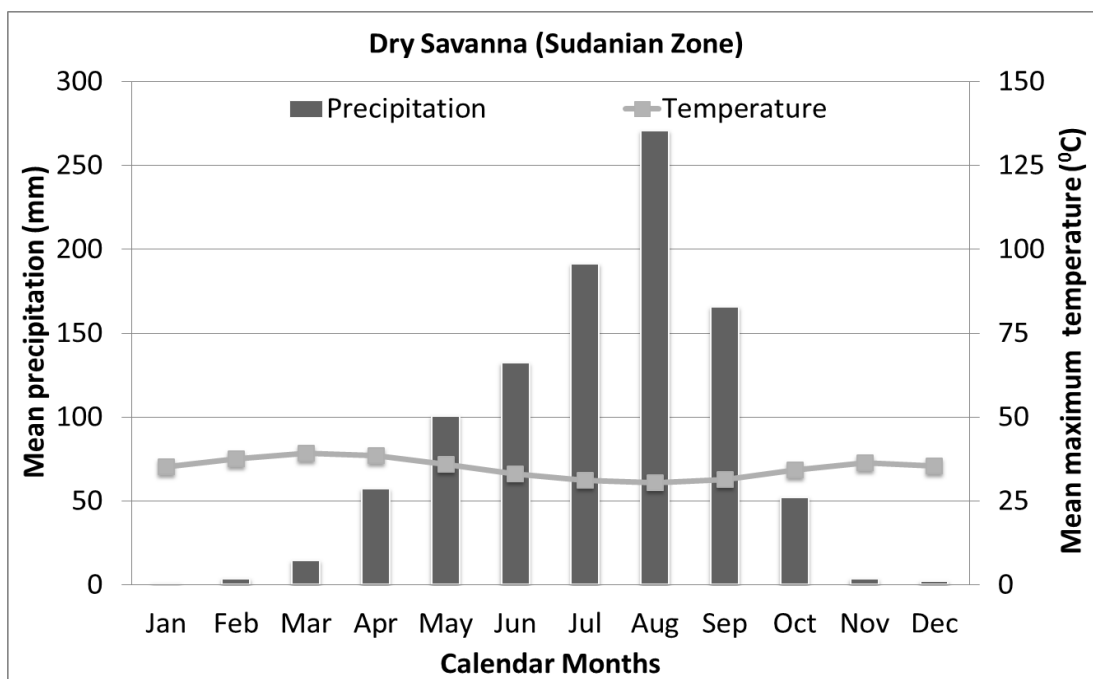


Figure 5: Study sites in two main ecological zones of the Volta basin in Ghana (West Africa)

(Source: de Condappa & Lemoalle, 2009).

Table 1: Description of Afram and Tankwidi river catchments

Item	Afram river catchment	Tankwidi river catchment
Climate	Guinean (Humid savanna)	Sudanian (Dry savanna)
Precipitation (mm)	1100	900
Mean maximum temperature (°C)	32	36
Soil type	Luvisol	Luvisol
Human activities	Farming, Fishing	Farming, Fishing
Area of Reserves hectares (ha)		
<i>Kogyae Strict Nature Reserve</i>	39,000	
<i>Tankwidi Forest Reserve</i>		19,221
Area of river catchment (ha)		
<i>Afram</i>	100,000	-
<i>Tankwidi</i>	-	27500



Jan      Feb      Mar      Apr      May      Jun      Jul      Aug      Sept      Oct      Nov      Dec  
 January   February   March   April   May   June   July   August   September   October   November   December

Figure 6: Temperature and precipitation patterns of the dry and humid savannas from averaged per month from 1961 to 2012

(Source: **Ghana Meteorological Service, 2014**)

### 2.1.2 Climate

The climate of Afram and Tankwidi riparian catchments within the Volta basin are controlled by two air masses: the North-East Trade Winds and the South-West Monsoons. The North-East Trade Winds, known as the Harmattan, blow from the interior of the continent and are dry and dusty. In contrast, the South-West Monsoons, blow from over the seas and are moist. The inter-phase of these two air masses is called the Inter-tropical Convergence Zone (ITCZ). There is a lot of convective activity in the region of the ITCZ; hence the region is associated with a considerable amount of rainfall. The ITCZ moves northwards and southwards across the basin from about March to October when rainfall is received in the region (**UNEP-GEF, 2012**). In the south, rainfall follows a pseudo-bimodal regime with a humid period during May–October and reduced rainfall in July and August. In the north, we find a mono-modal rainfall regime with rainfall from May/June through September (**UNEP-GEF, 2012**).

The mean annual temperature ranges from 27°C in the south to 36°C in the north. In March, the hottest month of the year, mean daily temperatures in the southern parts may rise from a mean of 24°C to 30°C. The daily temperature range in this area is about 3-5°C. There are vast variations in mean daily humidity; varying between 6% and 83% depending on the season and the location (**UNEP-GEF, 2012**). The potential evapotranspiration of the study areas ranges between 1600 mm to 2100 mm per annum (Figure 7). The values are high during the dry seasons and attenuated during rainy season. It is estimated that nearly 80 % of the rainfall is lost to evapotranspiration during the rainy season (**Volta Basin Authority, 2000**).

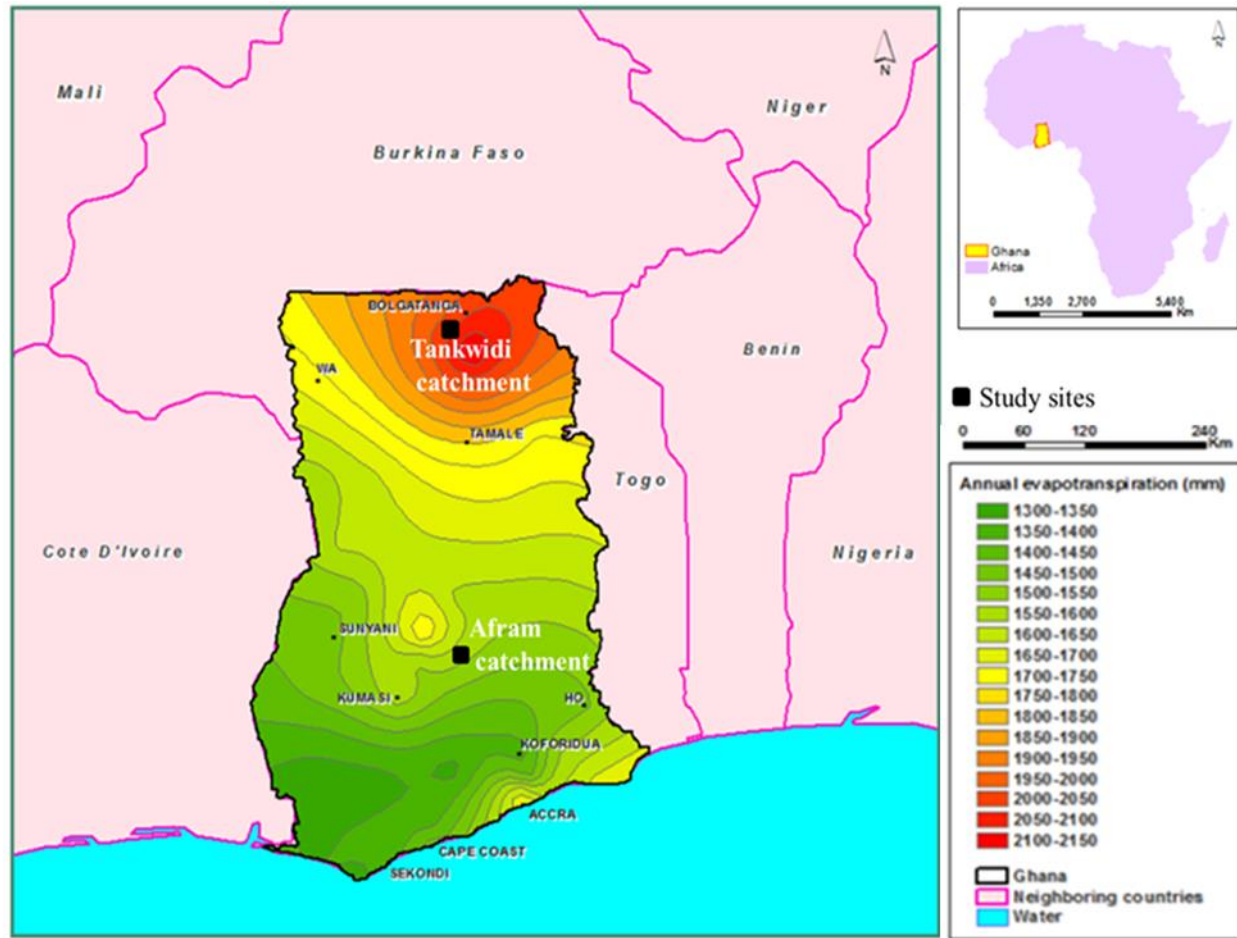


Figure 7: Potential evapotranspiration rates per annum in Ghana indicating the study sites

(source: **Volta Basin Authority, 2000**)

### **2.1.3 Hydrology, surface waters and relief**

The Volta basin is drained by 4 main river systems (Figure 8): the Sourou and Mouhoun in Burkina Faso which become Black Volta in Ghana; the Nakambe in Burkina Faso which becomes the White Volta in Ghana; the Pendjari in Benin which becomes the Oti in Togo and Ghana, and; the Lower Volta system in Ghana. The Black Volta is a perennial river. It flows from Mali flows into Burkina Faso and joins the Mouhoun, which flows downstream to Ghana as the Black Volta. White Volta river flows from Burkina Faso. The Pendjari or Oti River begins from Benin and flows through Togo to Ghana. The Lower Volta is fed by three major tributaries. To the West, the Black Volta drains western Burkina Faso and small areas within Mali and Cote d'Ivoire; the White Volta drains much of northern and central Ghana and Burkina Faso and to the east, the Oti drains the north western regions of Benin and Togo. Waters from all 4 river systems flow into the Volta Lake in Ghana, which was created by the construction of the Akosombo Dam in 1964. The Tankwidi river of this study is located in the Red and White Voltas. The Afram river is found in the lower Volta (**Callo-Concha *et al.*, 2012; UNEP-GEF, 2012**).

The Volta basin, where Afram and Tankwidi catchments are found is described as lowland basin with maximum elevation ranging from 120-150m (Figure 9). All tributaries of the river Volta (such as Afram, Tankwidi, Pru, Black and White Volta) flow directly towards the Atlantic sea. Most of the well-developed alluvial flood plains and terraces of the river Volta are under the man-made Volta lake established in 1963 (**Salifu & Agyare, 2012; Callo-Concha *et al.*, 2012**).

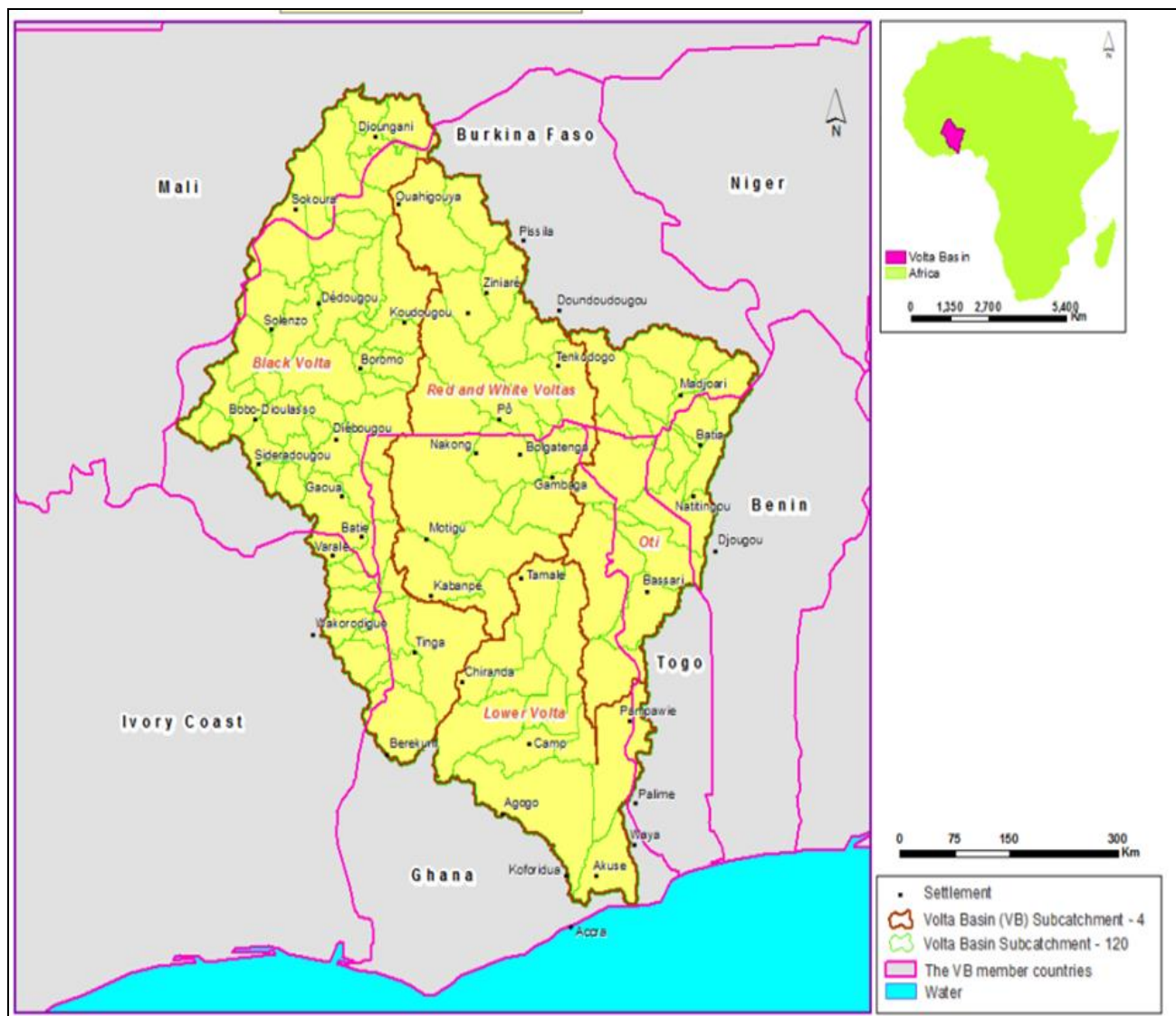


Figure 8: Volta Riparian Basin sub-catchments

(source: **Volta Basin Authority, 2000**)

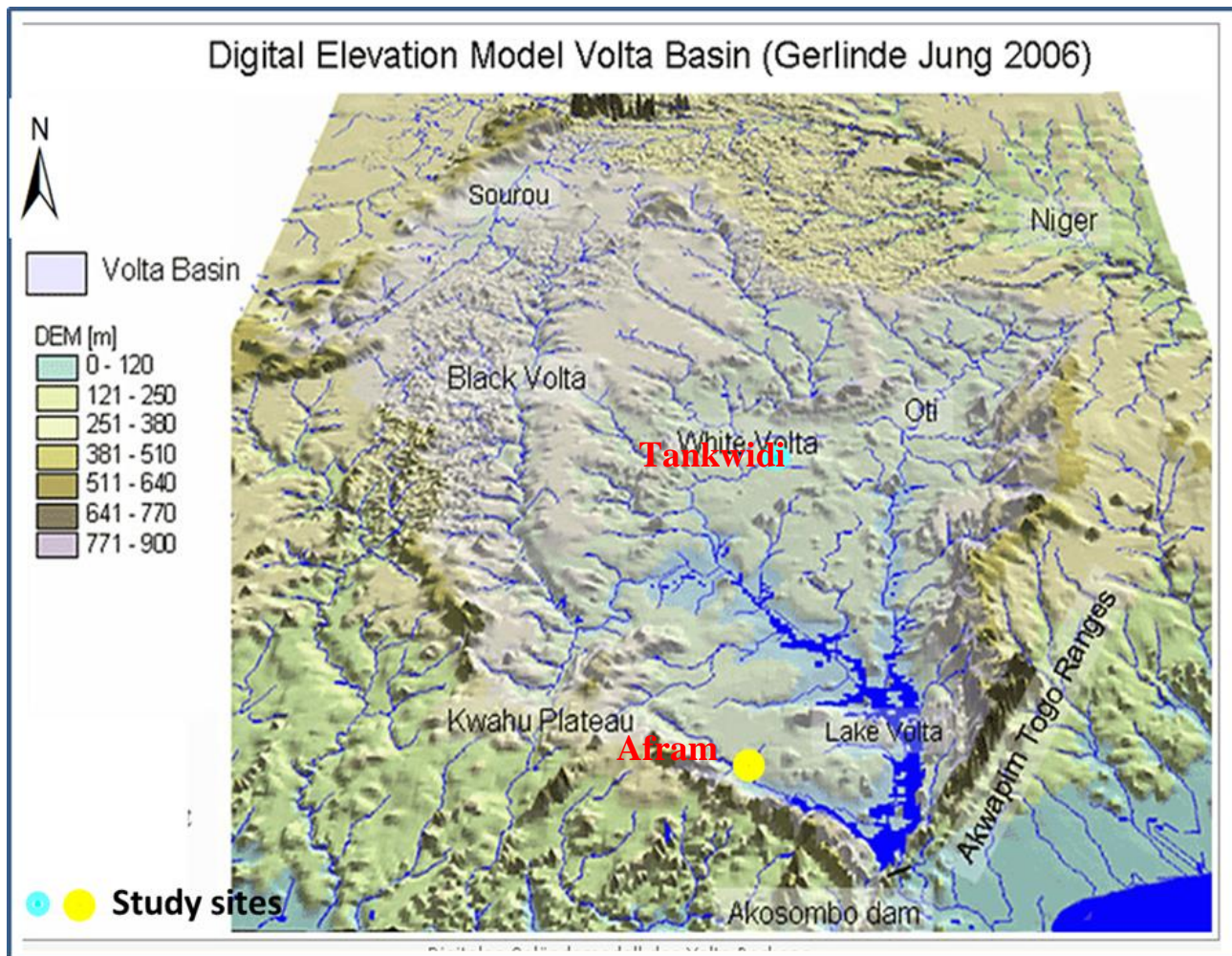


Figure 9: Relief of the Volta basin

(Source: **Volta Basin Authority, 2000**)

#### 2.1.4 Soil

Soils in the savanna of the Afram and Tankwidi catchment developed on acidic metamorphic rocks have low activity kaolinitic clay, coarse textured topsoils, low water holding capacities and, depending on the cultivation history, low levels of organic matter, a low supply of nitrogen (N) and phosphorus (P) and sometimes phosphate (K), sulfur (S) and zinc (Zn). In addition, they are very susceptible to erosion and compaction. Soil texture in the top layer is mainly sandy (>80% sand), which is due to the loss of dispersible clay through erosion or leaching to the subsoil. A number of soils with high clay content occur either in valley bottoms or in alluvial plains or in deeper horizons; the change in texture from the top to the subsoil provokes waterlogging (especially after heavy rains), surface run-off and restriction of the root growth (**Callo-Concha *et al.*, 2012; UNEP-GEF, 2012**).

#### 2.1.5 Geology

The geology of the Afram and Tankwidi riparian catchment within the Volta basin is dominated by the Voltaian system (**Callo-Concha *et al.*, 2012**). Other geological formations include the Buem formation, Togo series, Dahomeyan formation, and Tertiary-to-Recent formations. The Voltaian system consists of Precambrian to Paleozoic sandstones, shales and conglomerates (**UNEP-GEF, 2012**).

The Buem series lies between the Togo series in the east and the Voltaian system in the west. The Buem series comprises calcareous, argillaceous, sandy and ferruginous shales, sandstones, arkose, greywacke and agglomerates, tuffs, and jaspers. The Togo series lies to the eastern and southern part of the main Volta and consists of alternating arenaceous and argillaceous sediment. The Dahomeyan system occurs at the southern part of the main Volta basin and consists of mainly metamorphic rocks, including hornblende and biotite, gneisses, migmatites, granulites, and schist (**UNEP-GEF, 2012**).

The Oti basin is underlain mainly by the Voltaian system, the Buem formation and the Togo series. The White Volta basin is composed of the Birimian system and its associated granitic intrusives and isolated patches of Tarkwaian formation. The other significant formation is the Voltaian system. The Birimian system consists of metamorphosed lavas, pyroclastic rocks, phyllites, schists, tuffs, and greywackes. The Black Volta basin consists of granite, the Birimian and Voltaian systems, and, to a minor extent, the Tarkwaian system. The Tarkwaian formation consists of quartzites, phyllites, grits, conglomerates, and schists (**UNEP-GEF, 2012**).

### 2.1.6 Vegetation and land use

The Volta basin is divided into 3 main agro-ecological zones: the Sudan-Sahel savanna, the Sudan savanna and Guinea savanna. The Sudan-Sahel savanna is predominantly desertification-prone. The Sudan Savannas are found in the northern parts of the basin. The Guinea savanna consists of a mosaic of forests and savanna woodland. Vegetation cover includes grasslands, shrublands and tree savannas, semi-deciduous forest and mangroves along the coast (UNEP-GEF, 2012). There are also azonal ecosystems such as riparian forests, mangroves, lakes and lagoons as well as protected areas and forest plantations.

The principal land use and livelihood is agriculture for subsistence and commercial purpose (Agyare, 2004). Various food crops cultivated include: *Manihot esculenta*, *Mangifera indica*, *Anacardium occidentale* and *Dioscorea spp.* *Sorghum bicolor*, *Zea mays* and *Oryza spp.* (Salifu & Agyare, 2012).

### 2.1.7 Demographic trends

The major population areas in the Volta Basin include Ouagadougou in Burkina Faso; Tamale in Ghana; Bolgatanga in Ghana in the White Volta sub-basin; and Bobo Dioulasso in Burkina Faso in the Black Volta sub-basin. Others are the Kara region of Togo in the Oti River sub-basin and in the lower reaches of Lake Volta and the Lower Volta in southern Ghana. According to demographic statistics, the population of the basin was 18.6 million in 2000 and is forecasted to reach 33.9 million in 2025 (Table 2). At current rates, the basin's population will have doubled in the thirty-year period between 1990 and 2020. If this trend continues, the basin's population will reach 45 million by 2050. In Atacora and Donga provinces in Benin, the population is estimated to have grown from 755,000 in 1997 to more than 1 million in 2007, an average annual growth rate of slightly more than 3 per cent. The Volta Basin population in Burkina Faso grew from more than 8.1 million to more than 10.9 million between 1996 and of 2006, an annual increase of 3 per cent. The population of Burkina Faso's Nakambé region alone will account for approximately 61 per cent of the total population of the basin by 2025, a rise of 2 per cent from 2010 (UNEP-GEF Volta, 2013)..

Ghana's national population was estimated at nearly 25 million for the year 2010, and is projected to surpass 30 million by 2025. About 37 per cent of the country's inhabitants live within the Volta Basin. In Mali, the Volta Basin covers Bankass, Koro and Douentza, with a population estimated at almost 620,000 in 1998, growing to more than 873,000 in 2009, and projected to reach nearly 1.4 million by

2025. The population of the Volta Basin in Togo was estimated at nearly 1.6 million in 2000, growing to more than 2.1 million inhabitants in 2010 and expected to rise to 2.9 million in 2020 and almost 3.9 million by 2030. The demographic trends have environmental impacts: water pollution (agricultural, domestic and industrial), rapid mining of non-renewable resources, deforestation, land degradation, sedimentation of riverbeds, invasion of non-indigenous species, and loss of habitats (UNEP-GEF, 2013).

The demography of the Volta Basin has several notable characteristics that are pertinent to the integrity of its natural resources:

- Rapid population growth suggests that there will be increasing pressure on natural resources, notably water. This population growth will also impact on existing infrastructure and will have social and political consequences.
- The largely rural nature of the population implies a higher direct dependence on the natural resources base. Between 64 and 88 per cent of the population of the Volta Basin is rural and depends directly on natural resources.
- Despite the high population growth, population density remains relatively low.
- People continue to move to urban areas, mostly in search of work. Population growth in urban areas will be even greater than in rural areas, leading to high concentrations of demand for water and natural resources, and to major sources of point pollution.

In terms of density, the Volta Basin remains relatively sparsely populated compared to most of the land in the basin countries. The population density was estimated at 72 per km<sup>2</sup> in the basin in 2010, though it is expected to rise to 83 per km<sup>2</sup> by 2015, and to more than 100 inhabitants per km<sup>2</sup> by 2025 if current trends continue (UNEP-GEF, 2013).

Some areas of the basin are also experiencing depopulation. In Ghana, for example, the decline of upstream fishing due to the creation of Lake Volta led to the movement of people to settle in the immediate vicinity of the lake. In Togo, some people, particularly in Savanna and Kara regions, who had previously migrated south in 1990, had to retrace their steps in response to socio-political conflicts. There is also significant migration (and emigration) in Mali, with migrants aiming to find new land in the forest of Samori. Migration also took place during the drought of 1984–1985, with the dispersion

of part of the basin population to Seno, a sub-basin of the Volta River in Mali, which led to the depletion of fallow land and, in turn, led to the continued loss of soil (UNEP-GEF, 2013).

All over the basin, dissatisfaction with livelihoods motivates people to migrate, both internally and outside the country. People go in search of employment, food, schooling or agricultural land and can be motivated by climatic or edaphic conditions. The population group most affected consists of men and women between the ages of 15 and 59. In Benin, this population group represents 88 per cent of migrants, and, specifically, 96 per cent of migrants in the regions of Atacora and Donga. In Burkina Faso, the source country for much international migration, waves of departures have been recorded, with the most able-bodied generally being the most likely to leave the country. The pattern of migration is clear: young men aged 15 to 29 are the first demographic group to leave, followed by adults aged 30 to 44 years, and then women aged 15 to 24 years. In 2006 alone, over 60,000 people left Burkina Faso (UNEP-GEF, 2013).

A growing phenomenon is migration from rural to urban areas, for example, amongst the Lobi people of Côte d'Ivoire. This form of migration is not new within the Volta Basin but it has increased in recent years and is projected to grow in the future. Part of this migration is due to agricultural and livestock conflicts. As previously discussed, a large number of people from the Volta Basin region have emigrated to other countries and regions. Many are now in other African countries, in Europe or North America, either studying or seeking employment. In many cases, these temporary emigrants send a part of their earnings back to their family – providing an input into the local economy that can be used to invest or to purchase essential goods. This certainly has an indirect impact on the utilization and management of natural resources, including water, in the basin (UNEP-GEF, 2013).

Table 2: Population data (2008) for countries in the Volta Basin and projections for 2025

National population		Year 2008				Year 2025
		Basin population				
Total  (thousands)  (thousands)		Total (thousands)	Basin as a percentage of country	Rural (thousands)	Rural as a percentage of total basin	Projection  Total (thousands)
Benin	8290	590	7.12	378	64	820
Burkina Faso	15850	11227	70.8	7186	77	15997
Côte d’Ivoire	18400	497	2.70	318	77	718
Ghana	23383	8570	36.6	5484	84	11696
Mali	14517	880	6.06	563	88	1260
Togo	5870	2154	36.7	1378	70	3385
Total	86310	23918	27.7	15307	-	33876

Source: UNEP-GEF Volta Project (2013).

## **2.2 Methods**

### **2.2.1 Assessment of forest cover dynamics in the Afram and Tankwidi riparian catchments between 1986 to 2014**

- **Selection of images**

Satellite data inputs for multi-temporal studies of forest cover (1986, 2000 and 2014) for both Afram and Tankwidi riparian catchments were obtained from the Landsat Thematic Mapper (TM), Landsat Enhanced Thematic Mapper Plus (ETM+), and Landsat Operational Land Imager (OLI). The images (Table 3) were freely available and downloaded from the United States Geological Survey National Center for Earth Resources Observation and Science. Images with no cloud cover were downloaded. All the dates of the selected images were within the dry season when the grassy layers have been scorched thereby increasing the detectability of forests vegetation.

Preprocessing of satellite images were done at the University of Wurzburg, Germany. The Landsat images were geo-referenced to UTM projection WGS 84 and co-registered with each other using GPS-collected (Global Positioning System) ground control points, achieving inter-scene compatibility of less than one pixel. Radiometric calibration and solar atmospheric correction were performed on all images to derive surface reflectance pixel values in each band.

Table 3: Attributes of the Landsat TM, ETM+ and OLI imagery used in the study

Acquisition	Sensor	Spatial resolution (m)	Path/row
Afram riparian catchment			
9/02/1986	TM	30	194/55
14/03/2000	ETM+	30	194/55
8/01/2014	OLI	30	194/55
Tankwidi riparian catchment			
11/01/1986	TM	30	194/53
26/01/2000	ETM+	30	194/53
24/01/2014	OLI	30	194/53

- **Collection of ground control points**

During the fieldwork from September-December, 2013, ground control points and forest canopy density data were collected using GPS and spherical densiometer respectively. The data from this fieldwork was used to classify the 2014 Landsat images into “forest” and “non-forest” areas (Figure 10). Further, ground control points (GCP) for the classification of the 2000 Landsat image was also collected on the field with the aid of historic Landcover map prepared for the study area under the GLOWA-Volta (**Volta Basin Authority, 2000**). This was done by first identifying the features on the Landcover map prepared in 2000 and which could still be verified during fieldwork. This entailed identifying stable landcover in the protected area, along the Afram and Tankwidi rivers, farms and settlements, which had been in existence since 2000 (Figure 10). Similar exercise was conducted for the 1986 maps of both catchments but in this case no satellite derived Landcover map was available for reference. A total of 160 and 132 GCPs were collected for the Afram and Tankwidi riparian catchments respectively.



a) Forest/woodland (**FOREST**)



b) Riparian forest (**FOREST**)



c) Grassland (**NON-FOREST**)



d) Settlement (**NON-FOREST**)



e) Farmland (**NON-FOREST**)

Figure 10: Landcover types in the Afram and Tankwidi riparian catchments

- **Landcover classification (1986, 2000 and 2014)**

Supervised classification procedures using ERDAS Imagine 2011 software were implemented to classify the Landsat images of 2000 and 2014 using Maximum Likelihood Classification algorithm. Supervised classification was used because of the availability of ground control points to train the computer for classification. Areas with tree canopy of 20% and greater were located on the image and signature were selected and used as training set for classifying “forest areas”. Areas with less than 20% of canopy were classified as “non-forests”. This procedure was undertaken with reference to **Potapov *et al.* (2009)**. In the case of the 1986 image, “forest” was selected from stable vegetation along rivers. Qualitative assessments of the classified images were further done by examining the classified images visually and relating it to the knowledge obtained from the interview of local people. This ensured that the classified map output reflected reality. Forest reserve boundary layout of the two study sites were obtained from the geodatabase of the Forestry Commission of Ghana. Analysis of forest cover in terms of area (ha) for 1986, 2000 and 2014 were carried out in ArcGIS 10.1.

The annual rate of deforestation was computed by following the formula suggested by Puyravaud (2003):

$$r = (1 / (t_2 - t_1)) \times \ln(A_2 / A_1)$$

where:

r=rate of deforestation. Rate is presented in percentage ( $r \times 100$ )

t<sub>2</sub> and t<sub>1</sub> = time

A<sub>2</sub> and A<sub>1</sub>=forest cover at time t<sub>2</sub> and t<sub>1</sub>

- **Accuracy assessment of landcover classification**

Fifty percent (50%) of the collected ground control points (test data set) were used for the accuracy assessment of the Landsat map of 2000 and 2014. The classified images were crossed with the test data to generate confusion matrix. The confusion matrix calculates different accuracy measures i.e., producer's, user's, and overall map accuracies. Producer's accuracy estimates the probability of a reference sample to be correctly classified for each class of the map. User's accuracy evaluates the probability of a sample from a classified data belonging to the same category actually on the ground. Overall accuracy is used in illustrating the probability of correct classifications for randomly selected points on the map. Kappa statistics were also calculated as additional information for evaluating the accuracies of the maps. Kappa statistic determines the extent at which the map classification result

surpasses random assignment of pixels (**Lillesan *et al.*, 2004; Chai *et al.*, 2009**). It was not possible to carry out accuracy assessment for the 1986 map because of the lack of a satellite derived historical reference map. It is however, assumed that the accuracy assessments for the Landcover maps of 2000 and 2014 are sufficient to shed light on the overall classification procedures adopted for this study.

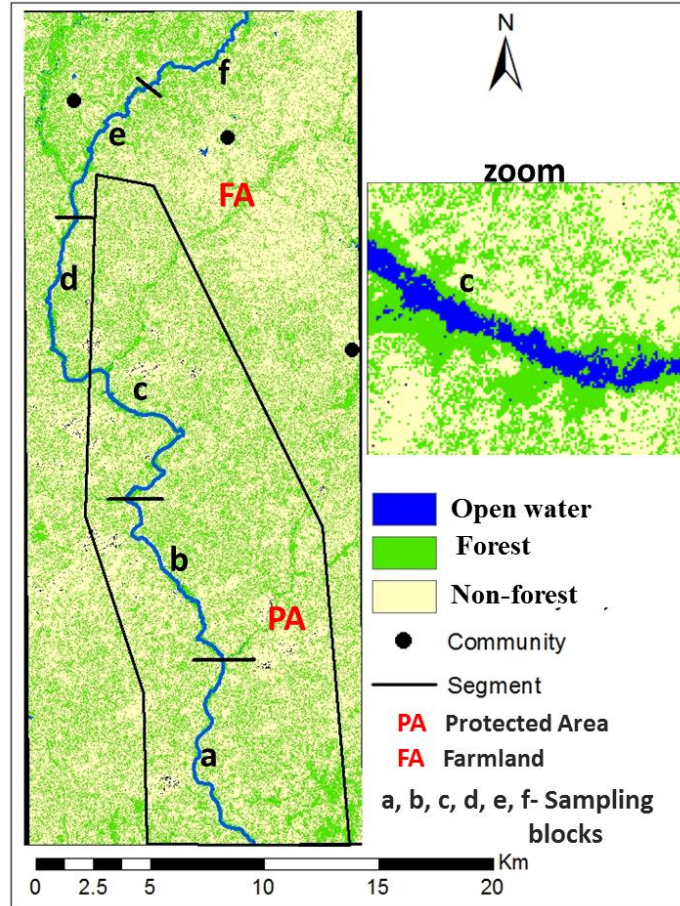
### **2.2.2 Assessment of woody plant diversity and structure and soil properties of riparian forests between protected area and farmland in the humid and dry savanna zones**

- **Design**

The study used high resolution satellite image (ALOS AVNIR) for mapping riparian forests to support the field sampling (Figure 11). This is because riparian forests are often too small to be detected using traditional satellite remote sensing data such as Landsat (at 30m resolution) or any broad scale GIS data (**Johansen *et al.*, 2010**). The ALOS AVNIR image comprises 4 bands from visible to the near infra-red range (0.42-0.89 $\mu$ m) and has spatial resolution of 10m. It is managed by Japanese Aerospace Exploration Agency (**Bagan *et al.*, 2012**). The ALOS AVNIR images were obtained from the Remote Sensing Unit of the Forestry Commission of Ghana. The date of the space acquisition of the two satellite images was 27 February, 2011. Maximum likelihood classification algorithm was used for mapping “forest” along the Afram and Tankwidi rivers.

The map classification accuracies for the Afram and Tankwidi rivers were 89 and 84% respectively (Table 4 A and B). The two maps facilitated the inventory of the riparian woody plants with stratified randomized design in farmland (FA) and protected reserve (PA) along both Afram and Tankwidi rivers. The maps were also used for selecting the positions of random plots along the riverine area. Whether in PA or FA, the river course was divided into 3 segments, at a buffer zone of 50m on each side of the river. The buffer zone (50m) was chosen as it is a prescribed width for temporary rivers enshrined in the Ghana Riparian Buffer Zone Policy for managing freshwater bodies (**Government of Ghana, 2011**). The length of each segment along the Afram and Tankwidi rivers were approximately 7 and 8 km respectively.

### Tankwidi catchment (Dry Savanna)



### Afram catchment (Humid Savanna)

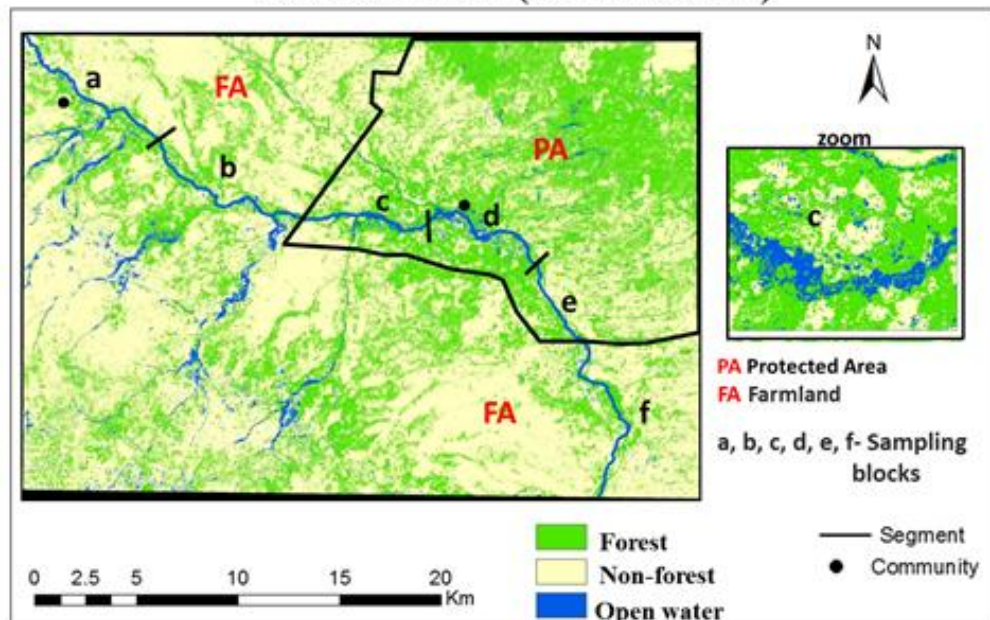


Figure 11: Sampling sites in the Afram and Tankwidi riparian catchments

Table 4: Confusion matrix of Landcover map of Afram and Tankwidi riparian catchments using ALOS AVNIR imagery (2011)

A. Afram riparian catchment

Landcover	Reference data				Accuracy total			
	Forest	Non-forests	Open water	Classified total	Number correct	Producers Accuracy %	User Accuracy %	Kappa
Forest	30	4	0	34	30	90.9	88.2	0.78
Non-forest	3	32	0	35	32	86.5	91.4	0.82
Open water	0	1	2	3	2	100	66.7	0.66
Total	33	37		72	64			
Overall Accuracy = 89%								
Overall Kappa = 0.79								

B. Tankwidi riparian catchment

Landcover	Reference data				Accuracy total			
	Forest	Non-forests	Open water	Classified total	Number correct	Producers Accuracy %	User Accuracy %	Kappa
Forest	25	3	1	29	25	83.3	86.2	0.73
Non-forest	4	21	1	26	21	87.5	80.8	0.69
Open water	1	0	6	7	6	75	85.7	0.84
Total	30	24	8	62	52			
Overall Accuracy = 84%								
Overall Kappa = 0.73								

- **Woody vegetation assessment**

The woody vegetation data was collected using stratified randomised design with river segments as stratum (Figure 11 & 12). The minimum disturbance between random samples as generated using ArcGIS 10.1 was 100 m along the river. In the overall, the inventory of woody plants with diameter at breast height (DBH)  $\geq 5\text{cm}$  was conducted in sixty random rectangular plots ( $500\text{m}^2$  per plot), 30 each in protected area (PA) and farmland (FA) and 10 plots per segment within a buffer zone of 50m. This was done for both Afram (humid savanna zone) and Tankwidi (dry savanna zone) rivers making up a total of 120 established plots. The woody species were identified with the aid of a forest botanist from the Forest Research Institute of Ghana following the identification key by **Irvine (1961)**, **Hawthorne (1990)** and **Hawthorne & Jongkind (2006)** and further confirmed online using the University of Oxford virtual field herbarium. The relatively higher number of random plots (120) used in this woody vegetation inventory was to increase the chances of locating all riparian trees species in order to facilitate selection of individuals of targeted species for dendrochronological studies.

Tree calliper was used to measure the DBH of the species. Ground slope and tree height was measured with Vertex IV and Transponder III, Haglof Sweden. Canopy cover was measured using spherical densiometer. Specimens of the species recorded were taken to the herbarium of the Forestry Research Institute of Ghana for confirmation of identification.

The publications of **Keay & Hepper (1954-1972)**, **White (1983)** and **Aké Assi (2001 & 2002)** was used to determine the chorotype (*i.e.* range of distribution type) of each species. The five main chorotypes used are as follows: GC Guineo-Congolian species, S Sudanian species, SZ Sudano-Zambesian species, GC-S Guineo-Congolian/Sudanian transition species (linking elements between the Guineo-Congolian and Sudanian regions) and Wd species with wide distribution such as Cosmopolitan, Pantropical and Paleotropical.

Shannon-Wiener (SWI) (**Shannon, 1948**) index was calculated as measures of woody species diversity within riparian plant community of a particular land use (protected area or farmlands) and compared with literature to understand the level of diversity. The index is commonly used for forest and savanna diversity assessment in Ghana and West Africa in general (**Traoré *et al.*, 2012**; **Tom-Dery *et al.*, 2013**). They were adopted in the study to facilitate comparison of the findings. Species richness (SR) used in this study refers to the number of different species recorded in a plot.

Shannon-Wiener index (SWI) =  $-\sum p_i \ln p_i$  where  $p_i = n_i/N$  with  $n_i$  = number of individuals of species  $i$  and  $N$  = total number of individuals in a plot.

Jaccard Index (JI) was used to examine  $\beta$ -diversity in the case of similarity (**Jaccard, 1908**) of riparian forests between protected area and farmlands for both the humid and dry savanna zones. The index measures the degree of similarity between the two localities using the number of species ( $c$ ) shared by the two localities, the number of species present in locality A ( $a$ ), and the number of species present in the locality B ( $b$ ), as described below:

$$JI = 100 \times c / (a+b+c)$$

The JI values range between 0 and 100, the maximal value expressing a complete similarity.

Again, for each land use management regime (PA or FA), the following structural parameters were calculated:

1. Woody species density (N); the average of the number of individual trees per plot expressed as trees/ha.
2. Basal area; the average cross-sectional area of woody species per plot (expressed in m<sup>2</sup>/ha) was calculated from the DBH below (**Van Laar & Akça, 2007**):

$$\text{Basal area} = \sum (\text{DBH}^2 \pi 4^{-1}) \text{ where } \pi = 3.14$$

To establish the size-class distributions, diameters of all species were used to construct histogram with size classes of 5 cm interval. This was similarly done for the heights of species at 5m interval classes.

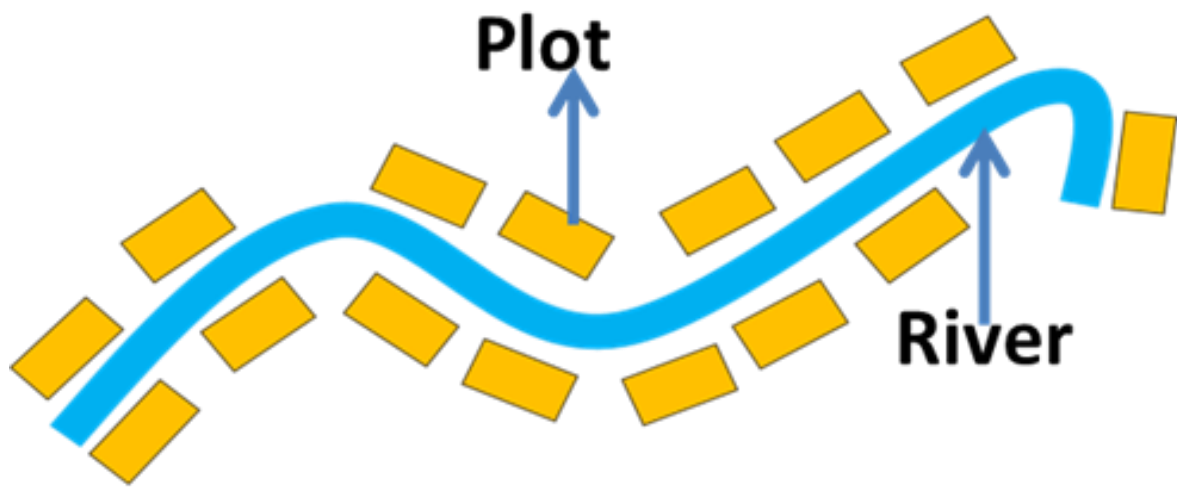


Figure 12: Plot layout for vegetation survey

- **Soil assessment**

Soil samples were collected in 60% of the stratified random plots (120) used for vegetation inventory in both protected area (PA) and farmland (FA) (total 36 plots with 18 plots each in PA and FA). This was done for both the humid and dry savanna zones (72 plots in total). For each rectangular plot (500m<sup>2</sup> per plot), five soil samples were collected at four points including one at the center at the following depth layers, 0 – 20 cm (top soil) and 20 – 40 cm (bottom soil). The five samples were thoroughly mixed and sub-samples taken in duplicate for Laboratory analysis. Further, cylindrical core sampler was used for collecting soils for bulk density determination at 0–20 cm and 20–40 cm depth in each plot at an undisturbed surface.

The soil samples were analyzed at the Laboratory of the Faculty of Renewable Natural Resources of the Kwame Nkrumah University of Science and Technology (KNUST, Ghana). The soil samples were air-dried, hand-milled with a roller and homogenized to pass through a 2mm sieve. The following basic soil chemical and physical properties were measured: Nitrogen (N), Phosphorus (P), Potassium (K), Organic Carbon (C), pH, texture, bulk density and moisture content. The procedures followed for each are narrated below:

1. *Total Nitrogen (N)*: Samples were analysed for total N using Kjeldahl method (**Bradstreet, 1965**) by wet-digesting 0.5 g samples in 5.0 ml concentrated H<sub>2</sub>SO<sub>4</sub> using a catalyst mixture (K<sub>2</sub>SO<sub>4</sub> and selenium powder) and distillation with colorimetric determination by spectrophotometer.
2. *Available Phosphorus (P)*: Available P was extracted with an HCl: NH<sub>4</sub> mixture using the method of **Bray & Kurtz (1945)**. Phosphorus in the extract was subsequently determined on a spectronic 21D spectrophotometer by blue ammonium molybdate method with ascorbic acid as reducing agent.
3. *Exchangeable Potassium (K)*: Exchangeable bases were extracted with 1.0 M NH<sub>4</sub>OAc (pH 7.0), exchangeable K in the extract was determined by flame photometry.
4. *Soil organic carbon (C)*: Soil organic carbon was determined using the **Walkley & Black (1934)** wet oxidation method. The procedure involves wet combustion of the organic matter with a mixture of acidified potassium dichromate and titrating excess dichromate after reaction against ferrous sulphate using diphenylamine as indicator.
5. *pH*: Soil pH was determined potentiometrically in 0.01M CaCl<sub>2</sub> solution using a soil to solution ratio of 1:2 (McLean, 1982).

6. *Texture or particle size distribution*: Soil particle size distribution was determined using hydrometer method after dispersing soil with sodium hexametaphosphate solution (**Bouyoucos, 1962**). The USDA particle size classes, namely, sand (2.0-0.05mm), silt (0.05-0.002mm) and clay (<0.002mm), were used to classify the textural classes.
7. *Soil bulk density* was determined on all the recording plots from soil samples taken at the top (0-20cm) and bottom (20-40cm). Prior to the oven drying of the soil at a temperature of 105°C to a constant weight, the initial weight of the soil was recorded. After drying, the weight was re-taken again. The following formula was used for the bulk density determination:

$$\text{Soil bulk density (g/cm}^3\text{)} = \frac{\text{Oven dried weight}}{\text{volume of soil}}$$

8. *Moisture content* was expressed by weight, as the ratio of the mass of water present to the dry weight of the soil sample (Black, 1965).

- **Statistical analysis**

Shapiro-Wilk's test for normality and Levene's test for equality of variances were used to test the normality and the homoscedasticity assumptions respectively in SPSS Statistics 17. Those data not normally distributed were subjected to transformation to meet the normality and homoscedasticity assumptions. This was done to support the use of parametric tests in this study.

Student's t-test was used to estimate the significance of the differences of the soil parameters between the protected area and farmland for both the humid and dry savanna zones.

Further, two-way ANOVA and Bonferoni post-hoc test were conducted in GraphPad Prism 5 to assess: (1) if the savanna type have effect on the soil properties; (2) if the land use types have effect on the soil properties; and (3) if the interaction between savanna type and land use have effect on soil properties.

Linear regression analyses were conducted to clarify the relationship between plant density and soil variables (C, N, P, K, C/N ratio, pH, slope and soil moisture content, Sand, Clay and Silt). All results were considered significant at  $P \leq 0.05$ .

### 2.2.3 Assessment of the growth of riparian wood species in the humid and dry savanna zones

- **Sample collection**

Since no previous dendrochronological studies have been carried out anywhere in the humid and dry savanna zones of Ghana, it was necessary first, to identify the riparian woody species that produce discernible rings. Therefore, during the intensive fieldwork for inventorying riparian woody species in 2013, a Haglof increment borer of diameter, 5 mm was used to extract sample cores of the woody species in both the Afram (humid savanna) and Tankwidi (dry savanna) riparian forests for visual inspection. The targeted species common to both riparian forests in the humid and dry savanna zones were *Afzelia africana* Smith ex Pers., *Anogeissus leiocarpus* (DC.) Guill. & Perr., *Azadirachta indica* A. Juss., *Daniellia oliveri* (Rolfe) Hutch. & Dalz, *Diospyros mespiliformis* Hochst. ex A. DC., *Khaya senegalensis* A. Juss., *Mitragyna inermis* (Willd.) O. Kuntze, and *Vitex doniana* Sweet.

After scanning through the sample cores of the different riparian trees, two species having highly visible growth rings, relatively dominant and belonging to different functional groups were selected. The species were *Afzelia africana* (Fabaceae) and *Anogeissus leiocarpus* (Combretaceae). According to the classification of **Sarmiento & Monasterio (1983)** and **Seghieri et al. (2012)**, *Anogeissus leiocarpus* is considered as short-deciduous species with a short leafless period. *Afzelia africana* is semi-evergreen species, shedding its leaves during a period not more than two months. Both *Afzelia africana* and *Anogeissus leiocarpus* have socio-economic importance and used for furniture, firewood and charcoal. The foliage of *Afzelia africana* is used as source of fodder for livestock whereas the seeds of *Anogeissus leiocarpus* is used in traditional medicine (**Andary et al., 2005; Gérard & Louppe, 2011**).

For thorough study, a total of 31 stem discs of *Afzelia africana* and *Anogeissus leiocarpus* within the diameter class of 25 – 40 cm were collected along the Afram (humid savanna) and Tankwidi (dry savanna) rivers. Stem discs were collected as no studies have ever been conducted in Ghana and therefore, there was the need to be certain about the annual nature of the rings. In order to minimize edge effects, samples were collected at a minimum distance of 10m from the river but within a 50m riparian buffer zone. For each disc collected, the following information was recorded: (1) species name (2) location (3) date collected (4) species and site characteristics.

- **Sample preparation**

Standard dendrochronological methods were used to prepare the stem discs for measurement at the tree ring laboratory of Friedrich-Alexander University of Erlangen-Nurnberg, Germany. After air-drying the discs, they were polished mechanically and with sandpaper of progressively finer grit up to a grain of 1000. Wood dust was removed from the vessels with compressed air to improve visibility of the growth zone boundaries. In some cases, the surfaces of the wood samples were moistened to increase the contrast between different wood tissues and the distinctiveness of growth zones.

- **Growth ring measurements**

Prior to growth ring measurements, thin sections of 10 to 20- $\mu$ m thicknesses were cut from samples each of *A. africana* and *A. leiocarpus* (both humid and dry savanna) with a microtome to take microscopic pictures and to determine their rings boundaries. The sections were stained with solutions of safranin and astra blue, and dehydrated by washing with increasing concentrations of ethanol, following standards procedures (**Gärtner & Schweingruber, 2013**). The micro-sections were subsequently used to describe the wood anatomical features by following the classification in **Schweingruber et al. (2006)**.

During measurements (31 discs), each ring was marked on a sample disc on 2-4 radii and every tenth ring was interconnected between the different radii. This procedure helped to detect wedging rings, discontinuous growth zones as well as verifying the existence of each ring round a disc. When all the rings on a disc were detected and ring numbers and characteristics matched along different radii, ring width was measured along 2-4 radii of each stem discs. All ring widths were measured to the nearest 0.01mm along the pre-determined radii along a straight line and perpendicular to ring boundaries using a semi-automated device (LINTAB, Rinn tech, Heidelberg Germany). LINTAB consists of a stereoscope and a moveable board linked to a distance measuring device and a computer (**Rinn, 2012**). Mean curves (termed chronologies) were produced for each disc and per species using the radii after visual cross-dating with reference to pointer years (the position of very narrow or very wide rings to link rings detected on different radii). In addition to visual cross-dating (**Stokes & Smiley, 1968**), all ring-width series were statistically (**Cook et al., 1990**) cross-dated using computer program, Time Series Analysis and Presentation (TSAP). Two statistical indicators were used to evaluate the match between the time series: the “Gleichlaufigkeit” (GLK) which reflects the percentage of oscillations in the same direction in two time series within a certain period (**Eckstein & Bauch, 1969**) and the “t-

value BP” of Baillie-Pilcher (**Baillie & Pilcher, 1973**). These statistics were used for selecting the best correlated series to include in constructing sites chronologies.

- **Statistical analysis**

***Comparison of radial growth***

The study compared the mean radial growth (ring widths) among the species using t-test in Statistical Package Software for the Social Sciences, Version 17 after testing for normality. Results were considered significant at  $P \leq 0.05$ .

***Climate-growth relationships***

Before assessing the relationship between climatic parameters and radial growth of the trees, individual growth ring width series were detrended and standardized using the dendrochronology program library in R statistical software “dplR” (**Bunn, 2008 & 2010**). The detrending is the estimation and removal of the tree’s natural biological growth trend. The standardization is done by dividing each series by an estimated growth trend to produce dimensionless growth series free of autocorrelation caused by internal biological growth trends. The final mean chronology is a dimensionless ring-width index (RWI). In this study, a Spline function was used to fit each raw mean ring-width series with a frequency response of 0.50% at wavelength of 0.67 of each tree-ring series length.

Mean interseries correlation was used as a measure of the strength of the common growth signal within a chronology using the RWI. This index was calculated over a moving 30-year window with sample replication of 5. Expressed Population Signal (EPS) (**Wigley *et al.*, 1984**) measures the reliability of the chronology, if it reflects a hypothetically perfect or true chronology. EPS is a function of the interseries correlation and the series replication. EPS ranges from zero to one and is calculated according to the formula:

$$EPS(t) = \frac{n\bar{r}_{bt}}{n\bar{r}_{bt} + (1 - \bar{r}_{bt})}$$

Where:

$r_{bt}$  = mean correlation between all tree-ring series;

$n$  = number of correlated trees.

Pearson correlation analysis was conducted with a significance of 5% separately for the RWI of each species (*A. africana* and *A. leiocarpus*) of the humid and dry savanna zones to climatic parameters (monthly and yearly averages of precipitation and temperature). Climate data were obtained from the Ejura and Navrongo Meteorological Stations of the Ghana Meteorological Agency for the humid and dry savanna zones respectively (period=1961 to 2012). The correlation analyses were conducted in GraphPad Prism 5.

Spatial correlation analyses of RWI and Hadley Centre Sea Ice and Sea Surface Temperature (SST) ( $p \leq 0.05$ ) were also carried out with the KNMI Climate Explorer (**Royal Netherlands Meteorological Institute, 2015**). The SST dataset were from the Climate Research Unit of the University of East Anglia. This was done for *A. africana* and *A. leiocarpus* in both the dry and humid savanna zones.

### ***Cyclicity of tree growth fluctuation***

Wavelet transform was used to decompose the time series of *A. africana* and *A. leiocarpus* in the humid and dry savanna zones over a time-scale space (**Oberhuber et al., 2015**). Wavelet transform is a tool used to analyze non-stationary signals and it permits the detection of main periodicities in a time series and the evolution of their respective amplitude, frequency, and phase. We used the Morlet wavelet in package dplR (**Bunn, 2008**), which is a sine wave modulated by a classical Gaussian function, because it establishes a clear distinction between random fluctuations and periodic regions (**Torrence & Compo, 1998**). The output of Wavelet transform is the wavelet spectrum, which is a time-scale plot, where the x- and y-axis represent the position along time and periodicity scale, respectively, and the color contour at each x/y point represents the magnitude of the wavelet coefficient at that point. A dark red color is assigned to the highest value of the wavelet power spectrum, whereas a dark blue color is assigned to the lowest value. As continuous wavelet analyses are applied to the time series of finite length, edge effects may appear on the wavelet spectrum, leading to the definition of a cone of influence (**Torrence & Compo, 1998**), which is shown in a lighter shade in the wavelet spectrum.

#### 2.2.4 Assessment of Carbon-13 ( $\delta^{13}\text{C}$ ) isotope in riparian wood species in the humid and dry savanna zones

- **Selection and treatment of wood samples**

The study selected four (Table 5) cross-dated discs (individuals) from a larger tree-ring data set of 31 stem discs of *A. africana* and *A. leiocarpus* from both the dry and humid savanna zones for carbon-13 ( $\delta^{13}\text{C}$ ) isotope analysis (Total number of discs=16). The discs were collected between January and February, 2014. Ring widths of all samples were measured on 2-4 radii and properly cross-dated before annual rings were separated with a scalpel for stable isotope analyses. The study used two methods in preparing the wood samples for isotope measurements: (1) Bulk (whole) wood and (2) Cellulose extraction.

Earlier studies suggest that different isotope ratios exist between earlywood and latewood because earlywood carries the isotopic composition of stored carbohydrate synthesized in the previous year. However, since a clear distinction of earlywood and latewood was not possible due to the wood anatomy (structure) of the studied species that show a diffuse porous wood anatomy, the whole annual growth ring was used, resulting in an annual resolution of the final  $\delta^{13}\text{C}$  chronologies (**Gebrekirostos *et al.*, 2012; Krepkowski *et al.*, 2013**). The last year (2013) of each ring was excluded from analysis as the ring width was not yet complete.

Table 5: List of studied species with summary of their habit and annual growth increments

	Dry savanna		Humid savanna	
	<i>A. africana</i>	<i>A. leiocarpus</i>	<i>A. africana</i>	<i>A. leiocarpus</i>
Total length	101	41	84	76
Diameter (cm)	28-33	30-32	29-36	31-39
GLK	82	69	70	75
TV-BP	4.1	2.4	3.5	4.8
Mean	1.45	3.34	1.77	3.10
Std. Dev.	1.02	1.62	1.24	1.53
Maximum	3.15	5.7	7.18	7.61
Minimum	0.36	0.83	0.39	1.28

GLK: Gleichlaeufigkeit, TV-BP: t-value of Baillie-Pilcher

- **Bulk (whole) wood method**

The carbon-13 ( $\delta^{13}\text{C}$ ) measurements were done using bulk wood for each individual disc. Although earlier studies demonstrated that different wood components have different isotopic signatures, recent studies comparing the isotopic composition of different wood components (cellulose, lignin and bulk wood) have found a high correlation between cellulose and bulk wood as well as between cellulose and lignin (**Gebrekirstos *et al.*, 2012**). In some cases, bulk wood was found to be equally good and sometimes even better climate proxy than cellulose (**Krepkowski *et al.*, 2013**).

To use the bulk wood method, powdered samples were produced along one radius of each disc using a micro drill with a diameter of 0.5 mm. The powders were pooled into tin capsules and homogenized with a metal stick to represent the whole ring. Subsamples from each year were weighed into tin capsules (0.4–0.5 mg). Carbon isotope composition was measured (separation of carbon isotopes based on masses) with a mass spectrometer (Delta V Advantage, Thermo Electron, Bremen, Germany) coupled to a HekaTech Elemental Analyzer. The results are given in  $\delta$ -notation, which is the relative deviation from the PDB (Pee Dee Belemnite) standards:  $\delta^{13}\text{C} = [(^{13}\text{C}/^{12}\text{C})_{\text{sample}} / (^{13}\text{C}/^{12}\text{C})_{\text{PDB}} - 1] \times 1000\text{‰}$ .

- **Cellulose extraction**

Cellulose was extracted so that the pattern of  $\delta^{13}\text{C}$  obtained from measurement could be used to compare the values obtained using the whole wood method. This helps to know if the  $\delta^{13}\text{C}$  offsets is constant over time, thus helping to decide the effectiveness of  $\delta^{13}\text{C}$  archives of whole wood for paleoclimatic reconstruction or strength of climatic signal. Approximately 12 annual rings counted from the second ring (year=2012) from the outer part of each cross-dated disc of *A. africana* and *A. leiocarpus* in each savanna type (humid and dry) were used for the extraction of cellulose. The selected rings were cut into annual wood blocks with a razor blade under a binocular microscope. Each annual wood sample was put into an Eppendorf tube for subsequent cellulose extraction.

The cellulose extraction process was carried out according to the methods described in **Wieloch *et al.* (2011)** in the isotope laboratory of the Friedrich-Alexander University of Erlangen-Nurnberg, Germany. Accordingly, resin, fatty acids, etheric oils and hemicellulose were extracted with a solution of 5% NaOH for 2 hours at 60 °C. This operation was repeated twice. Then, lignin was extracted with 7% NaClO<sub>2</sub> solution for 40 hours at 60°C. We adjusted the 10 hours  $\times$  4 times process and adopted

instead an  $8 \text{ h} \times 5$  times process in order to achieve an adequate chemical treatment. Hemicelluloses were then extracted with 17% NaOH for 2 hours at room temperature. A washing procedure (until  $\text{pH } 7 \pm 1$ ) was interposed between the different steps. Finally, samples were washed once with 1% HCl and three times with boiled de-ionized water (until  $\text{pH } 7 \pm 1$ ) and transferred from the filter funnels into Eppendorf tubes with 1 ml de-ionized water.

Following **Laumer *et al.* (2009)**, ultrasonic homogenization was carried out for 15 seconds (cycle: 0.5, amplitude: 70) with a UP200s (Hielscher Ultrasonics GmbH, Warthestr. 21, D-14513 Teltow (Berlin), Germany). After freeze drying for 72 hours in an ALPHA 1-4/2-4 LSC lyophilisation unit, the dried cellulose was then weighed to determine the yield and finally measured by isotope ratio mass spectrometer.

- **Statistical analysis**

***Synchronization of  $\delta^{13}\text{C}$  series of species***

Tree ring isotopic data contain trends and variability unrelated to past climate. One non-climatic trend that can be removed from  $\delta^{13}\text{C}$  series is related to the decline in atmospheric  $\delta^{13}\text{C}$  values caused due to burning of  $^{13}\text{C}$ -depleted fossil fuels. This trend was removed by adding published annual values of the  $\delta^{13}\text{C}$  decrease in atmospheric  $\text{CO}_2$ , as demonstrated by **McCarroll & Loader (2004)**. Further, all  $^{13}\text{C}$  series were statistically compared for individuals within a species and between species using computer program, Time Series Analysis and Presentation (TSAP). Two statistical indicators were used to evaluate the match between the time series: the “Gleichlaeufigkeit” (GLK) which reflects the percentage of oscillations in the same direction in two time series within a certain period (**Eckstein & Bauch, 1969**) and the “t-value BP” of Baillie-Pilcher (**Baillie & Pilcher, 1973**).

***Measuring signal strength and chronology reliability***

Using the dendrochronology program library in R statistical software “dplR” (**Bunn, 2008 & 2010**), mean interseries correlation was calculated as a measure of the strength of the common growth signal within a chronology. This index was calculated over a moving 30-year window with sample replication of 4. Expressed Population Signal (EPS) measures the chronology reliability, if it reflects a hypothetically perfect or true chronology. EPS is a function of the interseries correlation and the series replication (**Wigley *et al.*, 1984**). EPS ranges from zero to one and calculated according to the formula:

$$\text{EPS}(t) = \frac{n\bar{r}_{\text{bt}}}{n\bar{r}_{\text{bt}} + (1 - \bar{r}_{\text{bt}})}$$

Where:  $\bar{r}_{\text{bt}}$  = mean correlation between all tree-ring series;

$n$  = number of correlated trees.

### ***Climate- $\delta^{13}\text{C}$ relationships***

Pearson correlation analysis was conducted separately for each species (*A. africana* and *A. leiocarpus*) in both the humid and dry savanna zones in order to determine the sensitivity of the  $\delta^{13}\text{C}$  to climatic parameters: mean monthly and average precipitation and temperature. The climate data were obtained from the Ejura and Navrongo Meteorological Stations of the Ghana Meteorological Agency for the humid and dry savanna zones respectively. The correlation analyses were conducted in GraphPad Prism 5.

# **III. RESULTS**

### **3.1 Trends in forest cover dynamics in the Afram and Tankwidi riparian catchments from 1986, 2000 to 2014**

- **Forest cover dynamics of the Afram riparian catchment in the humid savanna zone**

The results of the classification accuracy assessment for the 2000 and 2014 maps are presented in Table 6 and 7 respectively. Overall accuracies of 89% for the 2000 image and 91% for the 2014 image. The Kappa coefficient for 2000 and 2014 were 0.77 and 0.83 respectively. The “forest” and “non-forest” classes of both 2000 and 2014 had producer’s and user’s accuracies over 80%.

The quantified forest cover trends mapped between 1986 and 2014 are depicted in Table 8 and Figure 13. The trend generally shows increasing forest cover loss (deforestation) from 1986, 2000 to 2014. In 1986, the forest cover was estimated at 50% of the entire headwaters studied and was reduced to 37% by 2000. The area of forest cover as at 2014 was 31% of the headwaters of the Afram river catchment. The “non-forest” which comprises primarily of farmland and grassland have been increasing in area coverage since 1986 (50%) through 2000 (63%) to 2014 (69%).

Table 6: Confusion matrix of Landcover map using Landsat 2000 (Afram catchment)

	Reference data		Classified total	Number correct	Accuracy total		
	Forest	Non- forests			Producers Accuracy %	User Accuracy %	Kappa
Forest	29	2	31	29	80.56	93.55	0.88
Non-forest	7	42	49	42	95.45	85.71	0.68
Total	36	44	80				
Overall Accuracy = 89%							
Overall Kappa = 0.77							

Table 7: Confusion matrix of Landcover map using Landsat 2014 (Afram catchment)

	Reference data		Classified total	Number correct	Accuracy total		
	Forest	Non- forests			Producers Accuracy %	User Accuracy %	Kappa
Forest	36	1	37	36	85.71	97.3	0.94
Non-forest	6	37	43	37	97.37	86.05	0.73
Total	42	38	80	73			
Overall Accuracy = 91%							
Overall Kappa = 0.83							

Table 8: Landcover proportions from 1986-2014 at the Afram catchment

Landcover	1986	%	2000	%	2014	%	Rate % year <sup>-1</sup> (1986-2014)
Forest (ha)	143453	50	105595	37	87897	31	-1.7
Non-forest (ha)	142497	50	180355	63	198053	69	
Total	285950		285950		285950		

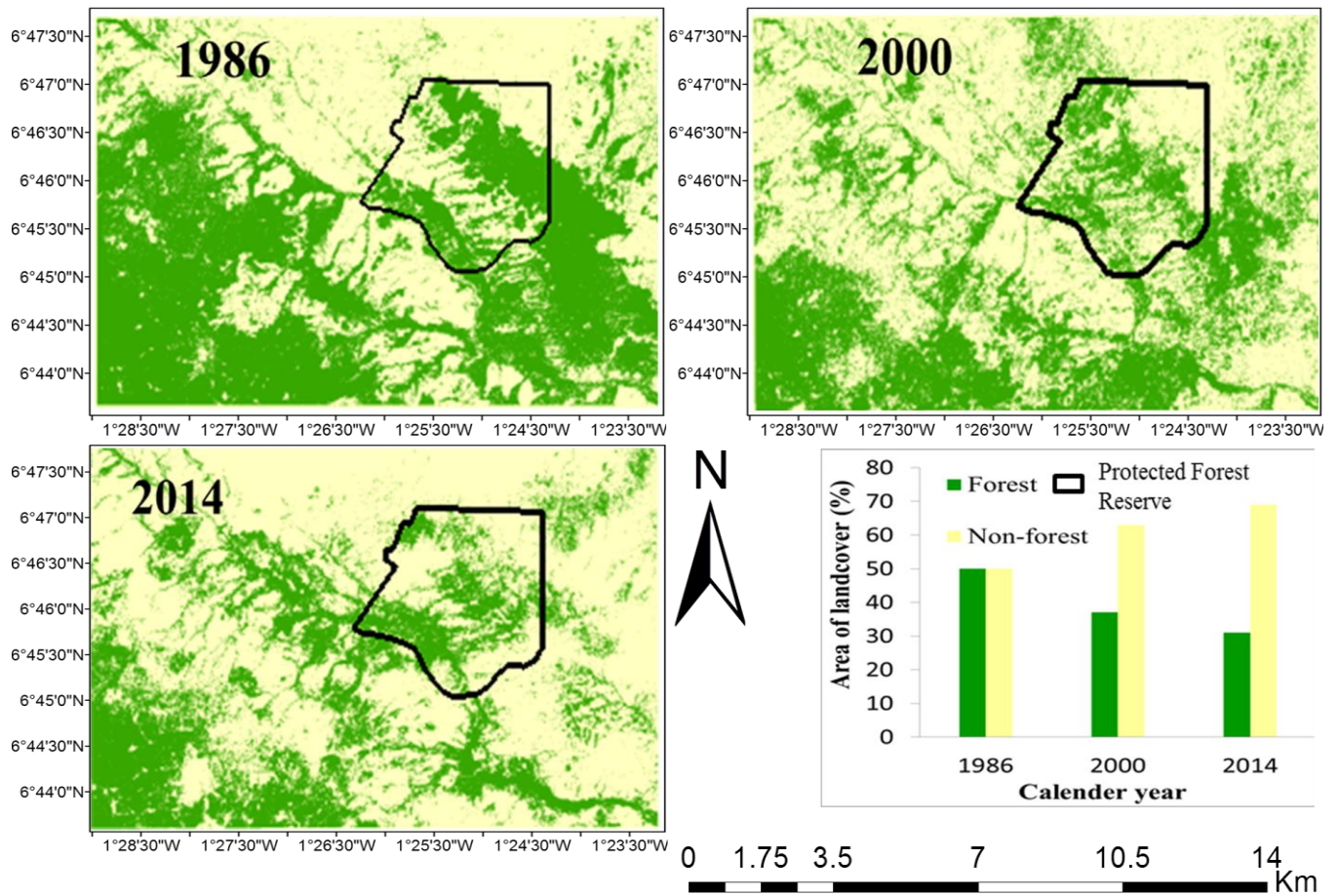


Figure13: Landcover in the Afram river catchment for the studied years (1986-2014)

- **Forest cover dynamics of the Tankwidi riparian catchment in the dry savanna zone**

The study observed overall accuracies of 71% for the 2000 image and 74% for the 2014 image. Kappa coefficient for 2000 and 2014 were 0.43 and 0.45 respectively. Producer accuracy of the “forest” for 2000 and 2014 were lower than the “non-forest”. The user accuracy of “forest” was nevertheless, higher than the “non-forest” for both 2000 and 2014. Results of the classification accuracy assessments for the maps of 2000 and 2014 are presented in Table 9 and 10 respectively

The quantified forest cover trends mapped between 1986 and 2014 are depicted in Table 11 and Figure 14. The trend generally shows increasing deforestation from 1986 to 2014. In 1986, the forest cover was estimated at 23% of the area studied. It was reduced to 11% by 2000. Currently, the area of forest cover is 7% of the study area. The “non-forest” which comprises primarily of farmland and grassland have been increasing in area coverage since 1986 (77%) through 2000 (89%) to 2014 (93%).

Table 9: Confusion matrix of Landcover map using Landsat 2000 (Tankwidi catchment)

Landcover	Reference data		Classified total	Number correct	Accuracy total		
	Forest	Non-forests			Producers Accuracy %	User Accuracy %	Kappa
Forest	15	1	16	15	46.88	93.75	0.87
Non-forest	17	29	46	29	96.67	63.04	0.28
Total	32	30	62	44			
Overall Accuracy		71					
Overall Kappa		0.43					

Table 10: Confusion matrix of Landcover map using Landsat 2014 (Tankwidi catchment)

Landcover	Reference data		Classified total	Number correct	Accuracy total		
	Forest	Non-forests			Producers Accuracy %	User Accuracy %	Kappa
Forest	13	1	14	13	44.83	92.86	0.87
Non-forest	16	36	52	36	97.30	69.23	0.30
Total	29	37	66	49			
Overall Accuracy		74					
Overall Kappa		0.45					

Table 11: Landcover proportions from 1986-2014 at the Tankwidi catchment

Landcover	1986	%	2000	%	2014	%	Rate % year <sup>-1</sup> (1986-2014)
Forest (ha)	33905	23	17090	11	10681	7	-4.1%
Non-forest (ha)	115755	77	132570	89	138979	93	
Total	149660		149660		149660		

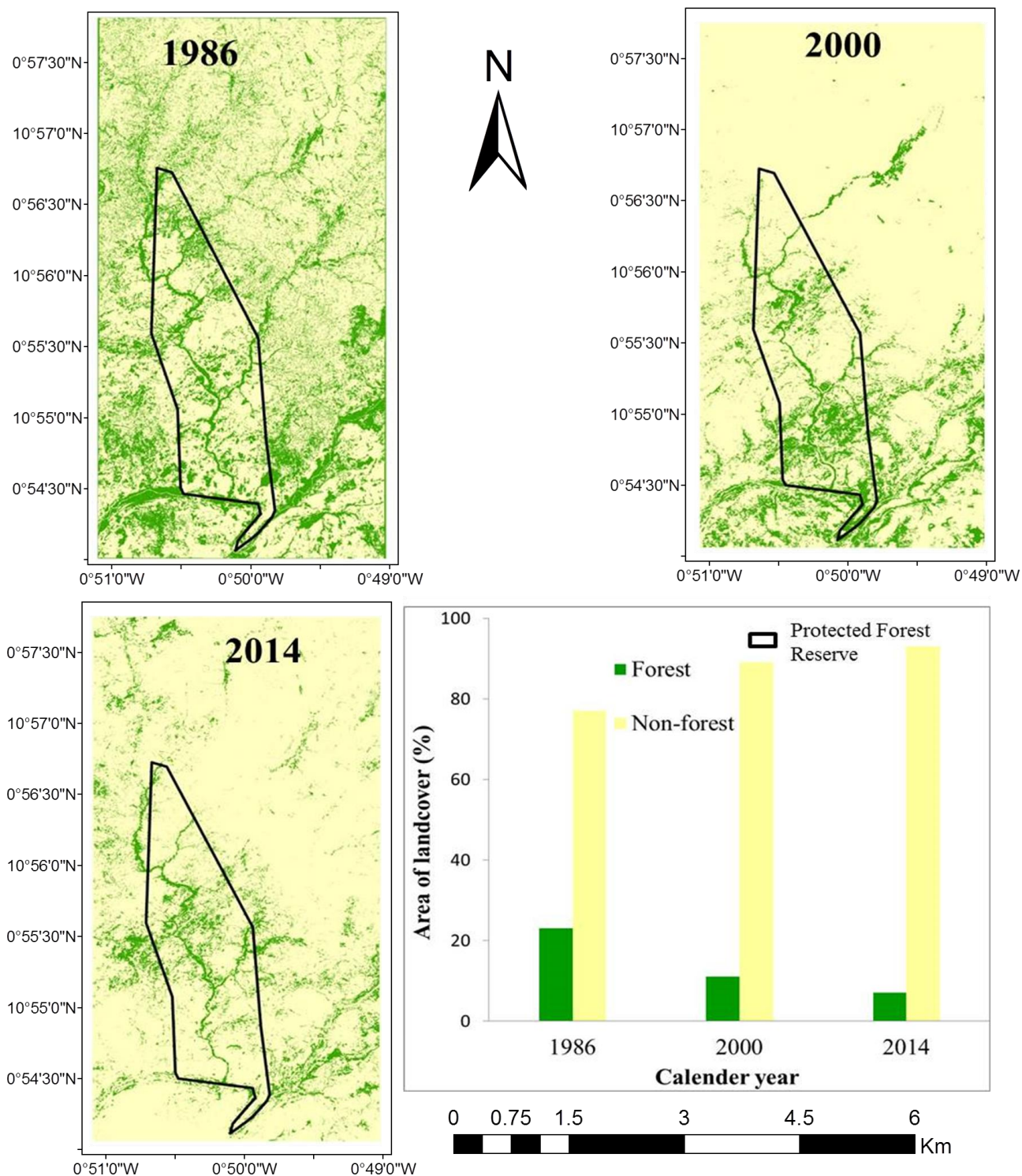


Figure14: Landcover in the Tankwidi river catchment for the studied years (1986-2014)

### **3.2 Comparison of woody plant diversity and structure of riparian forests between protected area and farmland in the humid and dry savanna zones**

#### **3.2.1 Density, basal area and size-class distribution of woody species**

Along the Afram river in the humid savanna, all structural parameters (tree canopy cover, density, basal area and height) significantly decreased from the PA to FA (Table 12). In terms of DBH, there was no significant difference between the PA and FA. In the case of the Tankwidi river of the dry savanna, the tree density and canopy cover were similarly higher in the PA than the FA. Nonetheless, the DBH, basal area and height of woody plants were significantly higher in FA than PA (Table 12).

Apart from the DBH, the tree canopy cover, density, basal area and height of the woody plants in protected areas (PA) showed a significant decrease from the humid (Afram river) to the dry savanna (Tankwidi river) zone (Table 12). On the other hand, the basal area, DBH and height in farmlands showed a significantly increase from the dry to the humid savanna zone (Table 12).

In both Afram (humid) and Tankwidi (dry) riparian forests, the size class distribution of woody plants in the different land uses (PA and FA) generally followed a reversed J-shaped structure with a high number of individuals of diameter and height less than 15cm and 10m respectively (Figure 15 & 16). The pattern in FA along the Tankwidi river (dry) nevertheless showed a deviation at the lower diameter (5-15cm) and height classes (0-10m) with fewer number of individuals.

Table 12: Stand structural characteristics of riparian buffer in protected area (PA) and farmland (FA) along the Afram river (Humid savanna) and Tankwidi river (Dry savanna)

		Humid savanna			Dry savanna		
Parameter	Land use	Mean	SE	P-value	Mean	SE	P-value
Density, N/ha	PA	545	18	0.00*	355	21	0.00*
	FA	277	13		146	11	
Canopy	PA	82.93	2.12	0.03*	75.30	1.77	0.00*
Cover, %	FA	74.50	3.28		21.13	3.16	
Basal	PA	19.63	1.74	0.01*	15.07	1.37	0.00*
Area, m <sup>2</sup> /ha	FA	14.10	1.22		29.03	3.71	
DBH, cm	PA	17.08	0.60	0.08	16.12	0.69	0.00*
	FA	15.70	0.46		23.95	1.24	
Height, m	PA	13.88	0.44	0.00*	10.17	0.43	0.00*
	FA	11.63	0.36		14.25	0.82	
		Protected area			Farmland		
Parameter	Land use	Mean	SE	P-value	Mean	SE	P-value
Density, N/ha	Humid	545	18	0.00*	277	13	0.00*
	Dry	355	21		146	11	
Canopy	Humid	82.93	2.11	0.01*	74.50	3.28	0.00*
Cover, %	Dry	75.30	1.77		21.13	3.16	
Basal	Humid	19.63	1.74	0.04*	14.10	1.22	0.00*
Area, m <sup>2</sup> /ha	Dry	15.07	1.37		29.03	3.71	
DBH, cm	Humid	17.08	0.60	0.30	15.70	0.46	0.00*
	Dry	16.12	0.69		23.95	1.24	
Height, m	Humid	13.88	0.44	0.00*	11.63	0.36	0.01*
	Dry	10.17	0.43		14.25	0.82	

SE: Standard Error, Number of observation for each, N=30; Degrees of freedom=58, Significant at  $P \leq 0.05$

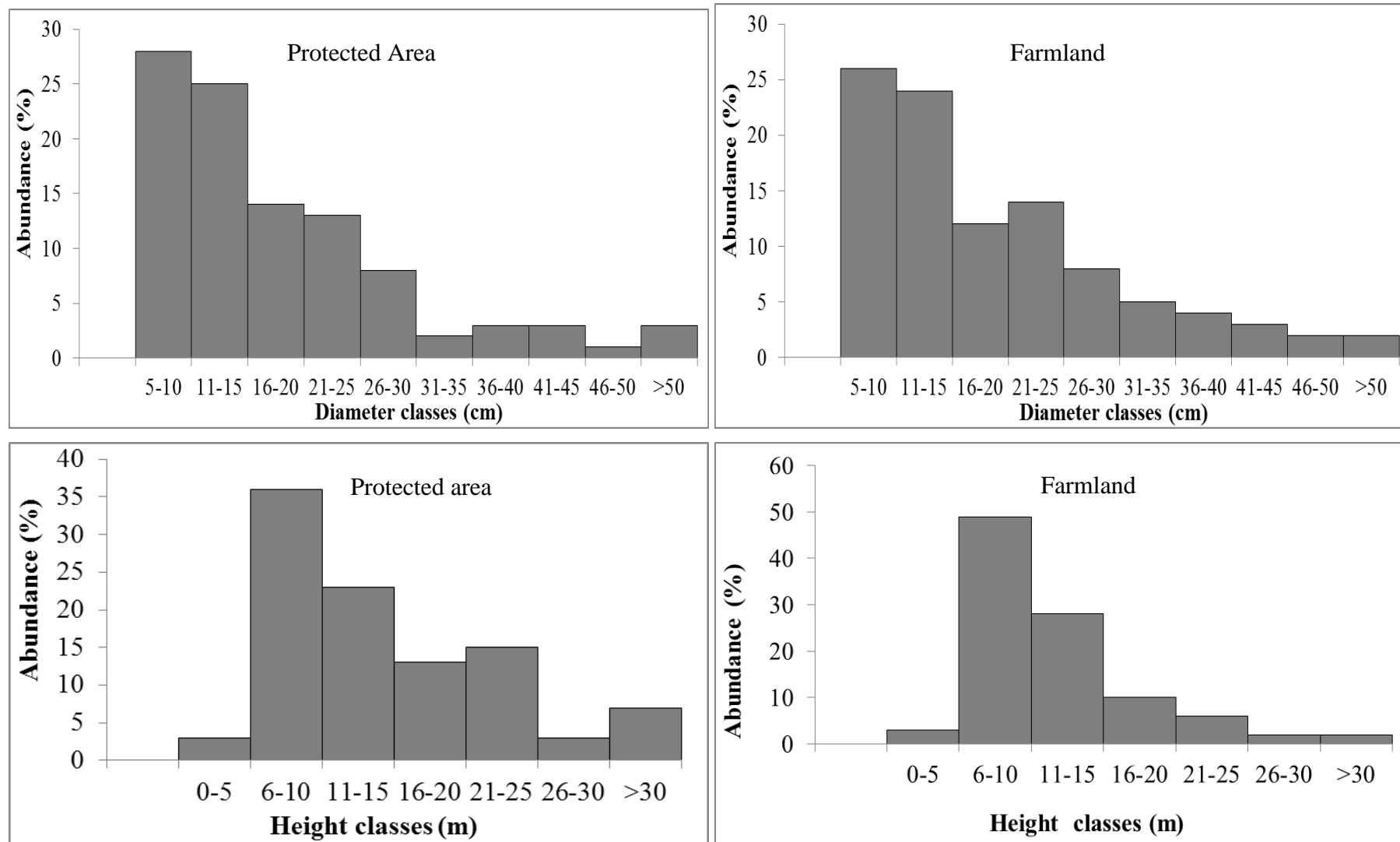


Figure15: Diameter and height class distribution of individuals'  $\geq 5$ cm DBH in riparian forests in protected area (PA) and farmland (FA) along the Afram river

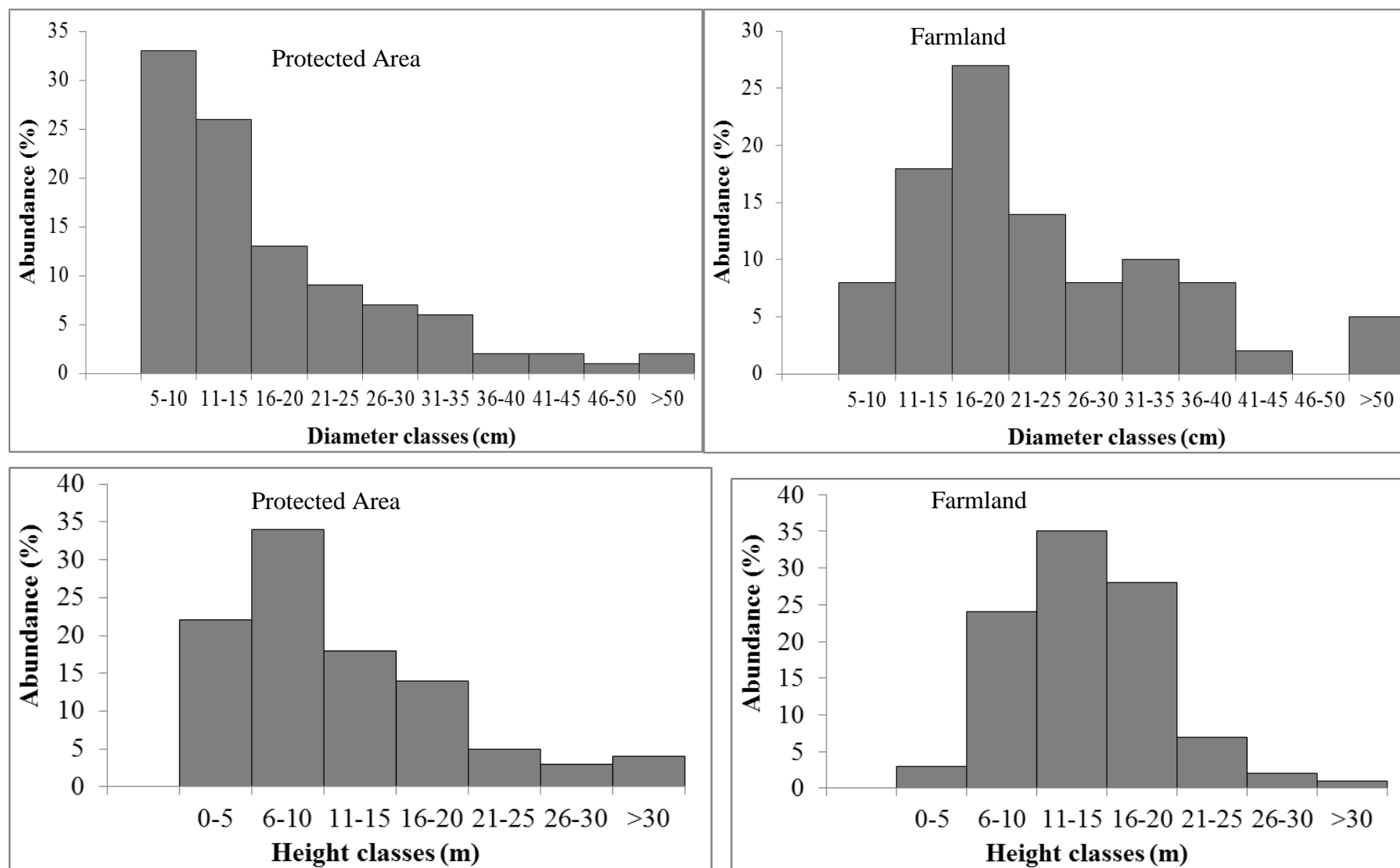


Figure16: Diameter and height class distribution of individuals'  $\geq 5$ cm DBH in riparian forests in protected area (PA) and farmland (FA) along the Tankwidi river

### 3.2.2 Woody species composition, diversity and similarity

A total of 95 species distributed within 26 families were recorded in the Afram and Tankwidi riparian forests located in the humid and dry savanna zones of Ghana respectively. Fabaceae (32%), Rubiaceae (15%), Combretaceae (10%), Moraceae (7%), Verbenaceae (4%) and Sterculiaceae (4%) were the dominant families in the riparian forests in both savanna types. In general, eight woody species were found common to both Afram (humid) and Tankwidi (dry) riparian forests. They were *Afzelia africana*, *Anogeissus leiocarpus*, *Azadirachta indica*, *Daniellia oliveri*, *Diospyros mespiliformis* ex A. DC., *Khaya senegalensis* A. Juss., *Mitragyna inermis* (Willd.) O. Kuntze and *Vitex doniana* Sweet.

In the humid savanna, a total of 63 woody species distributed within 24 families were recorded along the Afram river in both protected area (PA) and farmland (FA). The most species rich families in both PA and FA were Fabaceae (36%), Rubiaceae (13%), Moraceae (8%), Sterculiaceae (6%), Bombacaceae (5%), Combretaceae (4%) and Ebenaceae (4%). The total number of specimen recorded was 1232 with 817 in PA and 415 in FA. The number of species recorded decreased from PA (58) to FA (39). With this, 34 species were common to both PA and FA. Twenty four and 5 species were found exclusively in PA and FA respectively. Examples of the species found only in the PA were *Albizia glaberrima* (Schum. & Thonn.) Benth. (2%), *Albizia zygia* (DC.) J. F. Macbr. (1%), *Alchornea cordifolia* (Schum. & Thonn.) Müll. Arg. (1%) etc. The five species recorded exclusively in FA were *Acacia macrostachya* Reichenb. ex DC. (1%), *Anthocleista nobilis* G. Don (1%), *Azadirachta indica* A. Juss. (1%), *Canthium vulgare* (K. Schum.) Bullock. F.R. (2%) and *Raphia hookeri* Mann & Wendl. (1%). Some of the species common to the PA and FA were *Pterocarpus santalinoides* DC. (11%), *Mitragyna inermis* (11%), *Cynometra megalophylla* Harms (7%) etc.

Furthermore, six abundant species in the PA were *Pterocarpus santalinoides* (12%), *Mitragyna inermis* (11%), *Cynometra megalophylla* (7%), *Antiaris toxicaria* A. Chev. (6%), *Ceiba pentandra* (L.) Gaertn. (5%) and *Sterculia tragacantha* Lindl. (4%). Similarly, 6 abundant species on FA were *Mitragyna inermis* (12%), *Cynometra megalophylla* (9%), *Pterocarpus santalinoides* (8%), *Antiaris toxicaria* (6%), *Diospyros mespiliformis* Hochst. ex A. DC. (5%) and *Anogeissus leiocarpus* (4%).

In the dry savanna and along the Tankwidi river, a total of 40 woody species were recorded in both protected area (PA) and farmland (FA). All the 40 species were found in the PA and only 19 recorded in FA. There were 16 families in both PA and FA and the most species rich families were Fabaceae

(26%), Rubiaceae (20%), Combretaceae (20%), Verbenaceae (8%), Sapotaceae (7%) and Anacardiaceae (6%). The total number of specimen recorded along the Tankwidi river was 751 with 532 in PA and 219 in FA.

Woody species with the highest abundance in PA along the Tankwidi river were *Anogeissus leiocarpus* (17%), *Mitragyna inermis* (16%), *Vitex doniana* (7%), *Vitellaria paradoxa* C. F. Gaertn. (7%) and *Pterocarpus erinaceus* (7%). Others were *Daniellia oliveri* (5%), *Combretum nigricans* (4%) and *Lannea microcarpa* (4%). In the FA, the abundant woody species were *Anogeissus leiocarpa* (15%), *Mitragyna inermis* (17%), *Pterocarpus erinaceus* (7%), *Vitex doniana* (10%), *Vitellaria paradoxa* (9%), *Parkia biglobosa* (Jacq.) R. Br. ex G. Don f. (5%) and *Acacia sieberiana* DC. (7%).

Appendix 1 lists all the woody plants recorded in the Afram and Tankwidi riparian forests, their families, life form, chorotype and abundance.

The Shannon-Wiener diversity index (SWI) of the woody plants along the Afram river in protected area and farmland were 3.80 ( $\pm 0.05$ ) and 3.10( $\pm 0.08$ ) respectively. In the case of the Tankwidi river, the SWI was 2.5 ( $\pm 0.09$ ) for PA and 1.8 ( $\pm 0.014$ ) for the farmlands. According to Jaccard Index (JI) values, the two riparian sites in the protected area and farmlands in the Afram river (humid savanna) had a greater percent similarity (JI=53.97%) compared to the riparian forests of the same landuses along the Tankwidi river (dry savanna) (JI=47.50).

### **3.2.3 Soil physical properties in protected area and farmlands and between the humid and dry savanna zones**

The proportions of sand, clay and silt (Table 13) in the top soils (0-20cm) and bottom soil (20-40cm) varied moderately between farmland and protected area of the same site but greatly between the two savanna types. Using the USDA Soil Textural Triangle for assigning soil texture classification (Anderson & Ingram, 1998), the soils in all the land uses in the two savanna types were described as sandy loam (Table 13). In terms of bulk density, the study observed an increasing trend with increasing depth from the top (0-20cm) to the bottom (20-40cm) layer (Table 14) in both study sites. The differences were however, not significant. Although soil moisture content varied between PA and FA and between the humid and dry savanna zones, the differences were not significant (Table 15).

### **3.2.4 Soil chemical properties in protected area and farmlands and between the humid and dry savanna zones**

A comparison of soil chemical properties (C, N, P, K and pH) from top (0-20cm) to bottom (20-40cm) and between the protected area (PA) and farmland (FA) is shown in Table 16 and 17. All the mean values of the chemical properties measured (N, P, K, C, pH) decreased from the top to the bottom soils of the riparian forests in both the humid and dry savanna zones.

Along the Afram river, no significant difference was observed for C, N, P, K and pH of the riparian forests in protected area and farmlands. However, the CN ratio was significantly higher in the farmland than the protected area.

In the case of the Tankwidi riparian forests, the study observed that the content of C, K and C/N ratio of the riparian soils (0-40cm) in protected area were higher than on farmland (Table 18). There was however, no significant difference in the N, P and pH between the PA and FA.

Further analysis showed that the chemical properties (C, P, K, pH, C:N ratio) of riparian forests in protected areas in the dry savanna were higher than the humid savanna. Nitrogen contents of the riparian forests in the two savanna types however, showed no significant difference.

Additionally, the farmlands riparian soil chemical properties showed that P, K and C/N ratio in the humid was higher than the savanna zone. The farmland riparian forests in the humid savanna was

highly acidic than the dry savanna. There was no significant difference in the C and N content in farmlands between the humid and dry savanna zones.

The output of two-way ANOVA (Table 19) and Bonferroni's Post-hoc tests showed that there was significant interaction between savanna type and land use on soil C, K and C/N. No significant interaction was found between savanna type and land use on N, P and pH of the soils.

### **3.2.5 Relationship between woody plant density, and soil properties**

In both Afram and Tankwidi riparian forests, soil C, N, P, C/N ratio, pH and soil moisture content were the important soil attributes that in one way or another had significant relationships with the density of the riparian woody plants.

Within the protected area (PA) in the humid savanna (along Afram river), linear regression (Table 20) showed weak significant relationship between the density of woody plants and soil C content. In the farmlands the woody plant density also had significant relationships with C, P and soil moisture.

In the case of the PA in the dry savanna (Tankwidi river), there were strong significant relationships between the density of the woody plants with soil C and C/.N ratio For the farmland along this same river, the soil pH and N had significant relationship with the woody plant density. All other soil properties showed no relationship the density.

Table 13: Soil texture in protected area (PA) and farmland (FA) along Afram (Humid Savanna) and Tankwidi (Dry savanna) rivers

Parameter	Depth (cm)	Humid savanna		Dry savanna	
		PA	FA	PA	FA
Sand	0-20	75.13±2.39 <sup>a</sup>	70.91±2.50 <sup>a</sup>	52.14±2.80 <sup>a</sup>	68.12±2.94 <sup>b</sup>
	20-40	70.43±1.98 <sup>a</sup>	71.22±2.13 <sup>a</sup>	48.31±1.44 <sup>a</sup>	60.43±1.54 <sup>b</sup>
Clay	0-20	7.35±0.85 <sup>a</sup>	10.68±1.30 <sup>b</sup>	19.99±1.96 <sup>a</sup>	10.21±0.97 <sup>b</sup>
	20-40	14.12±1.09 <sup>a</sup>	18.42±1.78 <sup>b</sup>	22.50±2.31 <sup>a</sup>	17.80±1.03 <sup>a</sup>
Silt	0-20	17.52±1.67 <sup>a</sup>	18.41±1.38 <sup>a</sup>	27.87±1.20 <sup>a</sup>	21.67±2.05 <sup>b</sup>
	20-40	15.45±1.44 <sup>a</sup>	10.36±2.32 <sup>a</sup>	29.19±1.22 <sup>a</sup>	21.77±0.89 <sup>b</sup>
Soil type	0-20	Sandy Loam	Sandy Loam	Sandy Loam	Sandy Loam

Number of observation for each, N=18. Pairs of “Mean±standard error” in PA and FA followed by different letters are significantly different

Table 14: Soil bulk density and moisture content in Protected Area (PA) and Farmland (FA) in the humid and dry savanna zones

Bulk density (g/cm <sup>3</sup> )									
Parameter	Land use	Humid savanna				Dry savanna			
		Mean	SE	T	P	Mean	SE	t	P
Protected Area	Top	1.03	0.04	0.89	0.38	1.40	0.06	1.53	0.13
	Bottom	1.07	0.02			1.53	0.06		
Farmland	Top	1.13	0.05	0.59	0.56	1.51	0.05	0.81	0.42
	Bottom	1.17	0.05			1.58	0.06		
Total	PA	1.06	0.03	1.80	0.08	1.46	0.04	1.25	0.22
depth	FA	1.15	0.04			1.55	0.06		

Table 15: Soil moisture content in Protected Area (PA) and Farmland (FA) in the humid and dry savanna zones

Moisture content (%)									
Humid savanna						Dry savanna			
Parameter	Land use	Mean	SE	T	P	Mean	SE	t	P
Protected Area	Top	17.00	0.85	3.41	0.00*	12.40	1.7	1.93	0.06
	Bottom	12.60	0.97			8.50	1.1		
Farmland	Top	14.40	1.32	0.58	0.57	8.20	1.7	0.30	0.77
	Bottom	13.40	1.12			7.50	1.6		
Total	PA	14.76	0.89	0.53	0.60	10.55	1.23	1.40	0.17
depth	FA	14.02	1.09			7.88	1.45		

Degrees of freedom=34, Number of observation for each (N=18), Significant at  $P \leq 0.05$

Table 16: Riparian buffer soil in top and bottom layers of protected area and farmland along Afram (Humid savanna) and Tankwidi rivers (Dry savanna)

Humid savanna									
Protected Area						Farmland			
Parameter	Land use	Mean	SE	t	P	Mean	SE	T	P
Carbon (%)	Top	1.56	0.20	4.51	< 0.01*	1.49	0.20	3.22	<0.01*
	Bottom	0.65	0.06			0.72	0.13		
Nitrogen (%)	Top	0.18	0.04	2.76	0.01*	0.11	0.01	3.17	<0.01*
	Bottom	0.08	0.01			0.07	0.01		
Phosphorus (mgKg <sup>-1</sup> )	Top	5.91	1.34	0.41	0.69	5.60	0.96	1.77	0.09
	Bottom	5.12	1.39			3.49	0.70		
Potassium (cmolKg <sup>-1</sup> )	Top	0.66	0.09	2.53	0.02*	0.45	0.04	2.38	0.02*
	Bottom	0.36	0.07			0.31	0.05		
pH	Top	5.72	0.14	1.66	0.11	5.76	0.17	0.93	0.36
	Bottom	5.39	0.14			5.49	0.23		

Dry savanna									
Protected Area						Farmland			
Parameter	Land use	Mean	SE	t	P	Mean	SE	t	P
Carbon (%)	Top	2.35	0.19	4.69	<0.01*	1.07	0.21	1.54	0.13
	Bottom	1.18	0.16			0.71	0.12		
Nitrogen (%)	Top	0.17	0.02	3.74	<0.01*	0.16	0.02	4.53	<0.01*
	Bottom	0.09	0.01			0.06	0.01		
Phosphorus (mgKg <sup>-1</sup> )	Top	2.40	0.51	1.75	0.09	1.57	0.10	1.69	0.101
	Bottom	1.48	0.12			1.36	0.07		
Potassium (CmolKg <sup>-1</sup> )	Top	1.18	0.09	4.02	<0.01*	0.73	0.05	4.42	<0.01*
	Bottom	0.71	0.07			0.46	0.04		
pH	Top	6.26	0.10	1.61	0.12	6.45	0.11	1.28	0.21
	Bottom	5.93	0.17			6.26	0.09		

Top (0-20cm), Bottom (20-40cm), Degrees of freedom=34, Number of observation for each (N=18)

Table17: Riparian buffer soil in protected area and farmland

Parameter	Layer	Mean	SE	t	P	Mean	SE	T	P
Humid savanna					Dry savanna				
Carbon (%)	PA	1.14	0.11	0.19	0.85	1.77	0.12	5.07	<0.01*
	FA	1.11	0.11			0.89	0.13		
Nitrogen (%)	PA	0.13	0.02	1.95	0.06	0.12	0.01	0.99	0.33
	FA	0.09	0.01			0.11	0.01		
Phosphorus (mgKg <sup>-1</sup> )	PA	5.52	1.14	0.75	0.46	1.94	0.25	1.80	0.08
	FA	4.55	0.61			1.46	0.01		
Potassium (CmolKg <sup>-1</sup> )	PA	0.51	0.07	1.75	0.09	0.94	0.06	4.97	<0.01*
	FA	0.38	0.02			0.60	0.04		
pH	PA	5.56	0.10	0.45	0.66	6.10	0.11	2.04	0.49
	FA	5.63	0.10			6.36	0.07		
C:N ratio	PA	7.46	0.80	2.23	0.03	15.01	1.54	2.78	0.01*
	FA	10.95	1.34			9.70	1.52		

PA=Protected Area, FA=Farmland, SE=Standard Error, Soil depth=0-40cm, Degrees of freedom=34, Number of observation for each (N=18)

Table 18: Riparian buffer soil in the humid and dry savanna zones

Parameter	Layer	Mean	SE	t	P	Mean	SE	t	P
Protected area					Farmland				
Carbon (%)	HS	1.14	0.11	3.87	0.00*	1.11	0.11	1.29	0.21
	DS	1.77	0.12			0.89	0.13		
Nitrogen (%)	HS	0.13	0.02	0.47	0.64	0.09	0.01	1.23	0.23
	DS	0.12	0.01			0.11	0.01		
Phosphorus (mgKg <sup>-1</sup> )	HS	5.52	1.14	3.06	0.00*	4.55	0.61	4.97	0.00*
	DS	1.94	0.25			1.46	0.10		
Potassium (CmolKg <sup>-1</sup> )	HS	0.51	0.07	4.67	0.00*	0.38	0.02	4.90	0.00*
	DS	0.94	0.06			0.60	0.04		
pH	HS	5.56	0.10	3.70	0.00*	5.63	0.10	5.38	0.00*
	DS	6.10	0.11			6.36	0.07		
C:N ratio	HS	7.46	0.80	5.37	0.00*	10.95	1.34	0.61	0.54
	DS	15.01	1.54			9.70	1.52		

HS=Humid savanna, DS=Dry savanna, SE=Standard Error , Soil depth=0-40cm, Degrees of freedom=34, Number of observation for each, N=18, Significant at P≤ 0.05

Table19: Two-way Anova of the effect of savanna and land use types on riparian buffer soil chemical properties

	Savanna		Land use		Savanna $\times$ Land use		Residual
	F	P	F	P	F	P	MS
C (%)	13.63	0.00*	14.39	0.00*	14.71	0.00*	0.24
N (%)	0.09	0.77	4.73	0.03*	1.16	0.29	0.00
P (mgKg <sup>-1</sup> )	25.39	< 0.00*	1.20	0.28	0.14	0.71	7.85
K (CmolKg <sup>-1</sup> )	40.11	< 0.00*	21.76	< 0.00*	4.37	0.04*	0.05
CN ratio	6.529	0.01*	0.54	0.47	12.70	0.00*	27.40
pH	40.80	< 0.00*	2.78	0.10	0.96	0.33	0.18

Significant at  $P \leq 0.05$

Table 20: Regression analysis between riparian woody density and soil properties in Protected Areas and Farmlands in the humid and dry savanna zones

	Humid Savanna						Dry savanna					
	PA			FA			PA			FA		
	R <sup>2</sup>	β	P	R <sup>2</sup>	β	P	R <sup>2</sup>	β	P	R <sup>2</sup>	β	P
C (%)	0.32	0.56	0.02*	0.29	0.54	0.02*	0.23	0.48	0.05*	0.08	0.28	0.26
N (%)	0.16	0.40	0.10	0.02	0.13	0.61	0.20	-0.45	0.06	0.29	0.54	0.02*
P (mg/Kg)	0.00	0.02	0.93	0.25	0.50	0.03*	0.1	-0.24	0.34	0.19	0.43	0.08
K (Cmol/Kg)	0.10	0.28	0.27	0.18	0.42	0.08	0.01	0.24	0.33	0.01	0.11	0.65
pH	0.01	-0.14	0.59	0.03	0.16	0.53	0.02	-0.14	0.57	0.29	-0.54	0.02*
Sand (%)	0.02	-0.16	0.52	0.00	-0.04	0.88	0.10	0.23	0.36	0.00	-0.05	0.84
Clay (%)	0.00	-0.00	0.97	0.01	0.10	0.69	0.00	-0.02	0.94	0.00	0.00	0.99
Silt (%)	0.01	0.24	0.35	0.00	-0.07	0.77	0.11	-0.34	0.17	0.01	0.07	0.77
C/N ratio	0.16	0.40	0.10	0.16	0.40	0.10	0.39	0.63	0.00*	0.03	-0.16	0.52
Slope	0.1	0.32	0.20	0.07	0.26	0.30	0.03	0.20	0.44	0.00	0.05	0.86
Moisture	0.1	-0.31	0.21	0.34	0.58	0.01*	0.00	0.21	0.93	0.02	-0.15	0.54

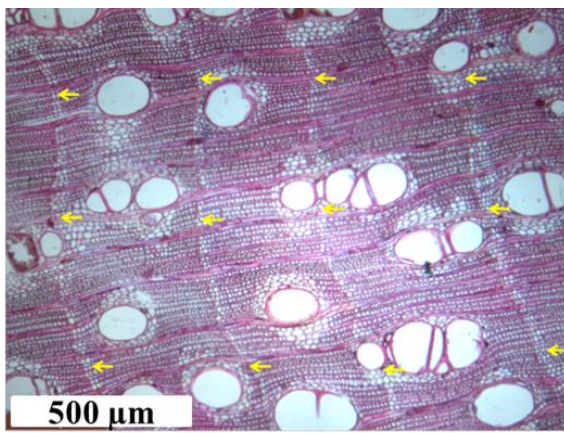
PA=Protected Area, FA=Farmland, R<sup>2</sup> = coefficient of determination, β = standardised coefficient, Significant at ≤ 0.05

### **3.3 Long-term growth patterns and the relationship between radial growth of riparian woody species and climatic parameters in the humid and dry savanna zones.**

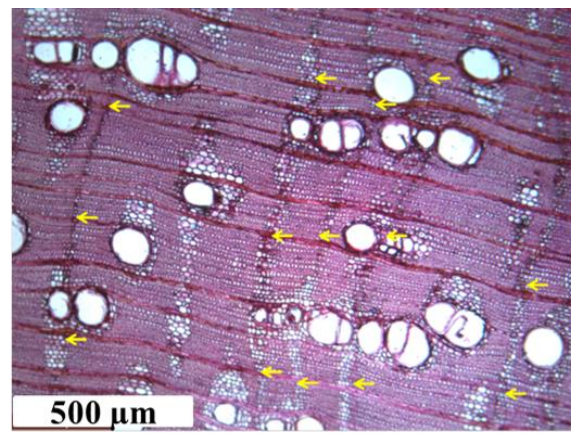
#### **3.3.1 Characteristics of trees growth rings**

Both *A. africana* and *A. leiocarpus* in the humid and dry savanna zones showed distinct growth rings (Figure 17). The growth rings of *A. africana* have been much more distinct than those of *A. leiocarpus*. The vessel sizes of *A. africana* also appeared to be larger than those of *A. leiocarpus*. The color of the wood is light-brown to red with coarse-grained, rough, hard wood texture. The wood structure is diffuse porous and vessels are circular to oval-shaped and occur solitary or in small groupings of 2-3 vessel elements in radial arrangement surrounded by paratracheal aliform or confluent parenchyma which are effective seals and protects the vessels from accidental air leak. The vessel sizes of *A. africana* and *A. leiocarpus* in the humid savanna were visibly larger than those of the dry savanna zone. Growth ring boundaries of *A. africana* in the two savanna types are demarcated by parenchyma bands. In some instances, wedging rings occurred and were determined by analyzing various radii on the stem discs. The ring widths were variable comprising both extremely narrow and wide rings.

The wood color is light-brown and darkens towards the pith. The species was characterized by a weak ring porous vessel distribution with no specific difference in pore sizes (Figure 17). Vessels are solitary or aligned in radial groups of up to more than 10 elements. Interestingly, trees growing in the dry savanna show higher numbers of vessel arranged in radial groups than in the humid savanna. The vessel sizes of *A. leiocarpus* in the humid savanna appear to be much smaller than in the dry savanna savanna. The ring boundaries of the species are demarcated by alternating bands of radially flattened fibres. Wide rings were generally distinct, but distinctiveness declined with decreasing ring width. *A. leiocarpus* rarely shows wedging rings, and if present they were determined by following the same procedure as in *A. africana*.

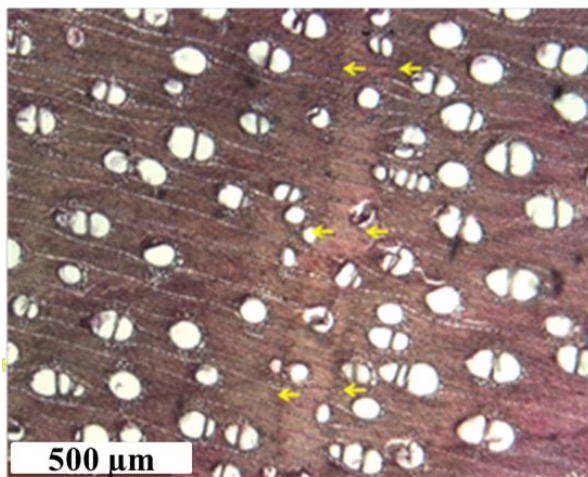


Humid savanna

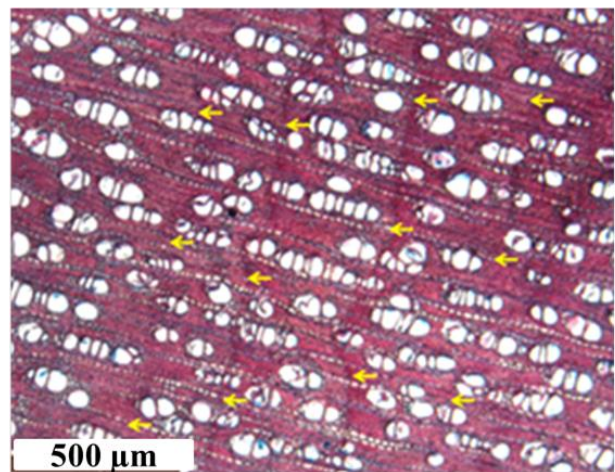


Dry savanna

*Afzelia africana*



Humid savanna



Dry savanna

*Anogeissus leiocarpus*

Figure 17: Transverse sections of *Afzelia africana* and *Anogeissus leiocarpus* in the humid and dry savanna zones of Ghana

Ovally-shaped objects are vessels; yellow arrows point to ring boundaries

### 3.3.2 Cross-dating of growth rings of riparian trees

Visual (Figure 18) and statistical (Table 21) cross-dating between radii of the same discs was successful for both *A. africana* and *A. leiocarpus* in the humid and dry savanna zones with significant TV-BP and GLK values. In the humid savanna zone, cross-dating of *A. africana* was successful for 7 out of 8 trees varying in lengths between 55 to 95 years. For *A. leiocarpus* of the same site, cross-dating was successful for 5 out of 7 trees also varying in length between 40 and 77 years. In the case of the dry savanna zone, cross-dating of *A. africana* was successful for 6 out of 7 trees of lengths ranging between 32 and 102 years. For *A. leiocarpus* of the dry savanna zone, cross-dating was successful for 7 out of 9 trees of lengths ranging between 26 to 42 years. In order to have an even number of cross-dated individuals for comparative analysis, the 5 best cross-dated individuals of each species were used for calculating the means of the ring width series or the sites chronologies. Further, all individuals that were less than 30 years in lengths were excluded from chronology building.

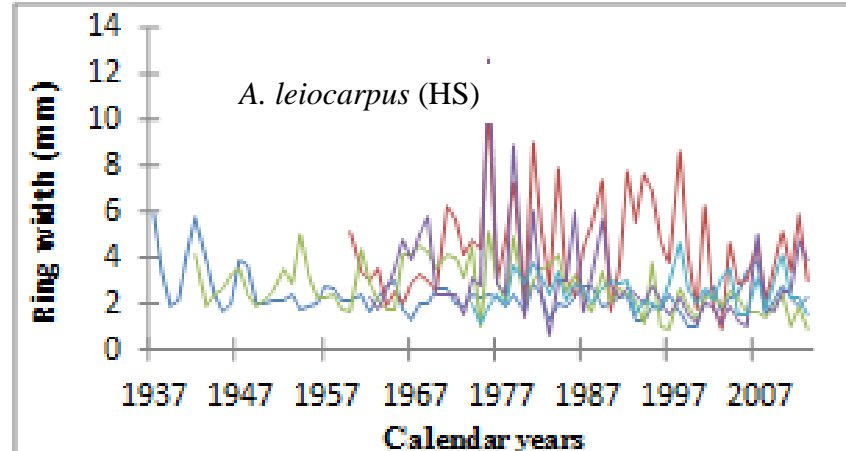
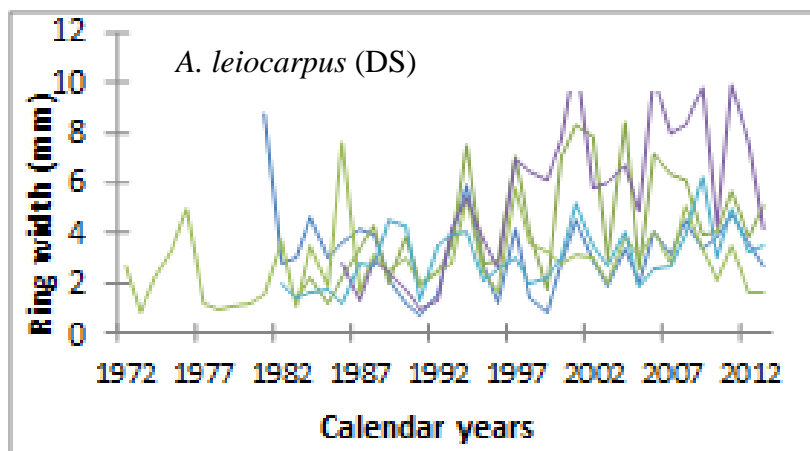
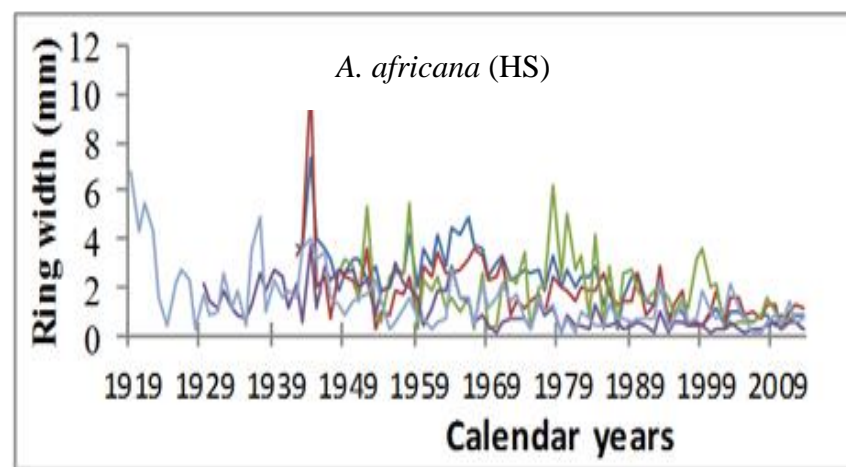
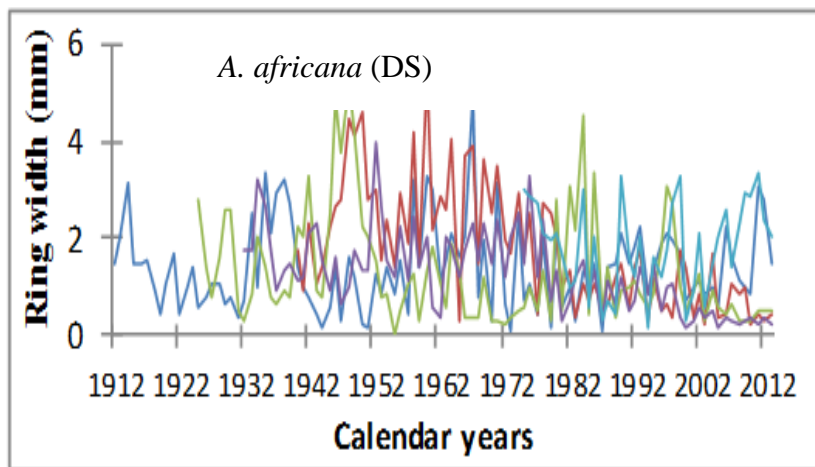


Figure18: Records of ring widths of the five best cross-dated individuals of *Azelia africana* and *Anogeissus leiocarpus* in the dry (DS) and humid (HS) savanna zones of Ghana

Table 21: Characteristics of tree ring series of *Azelia africana* and *Anogeissus leiocarpus* in the dry and humid savanna zones of Ghana

	Dry savanna		Humid savanna	
	<i>A. africana</i>	<i>A. leiocarpus</i>	<i>A. africana</i>	<i>A. leiocarpus</i>
No. trees	7	9	8	7
No. dated trees	6	7	7	5
Total length (years)	102	42	92	77
Diameter range (cm)	22-33	28-32	20-36	31-39
GLK	79	72	77	73
TV-BP	4.8	3.6	4.2	3.7
Mean (mm)	1.53	3.83	1.71	2.96
Standard error	0.10	0.31	0.13	0.16
Maximum (mm)	3.15	6.29	6.700	6.46
Minimum (mm)	0.35	0.98	0.32	1.42
Mean inter-series correlation	0.64	0.69	0.76	0.63
EPS	0.90	0.92	0.94	0.89

\*\*Computations are based on the contribution of 5 individual tree rings of each species

EPS is Expressed Population Signal , GLK: Gleichlaeufigkeit, TV-BP: t-value of Baillie-Pilcher

### 3.3.3 Radial growth of trees

Ranking of radial growth increments showed that *A. africana* in the humid savanna have the highest maximum growth followed by *A. leiocarpus* also in the humid savanna (Table 21). *A. leiocarpus* in the dry savanna followed up third in terms of maximum growth with the *A. africana* in the dry savanna having the smallest maximum growth. A comparison of the annual radial growth variation of *A. africana* and *A. leiocarpus* is presented in Figure 17. For both the dry and humid savanna zones, the mean annual growth of *A. leiocarpus* was significantly higher than for *A. africana* (Figure 19c & d). The results also showed no significant difference in the mean growth rate of *A. africana* between the humid and dry savanna zones (Figure 19a). In the case of *A. leiocarpus*, the mean growth rate in the dry savanna was significantly higher than in the humid savanna zone (Figure 19b).

### 3.3.4 Relationships between growth rings of trees in the humid and dry savanna zones

The detrended time series of *A. africana* in the humid savanna had the highest mean inter-series correlation and EPS (Table 21). This was followed by the *A. leiocarpus* in the dry savanna. The inter-series correlation and EPS values of the *A. africana* and *A. leiocarpus* respectively in the dry and humid savanna zones were similar with a small difference (0.01).

Correlation of detrended *A. africana* and *A. leiocarpus* time series collected from the same site in both the humid and dry savanna zones were positively weak as there were 1-time lags of the tree ring patterns in some years (Figure 20c and 20d). Nevertheless, correlation of *A. africana* and *A. leiocarpus* between the humid and dry savanna zones (Figure 20a and 20b) was positively strong as the species of the riparian habitats showed similar annual growth variability.

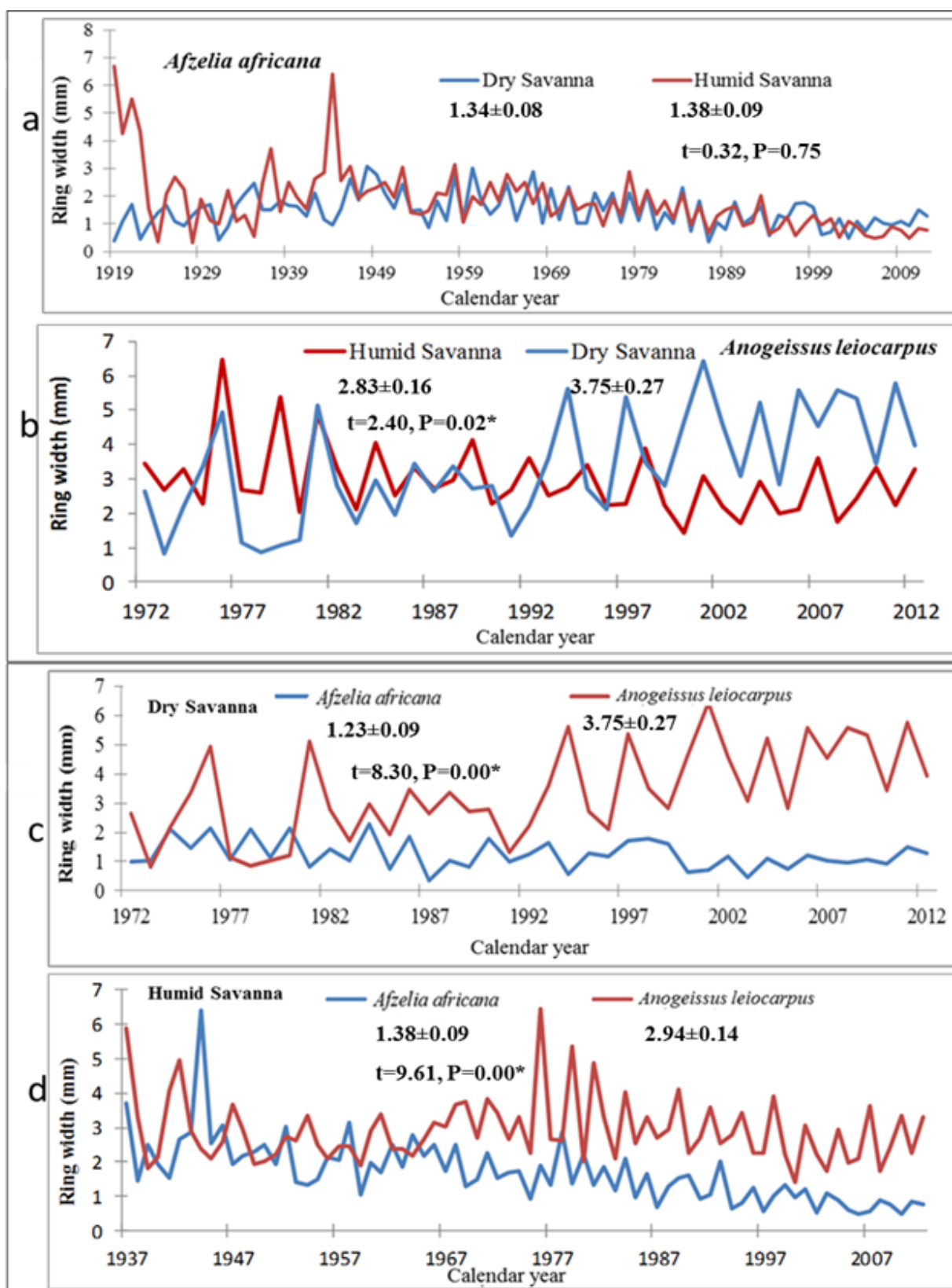


Figure19: Comparison of ring widths of *Afzelia africana* and *Anogeissus leiocarpus* in the dry and humid savanna zones of Ghana

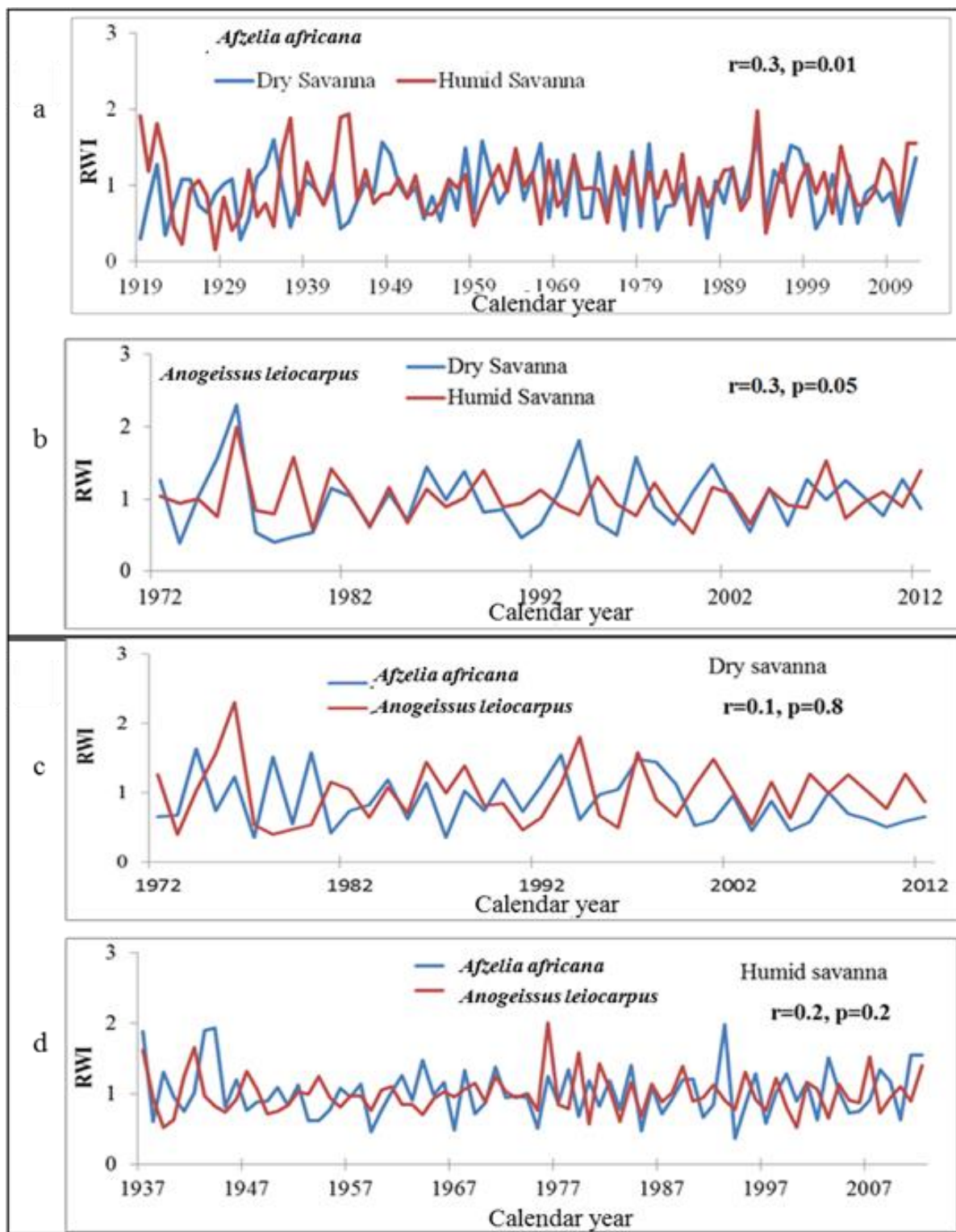


Figure20: Correlation of detrended time series of *Afzelia africana* and *Anogeissus leiocarpus* in the dry and humid savanna zones of Ghana

### 3.3.5 Relationships between growth rings of trees species and climatic parameters

- **Correlation of tree growth with precipitation variation**

The growth of *A. africana* and *A. leiocarpus* was positively correlated with the annual average precipitation (Figure 21). In the dry savanna, *A. africana* and *A. leiocarpus* respond strongly to precipitation in April, May, June and August. *A. leiocarpus* was positively correlated with June and August precipitation and negatively correlated with the precipitation of April. *A. africana* on the other hand had positive and negative relationships with May and June respectively. In the case of the humid savanna, *A. africana* and *A. leiocarpus* generally showed a positive response with precipitation for most of the months, except March.

- **Correlation of tree growth with temperature variation**

The study observed a strong negative correlation between the tree growth and temperature for both the humid and dry savanna zones (Figure 22). In the dry savanna, *A. africana* and *A. leiocarpus* were correlated to temperature in January, April, August, September and November. In the case of the humid savanna, *A. africana* and *A. leiocarpus* were strongly correlated to temperatures in January, February and April.

- **Correlation of tree growth with sea surface temperature variation**

There was weak positive correlation ( $r=0.3$ ,  $p=0.04$ ) of precipitation data from Ejura and Navrongo weather stations with annual sea surface temperature (SST) encircling the globe from 1961-2012. Similarly temperature showed in the two climatic stations showed weak significant negative correlation with the SST. In this regards also, the growth (RWI) of the species from the humid and dry savanna zones showed significant negative correlation with the annual SST (Figure 23). In both the humid and dry savanna zones, *A. africana* was more sensitive to the annual SST changes than the *A. leiocarpus*. *A. africana* showed strong negative correlation in the equatorial Atlantic as well as the Pacific and the Indian Ocean. The correlation of the SST with the growth of *A. leiocarpus* from the humid savanna was weak. The correlation of SST with *A. leiocarpus* of the dry savanna was strong and only possible for the Pacific and Indian Ocean.

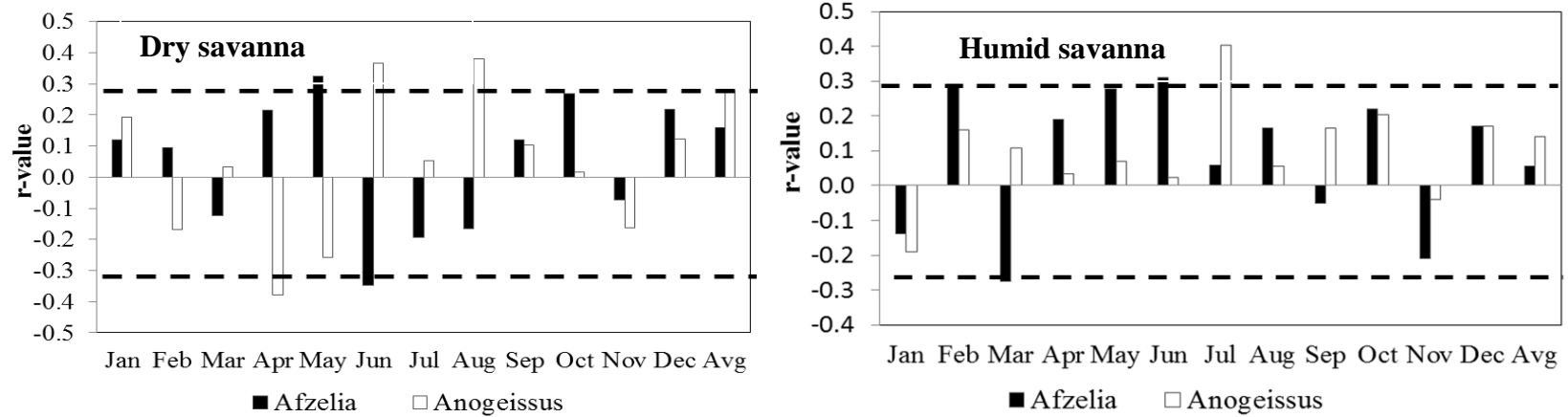


Figure 21: Correlation of *Afzelia africana* and *Anogeissus leiocarpus* individual chronologies from the dry and humid savanna to monthly and yearly average precipitation (Avg) data of climatic stations of each savanna types

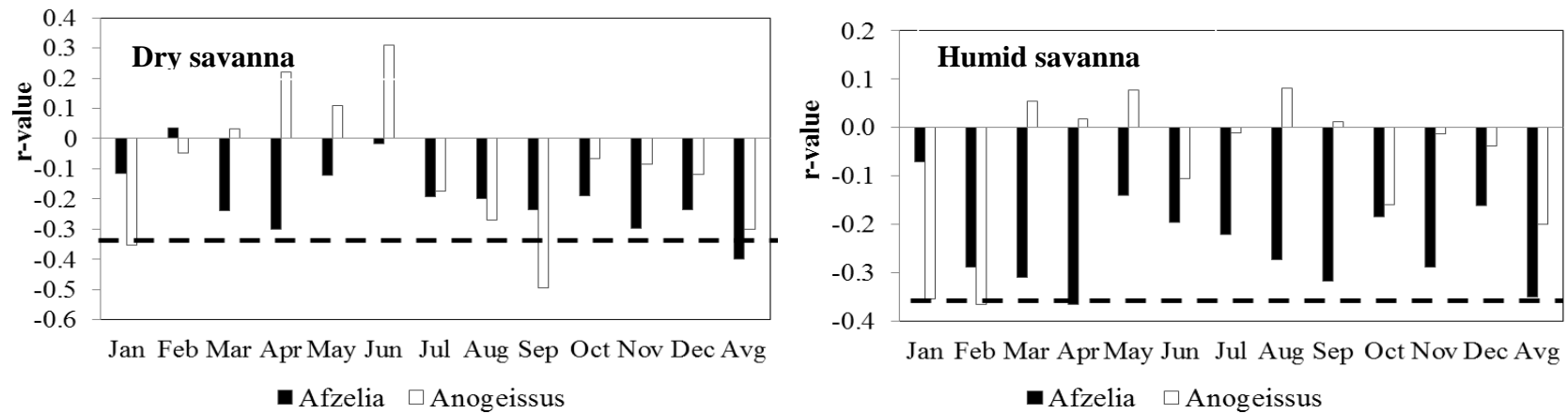
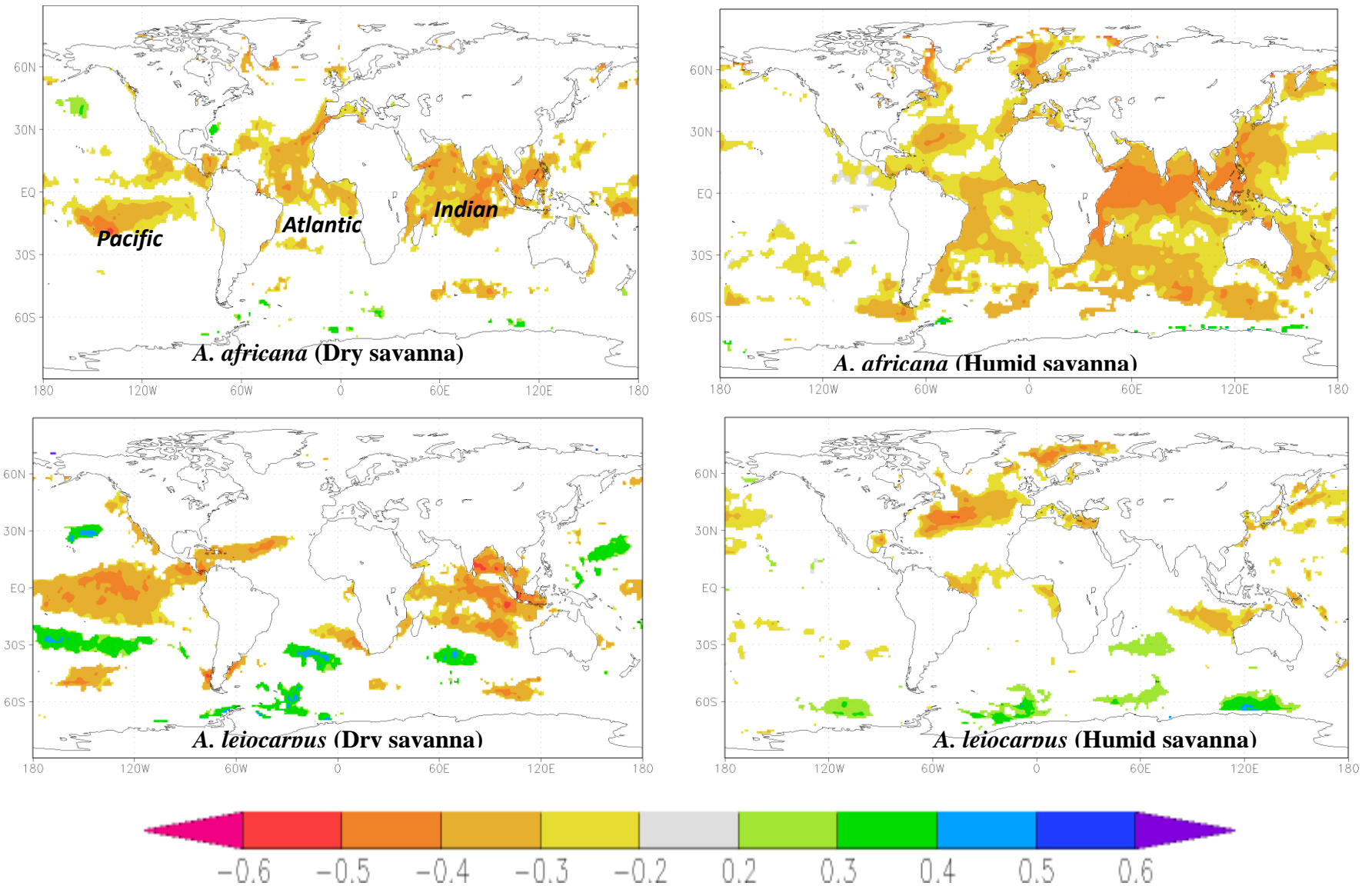


Figure 22: Correlation of *Afzelia africana* and *Anogeissus leiocarpus* individual chronologies from the dry and humid savanna to maximum mean monthly temperature (January to December) and yearly average (Avg) data of climatic stations of each savanna types

Dashed horizontal lines indicate significance ( $p \leq 0.05$ )



Scale bar shows correlation coefficient with a significant level  $\leq 0.05$ . **Period = 1961-2012**

Figure 23: Spatial correlation of growth rings of *Afzelia africana* and *Anogeissus leiocarpus* to Sea Surface Temperatures (SST)

### 3.3.6 Cyclicity in the growth of riparian trees

Morlet wavelet analysis on the detrended growth rings (RWI) of *A. africana* and *A. leiocarpus* of both the humid and dry savanna zones revealed a cyclic behaviour corresponding to the periods between 2-7 years. These growth fluctuations were concentrated in the years between 1960 and 2010. It was much more pronounced in the *A. leiocarpus* of the humid savanna zone and followed by *A. africana* in the dry savanna zone.

Figure 24 shows the Wave length spectra of *A. africana* and *A. leiocarpus* in the humid and dry savanna zones of Ghana. The black line outlines designate the 5% significance level. The ‘cone of influence,’ where edge effects become important and the results should be ignored, are shown in a lighter shade. Red and blue colours indicate high and low wavelet power spectrum values, respectively.

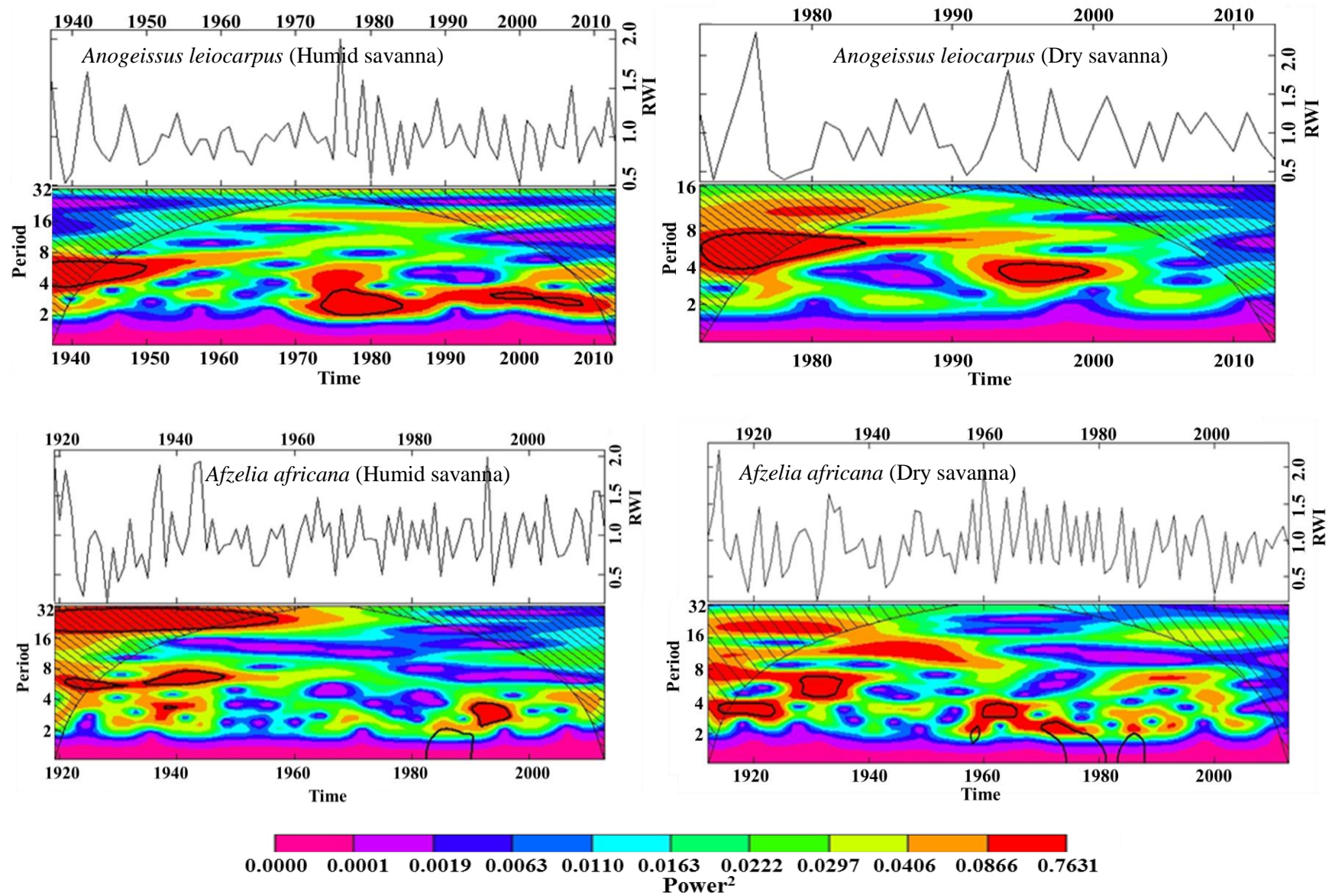


Figure 24: Ring Width Index (RWI) series and wavelet spectra with cone of influence (shaded area) for *Afzelia africana* and *Anogeissus leiocarpus* in the humid and dry savanna zones. Black contours show frequencies significant on the 0.05 confidence level.

### **3.4 Inter-annual variability of carbon isotope ratios of riparian trees in the humid and dry savanna zones to climatic parameters**

#### **3.4.1 Patterns of Carbon-13 of whole wood and cellulose**

Comparative analyses (Figure 25) of *A. africana* and *A. leiocarpus* in the humid and dry savanna zones show that on average Carbon-13 ( $\delta^{13}\text{C}$ ) of whole wood was isotopically lighter than the  $\delta^{13}\text{C}$  of cellulose. A positive correlation (Figure 25) was found between  $\delta^{13}\text{C}$  of whole wood and cellulose for all the species. However, the highest correlation was recorded for *A. africana* in the humid savanna. This was followed by the *A. africana* in the dry savanna. *A. leiocarpus* of the humid savanna followed up third with the *A. leiocarpus* in the dry savanna zone having the least correlations (Figure 25). The offset of the  $\delta^{13}\text{C}$  of whole wood and cellulose for *A. africana* and *A. leiocarpus* in the humid savanna were approximately 2 ‰. *A. africana* and *A. leiocarpus* in the dry savanna had offset of 1‰ and 2 ‰ respectively.

#### **3.4.2 Patterns of Carbon-13 in tree rings using whole wood**

Inter-annual patterns of Carbon-13 ( $\delta^{13}\text{C}$ ) of the four individuals of the *A. africana* and *A. leiocarpus* from both the humid and dry savanna zones were well synchronized with GLK and TV-BPs of each of the series greater than 60% and 9 respectively (Figure 26; Table 22). The highest GLK was recorded for *A. africana* in the humid savanna zone. This was followed by *A. leiocarpus* in the dry savanna. *A. africana* and *A. leiocarpus* of the dry and humid savannas respectively had the lowest GLKs (Table 22).

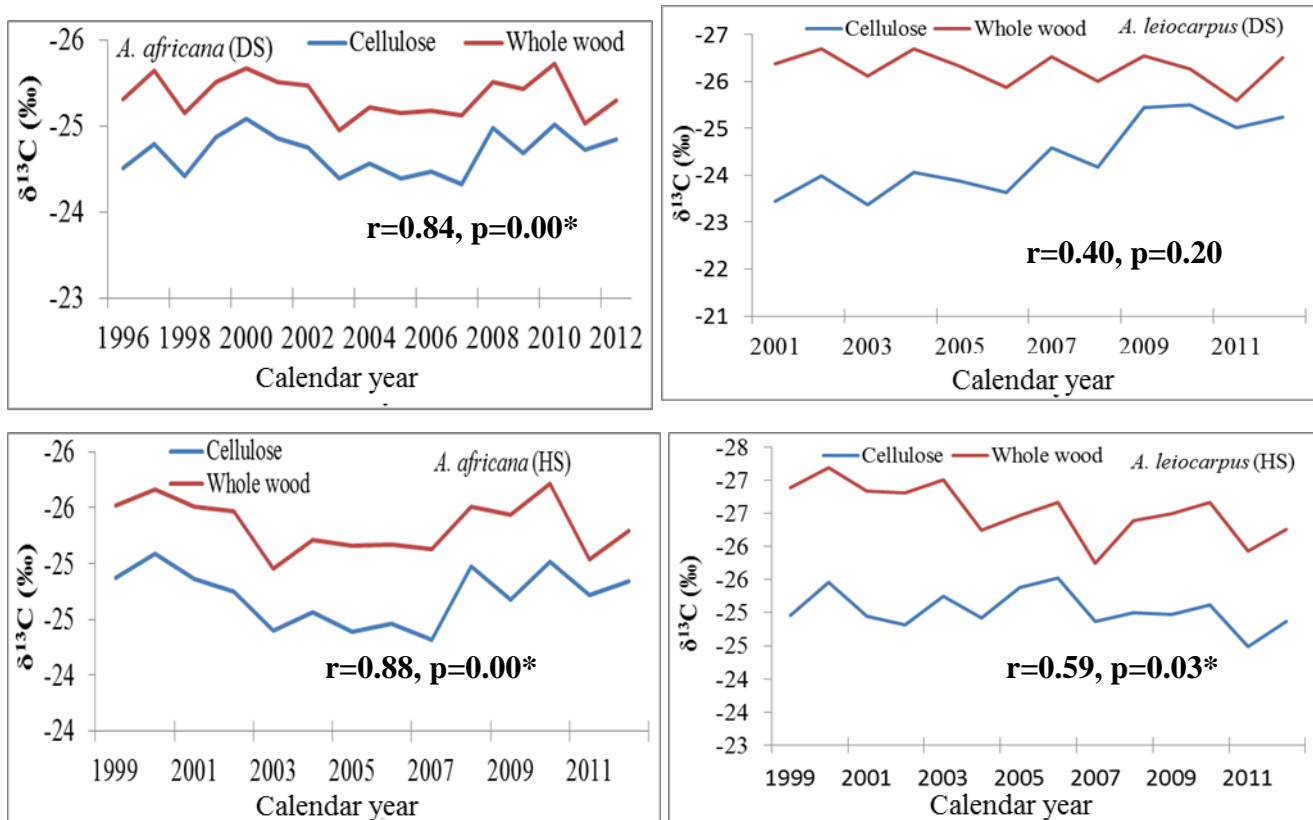
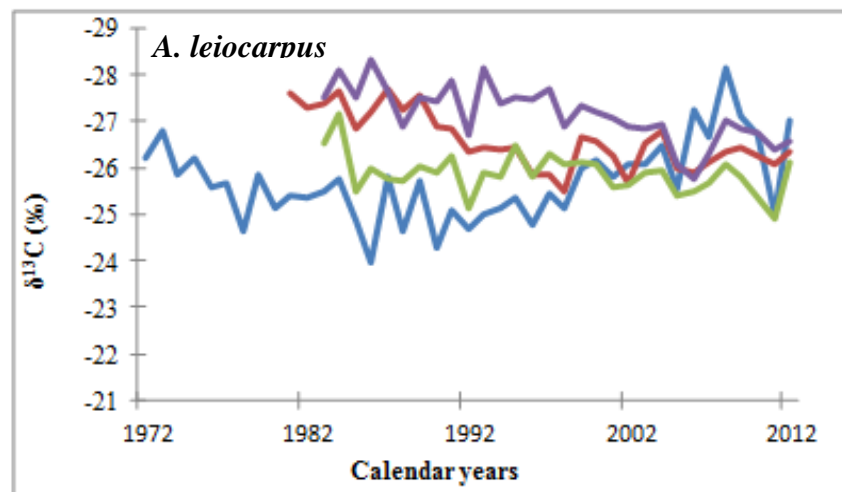
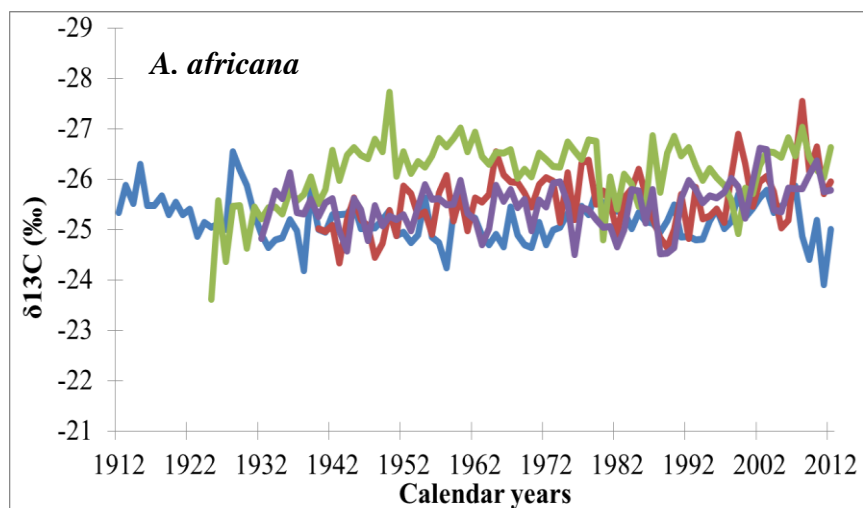
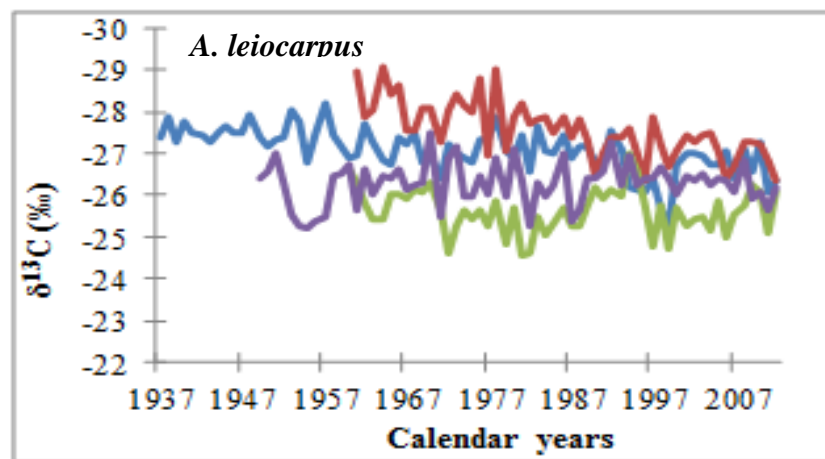
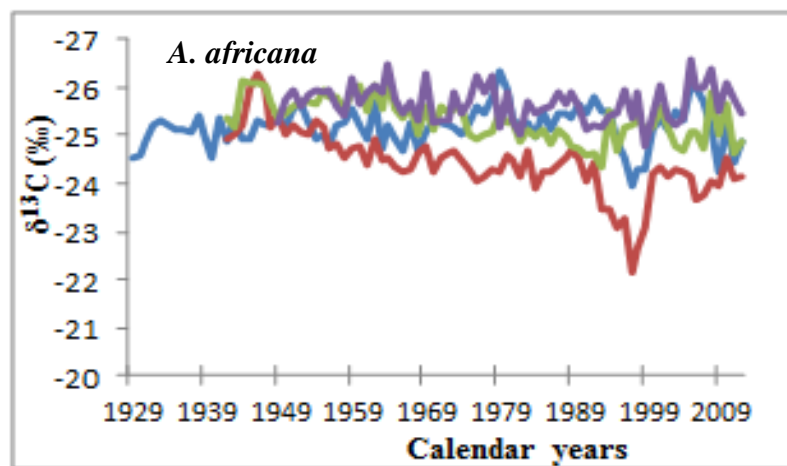


Figure 25: Correlation of the pattern of Carbon-13 ( $\delta^{13}\text{C}$ ) time series in whole wood and cellulose of *Azelia africana* and *Anogeissus leiocarpus* in the dry (DS) and humid (HS) savanna zones of Ghana

Significant at  $p \leq 0.05$



Dry savanna zone



Humid savanna zone

*Different colors represent different individuals of trees*

Figure 26: Time series of individuals of species-specific Carbon-13 ( $\delta^{13}\text{C}$ ) of *Azelia africana* and *Anogeissus leiocarpus* in the dry and humid savanna zones of Ghana

Table 22: Statistical characteristics of Carbon-13 ( $\delta^{13}\text{C}$ ) series of *Afzelia africana* and *Anogeissus leiocarpus* in the dry and humid savanna zones of Ghana

	Dry		Humid	
	<i>A. africana</i>	<i>A. leiocarpus</i>	<i>A. africana</i>	<i>A. leiocarpus</i>
Whole wood ( $\delta^{13}\text{C}$ )				
Total length	101	41	91	76
GLK	65	81	74	65
TV-BP	11	7.6	9.0	9.4
Mean (‰)	-25.64	-26.32	-25.14	-26.59
Std. Dev.	0.65	0.69	0.58	0.63
Maximum (‰)	-24.58	-24.62	-24.17	-25.80
Minimum (‰)	-26.94	-27.16	-25.90	-27.90
Inter-series correlation	0.63	0.56	0.66	0.61
EPS	0.87	0.84	0.89	0.86
Cellulose ( $\delta^{13}\text{C}$ )				
Mean (‰)	-24.18	-25.46	-23.53	-25.04
Std. Dev.	0.2	0.45	0.26	0.28
N	17	12	14	14

N=Number of samples, EPS is Expressed Population Signal, GLK: Gleichlaeufigkeit, TV-BP: t-value of Baillie-Pilcher

### 3.4.3 Patterns of Carbon-13 in whole wood of trees in the humid and dry savanna zones

The Carbon-13 ( $\delta^{13}\text{C}$ ) (Figure 27) of *A. africana* in the humid savanna had the highest mean inter-series correlation and EPS (Table 23). This was followed by the *A. africana* in the dry savanna. The inter-series correlation and EPS values of the *A. leiocarpus* had the dry savanna zone had the least interseries correlation and EPS.

The study compared  $\delta^{13}\text{C}$  of *A. africana* and *A. leiocarpus* in the humid and dry savanna zones. Correlation of the  $\delta^{13}\text{C}$  of *A. africana* and *A. leiocarpus* collected from the humid savanna was strong. Correlation of  $\delta^{13}\text{C}$  of *A. Africana* from both humid and dry savanna zone was strong (Figure 25). Nevertheless, correlation of *A. africana* and *A. leiocarpus* of the dry savanna was weak as there one time lag in some years. No significant correlation was observed for *A. leiocarpus* between the humid and dry savanna zones (Figure 27).

Comparison of species specific means of  $\delta^{13}\text{C}$  discrimination levels (Table 23) showed that in both the dry and humid savanna zones, the *A. africana* (evergreen) species are more enriched in  $\delta^{13}\text{C}$  whereas *A. leiocarpus* (deciduous) is more depleted in  $\delta^{13}\text{C}$ . Comparison of the same species between the two savanna types showed that *A. africana* in the humid savanna is more enriched in  $\delta^{13}\text{C}$  whereas it is more depleted in the dry savanna. In the case of *A. leiocarpus*, there was virtually no significant difference in the  $\delta^{13}\text{C}$  values between the humid and dry savanna zones.

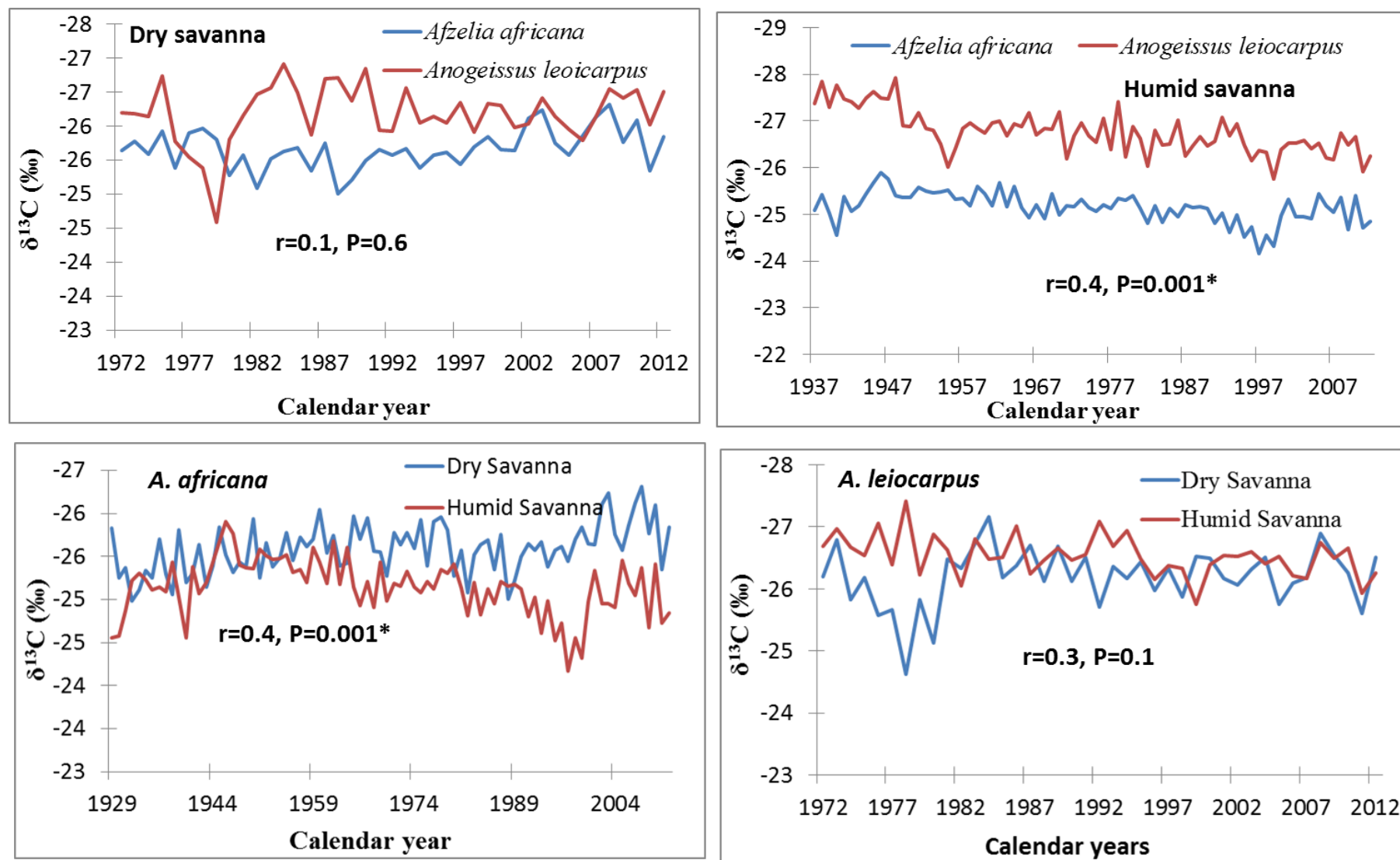


**Figure 27:** Comparison of Carbon-13 ( $\delta^{13}\text{C}$ ) of *Afzelia. africana* and *Anogeissus leiocarpus* in both the humid and dry savanna zones

Table 23: Comparison of Carbon-13 values of the *Afzelia africana* and *Anogeissus leiocarpus* in both the humid and dry savanna zones

For each comparison, the length was adjusted to the common period (N)

Savanna type	Mean	SE	N	t-value	d. f.	P-value
<u><i>Afzelia Africana</i></u>						
Dry savanna	-25.66	0.04	50	10.98	98	0.00*
Humid savanna	-25.03	0.04	50			
<u><i>Anogeissus leiocarpus</i></u>						
Dry savanna	-26.26	0.09	35	1.81	68	0.08
Humid savanna	-26.49	0.09	35			
<u>Dry savanna</u>						
<i>A. leiocarpus</i>	-26.20	0.09	35	3.908	68	0.00*
<i>A. Africana</i>	-25.74	0.07	35			
<u>Humid savanna</u>						
<i>A. leiocarpus</i>	-26.60	0.07	50	19.26	98	< 0.00*
<i>A. Africana</i>	-25.03	0.04	50			

\*\*SE=Standard Error, N=Number of observation

### 3.4.4 Relationship between Carbon-13 in whole wood of trees and climatic parameters

#### 1. Correlation of Carbon-13 ( $\delta^{13}\text{C}$ ) of trees to temperature

Temperature generally had significant positive correlation with Carbon-13 ratios of the trees. There were however, site specific differences. Example, in the dry savanna, *A. africana* and *Anogeissus leiocarpus* primarily had significant positive correlation with temperature from January to July. Exception was August and December where the plant had negative relationship with carbon-13 (Figure 28). *A. leiocarpus* rather had significant positive correlation for the month of January and negative correlation for March. In the humid savanna, *Anogeissus* had positive correlation with temperature for February, April, August and September. *A. africana* on the other hand only had positive correlation with temperature in November.

#### 2. Correlation of Carbon-13 ( $\delta^{13}\text{C}$ ) of trees to precipitation

Carbon-13 in *A. africana* and *A. leiocarpus* of the humid and dry savanna zones had mixed significant positive and negative relationships with precipitation variables (Figure 29). In the dry savanna, *A. africana* had strong negative correlation with precipitation in the month of July and October. In this region, *A. leiocarpus* only had significant negative relationship with precipitation for September. In the case of the humid savanna, *A. africana* had significant negative correlation with precipitation for the months of January and March. *A. leiocarpus* on the other hand had significant negative correlation with precipitation for the month of March and positive correlation for the month of January.

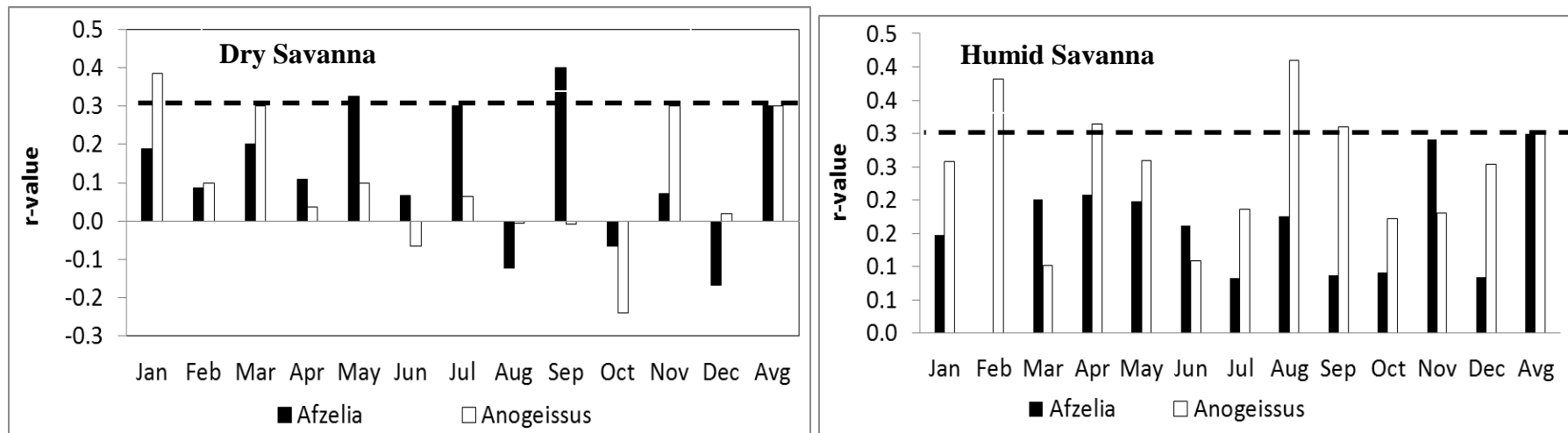


Figure 28: Correlation of *Afzelia africana* and *Anogeissus leiocarpus* individual chronologies from the dry and humid savanna to temperature

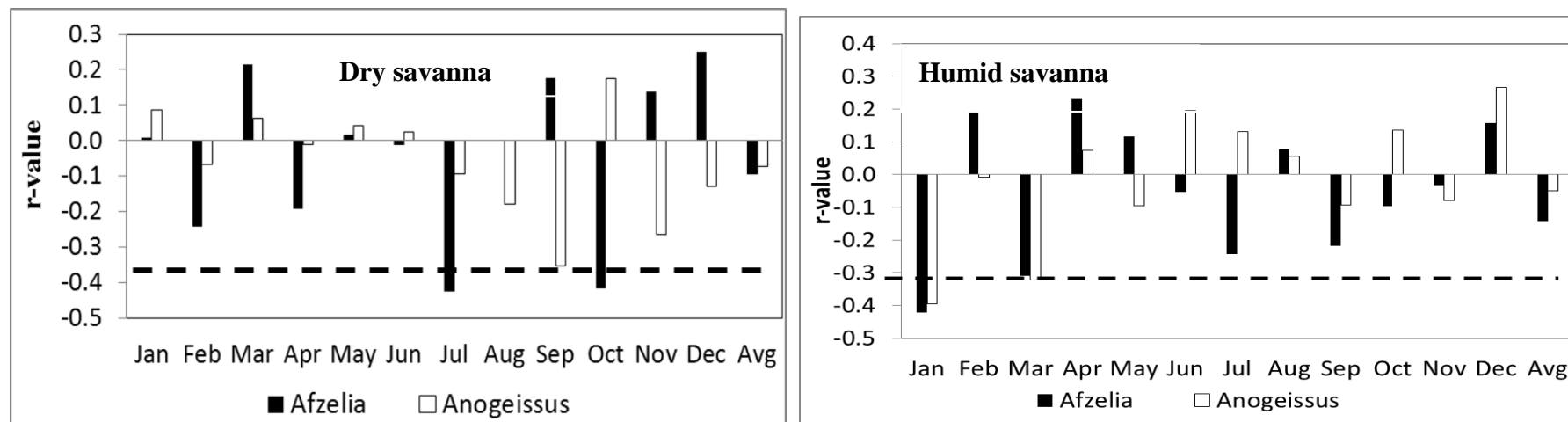


Figure 29: Correlation analysis of *Afzelia africana* and *Anogeissus leiocarpus* in both the humid and dry savanna zones with precipitation

Variables are monthly precipitation data (January-December) and yearly average (Avg). Significance levels shown as dashed lines ( $p \leq 0.05$ ).

## **IV. DISCUSSION**

## 4.1 Forest cover loss in Afram and Tankwidi riparian catchments

### 4.1.1 Map accuracies

The confusion matrix for Afram and Tankwidi catchments for the 2014 classifications were improvement over the 2000 classification maps (Table 6&7 and 9&10). This could be as a result of the use of current validation dataset as observed during fieldwork as opposed to the 2000 classifications where references were made to historic Landcover map and local knowledge in the collection of the validation data. For the 1986, 2000 and 2014 classifications, errors were minimized by choosing only two landcover classes (forest/non-forest), with spectrally distinct signatures. The accuracies of image classifications (2000 and 2014) for the Afram catchment in this study exceed the 85% overall accuracy threshold used by the US Geological Survey to determine acceptability (**Anderson *et al.*, 1976; Chai *et al.*, 2009**). In the case of the Tankwidi catchment, classification accuracy values for the 2000 and 2014 images were lower than the acceptable threshold (**Anderson *et al.*, 1976; Chai *et al.*, 2009**). Nonetheless, the values in the Tankwidi catchment are similar to studies reported in other savanna landscapes (**Ruelland *et al.*, 2010; Schetter & Root, 2011**). Generally, the lower accuracy of mapping in the savannas are as a result of the heterogeneity of forest patches, which according to **Ruelland *et al.*, (2010)** is difficult to detect in the savanna matrix by using medium resolution satellite image such as Landsat.

### 4.1.2 Forest cover change

Forest cover change assessment is an important starting point for understanding degradation patterns in any ecosystem. The result of the landcover change analysis shows the deforestation of both Afram and Tankwidi river catchments from 1986 through 2000 to 2014 (Table 8 and 11; Figure 13 and 14). The deforestation rate per annum of the Afram catchments (1.7 %) was similar to the national rate (1.3-2.3%year<sup>-1</sup>) (**FAO, 2007; Edusah, 2011**) but the rate of the Tankwidi was higher (4.1%year<sup>-1</sup>). This forest loss is however, attributable to farming activities in the catchments that remove woody vegetation and in turn replace them with crops. Also the farmers depend on fuelwood as their main source of energy, and the increasing demand by the populace contribute to the reduction in forest area (**Edusah, 2011**). Again due to the uncontrolled slash-and-burn activities of farmers which involve clearing of tree vegetation followed by burning, wildfire is prevalent within the protected reserve and farmlands of the study area, causing tremendous forest loss annually (**FAO, 2007**).

The deforestation observed in our study occurred in both farmlands and protected reserve areas (Figure 13& 14). This shows that the protected areas in both Afram and Tankwidi catchments have not been completely successful at preventing habitat destruction within its boundary. The finding is not peculiar to the study areas. This is because evidence of deforestation has been reported in protected areas across the tropics (**Chai *et al.*, 2009; Traore *et al.*, 2012**). Consequently, concerns have been raised on the effectiveness of protected area management for biodiversity conservation (**Chai *et al.*, 2009; Traore *et al.*, 2012**). The effect of the deforestation includes changes in elements such as light and wind which influence the microclimatic conditions of forest remnants to exert a strong effect on biological diversity (**Goetze *et al.*, 2006**). Additionally, the deforestation result in the modification of habitat structure (**Goetze *et al.*, 2006**), resource availability and distribution (**Morelli, 2013**), energy and nutrient cycling, temperature and moisture states of the forests (**Morandin & Winston, 2006**).

Generally, landcover conversions have significant effect on riparian ecosystems. Ecological effects of landcover conversions include changes in soil quality, soil erosion, water quality, biodiversity loss and habitat availability. As reported by **Mantyka-Pringle *et al.* (2012)**, expansion of agricultural area has significant impacts on riparian ecosystems. The process causes deforestation and lead to the loss of important riparian tree species including the sensitive ones that depend on water (**Azihou *et al.*, 2013**). The nutrient inputs from agricultural fields into rivers can lead to loss of biodiversity, shift in the structure of food chains and impairment of fisheries (**Schweiger *et al.*, 2011**). The landcover conversion could also lead to reduction in soil organic matter, depletion of nutrients in riparian soils and consequently alter the global carbon cycle. These effects have been reported in riparian catchments in other parts of the world (**Kayranli *et al.*, 2012; Mantyka-Pringle *et al.*, 2012**). It remains to be seen the impact of the deforestation on biological diversity and the functions of Afram and Tankwidi riparian forests.

## **4.2 Woody species diversity and structure in protected area and farmlands in the humid and dry savanna zones**

### **4.2.1 Plant density, basal area and size-class distribution**

The reversed “J” shaped structure (Figure 15 & 16) of the tree sizes of the riparian woody species in the two protected areas (humid and dry savanna zones) and the farmlands in the humid savanna zone suggests that they have the potential to regenerate naturally and face no danger of extinction (**Sambare *et al.*, 2011**). This observation is typical of secondary forests whereby light reaching the forest floor is able to support higher plant regeneration. The lower number of juveniles in the farmland along the Tankwidi river (dry savanna, Figure 16) however, suggested that the riparian buffer on the farmland is not being reproductive and resulting from the clearing of vegetation for farming activities. According to **Lykke (1998)**, for a plant community to maintain itself, it needs to have abundant juveniles which will recruit into adult size classes. This type of species distribution gives the plant community a stable structure for the sustenance of the ecological succession of riparian forests (**Sambare *et al.*, 2011**).

The lower density and higher average DBH and basal area of trees along the Tankwidi river (dry savanna) (Table 12) in the farmlands can be explained by the large old trees. From discussion with farmers, those trees are deliberately preserved because of their socio-economic importance. Generally, the decline in the density of woody species on farmlands in both Afram and Tankwidi rivers may be partly caused by the repeated manual weeding of the riparian area for crop cultivation (**Ceperley *et al.*, 2010**). Also the use of agro-chemicals for weeding may have affected the regenerative capacity since some of these chemicals kill the seeds that are dispersed (**Fischer *et al.*, 2009**; **Ceperley *et al.*, 2010**).

### **4.2.2 Plant diversity and similarity in protected areas and farmlands**

Shannon's diversity index is usually found to fall between 1.5 and 3.5 and is rarely above 5.0 (**Magurran, 2004**). This means that the Shannon values found in this inventory in protected areas and farmlands along both Afram and Tankwidi rivers are in the expected range. The fact that the Shannon index of farmlands were lower than that in the protected areas in the two riparian catchments confirm the negative effects of forest cover conversions of both Afram and Tankwidi river catchments. This could be attributed to the poor enforcement of the policy (**Government of Ghana, 2011**) prescription prohibiting agricultural activities in riparian buffer zone in the study areas.

The Shannon index of the riparian woody species in the protected areas of the two river catchments were higher because the controlled human activities in those sites reduce disturbance on plant species than the lands outside (**Okiror *et al.*, 2012; Traore *et al.*, 2012**). In contrast to this research, it has been found in other studies that the species diversity value on agricultural lands is enhanced by the deliberate preservation of trees or moderate disturbance of forests by farmers (**Boakye *et al.*, 2012; Traore *et al.*, 2012; Gray *et al.*, 2014**). Generally, the high diversity of riparian forest is driven by the intensity and frequency of floods, small-scale variation in topography, soils and canopy structure of the area that create a diversity of habitats for a wide variety of species to co-exist (**Sambare *et al.*, 2011**).

The similarity in plant species composition was generally higher between protected area and farmlands along the Afram river than the Tankwidi catchment. This low similarity between the site in the Tankwidi catchment could be explained by the difference in the agricultural disturbance which affects the habitat conditions of riparian forests.

The low similarity and diversity in the woody plants in the protected areas from the humid to the dry savanna zone may be as a result of many interacting biotic and abiotic factors. According to **Spasojevic *et al.* (2014)**, diversity is higher in places where climate is warm and moist rather than arid. This suggested that the abundant water and solar energy in the humid savanna zone permit a wider range of functional strategies and in turn higher numbers of species are able to tolerate such benign environments, whereas only smaller subsets of species can tolerate the more demanding conditions of aridity in the dry savanna (**Natta *et al.*, 2003**). **Poorter *et al.* (2004)** indicated that the amount of rainfall alone accounts for 74% of the variation in species composition at the vegetation level. In addition, the presence of different ecosystems in the humid savanna (mosaics of forest and grassland) provides conditions for different species to thrive (**Poorter *et al.*, 2004**). Studies have shown that plant shift their distribution range by spreading into areas with good representation of their ecological niche (**de Chazal & Rounsevell, 2009; Mantyka-Pringle *et al.*, 2012**).

#### **4.2.3 Relationships between woody plant density and soil properties**

The similarities in the soil textural class (sandy loam) in the different land uses (protected area and farmland) in both Afram (humid savanna) and Tankwidi (dry savanna) riparian forests indicated (Table 13) the homogeneity of soil forming processes and similarity of parent materials. Erosion, deposition

and weathering could have however, influenced the variations in the proportions of sand, clay and silt in both study sites (**Asiedu *et al.*, 2013; Dawoe *et al.*, 2014**).

The soil bulk densities ( $1.1\text{--}1.6\text{ g cm}^{-3}$ ) in both Afram and Tankwidi riparian forests under protected areas and farmlands (Table 14) were within the range reported in forests in Ghana (**Ampofo *et al.*, 2006; Dawoe *et al.*, 2014**). **Asiedu *et al.* (2013)** observed that the lower the bulk density, the more productive the soil is, as it allows for easy root penetration. In soils with higher bulk density, plant root growth is restricted because such soils serve as mechanical resistance to root penetration and limit the amount of air and water. In such soils, roots must exert greater force to penetrate, thereby lowering root length.

The lack of differences (Table 16 & 17) in soil chemical properties (C, N, P, K and pH) between protected area and farmland in spite of the reduced plant diversity and density in the latter along the Afram riparian forests (humid savanna) suggest that the ecological integrity of the riparian forests in retaining nutrients have not been completely destroyed. The disturbances on farmland may be minimum and recent to have resulted in such significant losses in chemical properties. Further soil nutrients washed from upstream could have supplemented the soil chemical conditions of the farmland riparian area (**Palmer *et al.*, 1996; Dawoe *et al.*, 2014**). C/N ratio is an index of nutrient mineralization where low C/N ratio indicates a high rate of mineralization (**Dawoe *et al.*, 2014**). This means that along the Afram river, protected area has high mineralization than the farmlands.

The reduction in key soil nutrients measures such as C and K in farmlands as opposed to that in the protected area along (Table 17) the Tankwidi river (dry savanna) reduces its ecological function as nutrient buffer. The low carbon content in the farmland may be attributed to: (1) the intensification of agricultural activities that remove forest and reduce the amount of organic material being returned to the soil; (2) the high rate of oxidation of soil organic matter; (3) continuous cultivation without fallowing; and (4) loss of organic matter by water erosion (**Dawoe *et al.*, 2014**). The annual recurrent wildfire of the adjacent savanna woodland in protected area could have also influenced the washing down of bases in the form of ash to the riparian area to increase its potassium content as opposed to that in the farmland. The higher C/N in the protected area of the Tankwidi river indicated increase in organic carbon gain and less nitrogen mineralization than the farmlands. Nitrogen and phosphorus did

not show any significant difference perhaps due to the addition of fertilizers to improve crop production in the overused agricultural landscape of the northern savanna of Ghana.

Given the high diversity, richness and density of woody plants in protected area in the humid savanna zone, it would have been expected that the soil nutrient attributes would be higher than the riparian buffer in protected area in the dry savanna zone. This is because diverse forests are known to contain species that use resources in a complementary manner, contributing to greater root biomass and soil nutrient retention throughout a growing season and across the soil profile (**Scherer-Lorenzen *et al.*, 2003**). The results (Table 18 & 19) however, showed that the soil of riparian buffer in the protected area in the dry savanna was richer in the soil nutrient attributes (C, K) than that found in the humid savanna zone. Carbon was lower in the humid savanna due to leaching or erosion of the dissolved nutrients in the soil profile with percolating water owing to the sandy nature of soils (**Dawoe *et al.*, 2014**). High addition of ash from upland savanna vegetation could have influenced K concentration in protected area in the dry savanna than the humid savanna zone. Phosphorus (P) is the primary limiting nutrients for plants in tropical soils, because of sorption of phosphate onto Al- and Fe-hydroxides where it is potentially, but not readily available to plants. It circulates rapidly between plant and soil through the litter fall and therefore the high plant density in the humid savanna could have resulted in significantly high concentration of P than in the dry savanna. Additionally, the relatively high soil acidity in the humid savanna as oppose to the dry savanna also increases nutrient leaching by restricting the rooting depth of sensitive plants. Soils in high rainfall areas are subject to nitrate leaching which is a significant source of soil acidification (**Dawoe *et al.*, 2014**).

In both Afram and Tankwidi riparian forests, soil C, N, P, CN ratio, pH and soil moisture (Table 20) were the most important parameters that had much significant relationships with the density of the riparian woody plants. It has been reported that the avoidance of deforestation prevents the exposure of riparian land surface which invariably minimizes decomposition and hence limits carbon release from soil microbial activities (**Scherer-Lorenzen *et al.*, 2005; Reddy & Delaune, 2008; Dawoe *et al.*, 2014**). Further, variations of soil moisture in riparian areas create different niches for different organisms. K had little influence on the density of species perhaps because the nutrient concentration of the riparian area are partly influenced by nutrients washed from upstream and upland areas (**Tilman, 1982; Mittelbach *et al.*, 2001; Enanga *et al.*, 2011; Nadeau & Sullivan, 2015**).

### 4.3 Relationship between radial growth of riparian woody species and climatic parameters in the humid and dry savanna zones

#### 4.3.1 Wood anatomical features

*A. africana* (evergreen) and *A. leiocarpus* (deciduous) in both the humid and dry savanna zones (Figure 17) showed distinct growth rings resulting from the periodicity of growth dormancy induced by seasonal precipitation patterns with a distinct dry season (**Schöngart *et al.*, 2006**). A dry season of more than three months with less than 60mm of monthly rainfall is found to be sufficient to invoke cambial dormancy (**Gebrekirostos *et al.*, 2008**). Generally, during the dry season, when plant water potential reaches the permanent wilting point, deciduous species shed their leaves. At this period both evergreen and deciduous species enter a state of cambial dormancy, which implies formation of visible growth boundaries (Gebrekirostos *et al.*, 2008). Previous studies in Benin and Cote d'Ivoire have also found the formation of growth rings in *A. africana* and *A. leiocarpus* and other tropical savanna tree species (**Schöngart *et al.*, 2006**).

The growth rings of *A. africana* (Figure 17) marked by parenchyma bands are more distinct than those of *A. leiocarpus* formed by tangential bands of fibres. Their distinctiveness is controlled by the differences in wood anatomy which are defined by the genetic constitution of the species (**Gebrekirostos *et al.*, 2008**). On the one hand, the primary function of parenchyma is starch storage for bridging the dry season. Parenchyma bands can promote conduction when growth is renewed and the provision of starch can support rapid flushes of growth, flowering, and fruiting (**Schöngart *et al.*, 2006**). On the other hand, fibres provide mechanical support and stability to the tree. The vessels grouping of *A. africana* and *A. leiocarpus* indicates a special adaptation of the species that facilitate transportation of water. In contrast to *A. leiocarpus*, *A. africana* maintains large vessels for the transportation of a large volume of water. *A. leiocarpus* maintained a higher number of smaller sized vessels in order to ensure sufficient transportation of water and minerals for tree growth while at the same time minimizing the risk of cavitation during the dry season (**Gebrekirostos *et al.*, 2008**; **Tomlinson *et al.*, 2014**).

#### 4.3.2 Cross-dating of growth rings

The successful cross-dating of ring width patterns of individuals of the same species (*A. africana* and *A. leiocarpus*) in the humid and dry savanna zones were indications that one ring is formed per year and that a common local factor (climate) could be influencing the ring formation. The GLK and TV-

BP values (Table 21; Figure 18) of the cross-dating process in this research were above the threshold generally applied in dendrochronology in temperate and boreal regions (TV>3.5 and GLK>70%) (**Trouet *et al.*, 2010**). The high Expressed Population Signal (Table 21) of the detrended time series of *A. africana* and *A. leiocarpus* in both the humid and dry savanna zones exceeded the recommended threshold 0.85 (**Wigley *et al.*, 1984**). This means that the chronologies of *A. africana* and *A. leiocarpus* in both the humid and dry savanna are reliable, sufficiently well replicated and showing a strong degree of consistency in the variability found among trees.

The significant correlation of each of *A. africana* and *A. leiocarpus* trees between the humid and dry savanna zones (Figure 20a & b) suggested that the growth of the species are influenced by a similar climatic fluctuation caused by the movement of the inter-tropical convergence zone (ITCZ) that distribute precipitation in the Volta basin of Ghana (**Schongart *et al.*, 2006**). ITCZ is the inter-phase of two air masses: the North-East Trade Winds and the South-West Monsoons. The North-East Trade Winds, known as the Harmattan, blow from the interior of the Africa continent and are dry and dusty. In contrast, the South-West Monsoons, blow from over the seas and are moist. The ITCZ moves northwards and southwards across the study area from about March to October when precipitation is received in the region (**UNEP-GEF, 2012**).

The weak correlation between *A. africana* and *A. leiocarpus* of the same site (Figure 20c & d) could be attributed to their differences in water use strategies resulting in different responses to local climatic conditions. Although species specific rooting depth ranges was not found in the literature, **Hasselquist *et al.* (2010)** indicated that evergreen species of Mexico have capacity to use deeper ground water to overcome seasonal water limitation than deciduous trees. Similarly, **Jackson *et al.* (1995)** and **Meinzer *et al.* (1999)** showed that evergreen species tap deeper water sources compared to deciduous species in Panama.

#### **4.3.3 Radial growth**

The higher growth rate of the *A. leiocarpus* compared to the *A. africana* in both savanna types (Figure 19c & d) may be driven by its high specific leaf area that maximise light interception and greater nitrogen concentration per unit leaf area for greater photosynthetic rate (**Ruiz-Robledo & Villar, 2005**). Deciduous may have adopted a strategy for avoiding drought and maximizing resource capture during a limited growing season and then avoids stress by shedding some of its leaves in the dry season.

Deciduous species may also have high root water content and such water storage in roots has been found to increase the drought survival of the species (**Poorter & Markesteijn, 2008**). Further the deciduous species allocate substantial carbohydrate resources to storage in their roots to support seasonal regrowth and this allocation is at the expense of allocation to leaf mass. *A. africana*, having evergreen characteristic have high biomass investment in enduring organs, minimize cavitation and transpiration in order to extend the functional longevity of their leaves to persist under dry conditions (**Tomlinson et al., 2014**).

The lack of significant differences in the mean growth of *A. africana* between the humid and dry savanna zones (Figure 19a) (**Gebrekirostos et al., 2008**) and the higher growth rate of *A. leiocarpus* of the dry savanna in comparison to the same tree in the humid savanna (Figure 19b) is an indication that species in drier environment can have higher growth rates if they are given suitable water conditions. In arid environments, forest species compensate the deficit in the rainfall by their proximity to rivers and this could have influenced particularly the growth rate of *A. leiocarpus* in the dry savanna to be higher than in the humid savanna. Generally, species in drier areas have adaptive traits that enable them cope with their environment. **Tomlinson et al. (2014)** indicated that species in drier environments tend to have small leaf sizes which result in thinner boundary layer and therefore allow greater vapour pressure for photosynthesis and greater sensible heat loss. The smaller size also allows species to adjust their leaf display more precisely under variable water supply conditions at low cost by rapidly dropping or producing leaf area. Further dry savanna species are known to have greater leaf P and K that controls the turgidity of stomatal guard cell that regulate gas exchange through stomata (**Tomlinson et al., 2014**). Increased concentrations may allow species to close down water loss rapidly under low water conditions. Maintaining cellular turgor through increased solute concentration can also help plants to cope with water stress. The lower growth rates of *A. leiocarpus* in the humid savanna may also be a result of competition of the species with others for sunlight for photosynthesis in that comparably, dense forest stands (**Fichtler et al., 2004; Gebrekirostos et al., 2008; Niles et al., 2010**). During our field campaign, it was observed that the soil nutrients of the Tankwidi riparian forests (dry savanna) were richer than in the Afram riparian forests (humid savanna) and this may have also contributed to the relatively high growth performance of *A. africana* and *A. leiocarpus* in the dry savanna zone.

#### 4.3.4 Climate-growth relationships

The growth of *A. africana* and *A. leiocarpus* in the dry and humid savanna showed positive correlations with annual mean precipitation (AVG) (Figure 21) because precipitation is important for maintaining high water levels of rivers and groundwater recharge for tree growth. There were however, variations in the response of the species to monthly precipitation values. The two species primarily showed positive correlations with some of the months between May and October because those months fall within the rainy season where plants are photosynthetically active. **Anyomi *et al.* (2007)** also reported significant positive correlation of the growth rings of *Tectona grandis* with rainy season precipitation for the savanna zone in Ghana. A second feature in the precipitation correlation function (Figure 19) is the negative growth response of *A. africana* for both the humid and dry savanna zones during the rainy season months of June and May, when the continuous rains may result in flooding of the riparian area. According to **Schifman *et al.* (2012)**, flooding creates a subsidy of high water and nutrient availability to individual terrestrial plants in riparian forests. Conversely, long-term soil moisture saturation induces soil anoxia, which limits nutrient availability and gas exchange for plants and consequently hinders the growth of trees. Growth of the previous year had little influence on the growth of the following year of the riparian trees. Instead, they were much more sensitive to environmental conditions during the current growing season.

Temperature (Figure 22) principally had negative correlations with the growth of *A. africana* and *A. leiocarpus* because plant transpiration and respiration increase with increasing temperature, resulting in a higher loss of assimilated carbon as a source of energy (**Fichtler *et al.*, 2004; Schöngart *et al.*, 2006**). During very dry periods the reduced water availability cause stomata closure to reduce excessive transpiration and consequently a reduction in photosynthetic capacity and growth. The response of tree growth to temperature was pronounced in the humid savanna with the strongest effect recorded within the dry season between January-April. **Anyomi *et al.* (2007)** however, reported positive effects of temperature and sunshine hours during the rainy season on the growth of *Tectona grandis* in the same savanna zone. This relationship was not surprising given that trees are photosynthetically active during the rainy season.

Sea surface temperatures (SST) are seen as the one of the best climate predictor variables. Consequently, tropical Atlantic SSTs account for the largest proportion of the variability observed in West African precipitation (**Odekunle & Eludoyin, 2008**). In spite of this, SSTs had a weak positive

correlation with precipitation amounts at the climatic stations Ejura and Navrongo in the humid and dry savanna zones of Ghana, respectively (Figure 23). According to **Balas *et al.* (2007)**, the positive effect of warm SSTs on precipitation is strong in coastal areas and weakens further inland. Regional SSTs however, showed a strong negative correlation with the growth of *A. africana* in both the humid and dry savanna and even with little effect for *A. leiocarpus* in the two savanna types. On the one hand, flooding resulting from excess precipitation limits plants growth (**Schifman *et al.*, 2012**). On the other hand, the negative correlation of tree growth with Pacific SSTs is explained by precipitation deficits in West Africa during warm Pacific SSTs; implying reduction in tree growth (**Schöngart *et al.*, 2006; Odekunle & Eludoyin, 2008**). Tree growth also revealed a negative link with Indian Ocean SSTs. This is in accordance with the results of **Balas *et al.* (2007)** who observed a growing importance of the Indian Ocean in controlling rainfall variability in the West African sub-region. Tropical-extra tropical climate links have been suggested by **Deser *et al.* (2004)** and **D'Arrigo *et al.* (2005)** by the movement of the Gulf stream that distributes heat across the globe, and by the El Niño-Southern Oscillation (ENSO) that causes torrential rainfall in parts of South America and droughts in the sub-Saharan Africa during El Niño events (**Schöngart *et al.*, 2006; Gebrekirstos *et al.*, 2008**).

#### 4.3.5 Cyclicity of growth fluctuation

The growth of the riparian trees in both the humid and dry savanna zones had cyclicity of 2-7 years in the time frame of 1960 and 2010 (Figure 24). This means that an external factor that re-occurs within such years could have influenced the annual growth fluctuation. A review of significant climatic incidences in the West African sub-region revealed that there were drought events during the years corresponding to 1968 and 1972; 1972 and 1973; 1982 and 1984; and 1997, which could have influenced the tree growth fluctuation (**Balme *et al.*, 2006; Ecowas/Swac, 2008**). It is worth mentioning that the different time span of growth fluctuation among the species could also be due to differences in physiology that influence the differences in the scale of responses to external climatic events (**Gebrekirstos *et al.*, 2008**).

## 4.4 Climatic signals in carbon isotope ratios of riparian trees in the humid and dry savanna zones

### 4.4.1 Patterns of Carbon-13 of whole wood and cellulose

Various wood components show different isotopic signals and therefore removal of the wood constituents such as lignin and resins enhances Carbon-13 ( $\delta^{13}\text{C}$ ) signals (**Battipaglia et al., 2008**). The trend of the  $\delta^{13}\text{C}$  series from whole wood and cellulose of *A. africana* and *A. leiocarpus* in this study suggests (Figure 25) that cellulose has higher isotopic signal than whole wood as found in many studies (**Borella et al., 1998; Battipaglia et al., 2008**). Furthermore, the  $\delta^{13}\text{C}$  offset (approximately 1-2‰) of the whole wood and cellulose of the species (Table 22) were similar to the already reported offset value (**Borella et al., 1998, Sidorova et al., 2008**). Because of the constant differences in  $\delta^{13}\text{C}$  of the whole wood and cellulose pattern, each could be equally well suited as climate proxies (**Sidorova et al., 2008**). It was for this reason that whole wood was adopted for further exploration of the  $\delta^{13}\text{C}$  of the species to climatic effects.

### 4.4.2 Patterns of Carbon-13 in tree rings using whole wood

The high correlation of carbon-13 ( $\delta^{13}\text{C}$ ) of tree individuals of the same species at the same site confirmed that one growth ring is formed per year and that the climate of the area could be influencing the stable carbon discrimination (Figure 26; Table 22). On one hand, the strong correlation between  $\delta^{13}\text{C}$  of *A. leiocarpus* and *A. Africana* in the humid savanna (Figure 24) agrees with numerous studies suggesting that different species growing in the same environment respond similarly to climate variations (**Schongart et al., 2006; Fichtler et al., 2010; Gebrekirstos et al., 2012**). On the other hand, the low correlation between  $\delta^{13}\text{C}$  of *A. leiocarpus* and *A. Africana* in the dry savanna (Figure 26) could have resulted from the differences in rooting depth or leaf architecture that cause species to respond differently to climatic conditions. **Hasselquist et al. (2010)** indicated that evergreen species (*A. Africana*) have capacity to use deeper water to overcome seasonal water limitation than deciduous trees (*A. leiocarpus*).

Apart from the 1-time lag observed in some years, the general trend suggested that, the pattern of  $\delta^{13}\text{C}$  of *A. africana* and *A. leiocarpus* trees between the humid and dry savanna zones (Figure 27) are influenced by a similar climatic fluctuation caused by the movement of the inter-tropical convergence zone (ITCZ) (**Schongart et al., 2006**). ITCZ is the inter-phase of two air masses: the North-East Trade Winds and the South-West Monsoons. The North-East Trade Winds, known as the Harmattan, blow

from the interior of the Africa continent and are dry and dusty. In contrast, the South-West Monsoons, blow from over the seas and are moist. The ITCZ moves northwards and southwards across the study area from about March to October when precipitation is received in the region (UNEP-GEF, 2012).

#### 4.4.3 Variation in Carbon-13 of whole wood between tree species

The significantly higher enrichment of Carbon-13 ( $\delta^{13}\text{C}$ ) in *A. africana* in both the humid and dry savanna zones means that the species is highly water stressed than the *A. leiocarpus* (Table 23). During long periods of water deficiency, *A. leiocarpus*, being deciduous avoids water stressing conditions by shutting down photosynthetic organs and then shedding leaves (Poorter & Markesteijn, 2008). Nevertheless, because *A. africana* is evergreen, it is able to extend the length of the photosynthetic season. This presents challenges to the plants as it has to tighten stomata closure to significantly reduce water loss (Hasselquist *et al.*, 2010). At the closure of the stomata,  $\delta^{13}\text{C}$  which remain in the leaf structure and less preferred by the plants is no more discriminated in the process of photosynthesis under this water stressing conditions. This therefore increases the proportion of  $\delta^{13}\text{C}$  in the leaf (Fichtler *et al.*, 2010).

Generally, comparing species in both the humid and dry savanna zones (Figure 27) have confirmed previous studies indicating that riparian trees irrespective of geographic location can be resistant to climatic stress (Hasselquist *et al.*, 2010). The study shows that the adaptation strategies of *A. africana* in the dry savanna enables it to cope with climatic stress. *A. leiocarpus* has also shown resilience to water stress even though it grows in the dry environment. According to Tomlinson *et al.* (2014) species in drier environments have smaller leaf sizes which result in thinner boundary layer and therefore, allow greater vapour pressure for photosynthesis and greater sensible heat loss. The smaller size also allows the species to adjust their leaf display more precisely under variable water supply conditions at low cost by rapidly dropping or producing leaf area. Further dry savanna species are known to have greater leaf P and K that controls the turgidity of stomatal guard cell that regulate gas exchange through stomata. Increased concentrations may allow species to close down water loss rapidly under low water conditions. Maintaining cellular turgor through increased solute concentration can also help plants to cope with water stress. (Fichtler *et al.*, 2004; Gebrekirstos *et al.*, 2008; Niles *et al.*, 2010). Further, *A. africana* in the humid savanna was enriched in  $\delta^{13}\text{C}$  perhaps because of competition for nutrients and light with other species in the dense riparian forests.

#### 4.4.4 Relationship between carbon-13 of whole wood of trees and climatic parameters

The months during which the most significant correlations occurred between the species Carbon-13 ( $\delta^{13}\text{C}$ ) and climatic variables varied according to the species studied. Temperature generally had positive correlation with the  $\delta^{13}\text{C}$  of *A. africana* and *A. leiocarpus* (Figure 28). This is so because  $\delta^{13}\text{C}$  increases with increasing temperature. In dry years, leaf stomata may close and hence  $\delta^{13}\text{C}$  may not be discriminated. This increases the enrichment of the  $^{13}\text{C}$  isotope in the tree rings (**Fichtler *et al.*, 2010**).

The correlation between precipitation and the  $\delta^{13}\text{C}$  of *A. africana* of the dry savanna zone was generally negative in the rainy season (Figure 29). This indicates that the trees are photosynthetically active during this period and growth rate may be higher. Mixed results were obtained in the humid savanna suggesting that precipitation in that area can be both a limiting resource and a stressor. According to **Schifman *et al.* (2012)**, intense precipitation causes flooding and creates a subsidy of high water and nutrient availability to individual terrestrial plants in riparian forests. Conversely, long-term soil moisture saturation induces soil anoxia, which limits nutrient availability and gas exchange for plants growth.

# **CONCLUSION, RECOMMENDATIONS AND PERSPECTIVES**

## Conclusion

In this study, a spatially explicit analysis of forest cover trends for both Afram and Tankwidi riparian catchments have been presented from 1986 through 2000 to 2014. The current rate of 1-2% per annum of forest cover loss in the two riparian catchments has serious environmental implications in terms of biodiversity and function of the riparian forests. This provided the basis to follow up research aimed at quantifying the impacts of the deforestation on riparian plant diversity and functions.

The low richness, diversity and density of riparian forests in farmlands as opposed to that in protected areas put the landscape at greater risk of harm of natural disturbances such as fires and flooding than would be the case if riparian forest cover and diversity had been retained similar to conditions found in protected areas. On one hand, the soil physical and chemical properties on farmland along the Afram river (humid savanna) is similar to that in protected area, indicating that the riparian forests in that area still has the potential to act as nutrient buffer, particle filter and carbon reservoir. On the other hand, the decline in soil nutrients in riparian buffer on farmland as opposed to the protected area along the Tankwidi river (dry savanna) suggests that the functional role of the buffer in that area may have been impaired.

The annual nature of the tree rings of *A. africana* and *A. leiocarpus* and the possibility of cross-dating using tree rings widths and carbon-13 isotope implies that there is a high potential for dendrochronological studies of riparian trees in the humid and dry savannas zones of Ghana. Although species specific, the correlations of precipitation and temperature with the growth of the trees suggests that there are opportunities for climate reconstruction and future projections on the impact of climate change on riparian ecosystems using tree rings as proxies. This would contribute to addressing the problem of the lack of adequate instrumental climate data for past climatic studies.

## Recommendations

1. Because of the declining richness, diversity and density of riparian woody plant on farmlands compared to protected areas, there is the need for enforcement of the freshwater buffer zone policy of Ghana in order to exclude farming activities within buffer zones. The enforcement of the policy should be done alongside farmer education on the importance of riparian forests for enhancing the resilience of farmlands to the negative effects of climate change.

2. For the ecological restoration of the degraded riparian forests, *Anogeissus leiocarpus* should be preferred than *Afzelia africana*. *Anogeissus leiocarpus* (fast grower and less water stressed) likely have a higher fitness (i.e., a higher contribution to future generations) than *Afzelia africana* (slow grower and highly water stressed). This is because *Anogeissus leiocarpus* has a greater chance of reaching reproductive size at a younger age than *Afzelia africana*. *Anogeissus leiocarpus* would boost canopy formation early because of its relatively high survival to reproductive size and short generation time. Furthermore, *Anogeissus leiocarpus* could be highly competitive due to shading of neighbors, enhanced seed dispersal over greater distances, and mitigation against disturbances such as surface fire and ground-based herbivory. The fast growth rates and large tree size of *Anogeissus leiocarpus* could however, come with some costs including reduced investment in defense (frequent infestations by insects or infections by fungi), low wood density, reduced mechanical strength, and high ratios of above- to belowground biomass, all of which increase risk of breakage and damage from wind.

### **Perspectives**

1. To improve understanding of long-term effects of climate warming on riparian forest, further investigations are needed of relationships between growth rate, tree longevity, and forest turnover rates.
2. Carbon isotopes exhibited higher sensitivity to climate and fewer trees were needed to produce a reliable chronology. In riparian areas with high diversity but low density of species, isotopic data be used to strengthen climatic reconstructions.
3. Further studies are needed to explore the reasons for temporally changing correlations observed between the *Anogeissus leiocarpus* and *Afzelia africana* from the different savanna types.

# REFERENCES

- Aké Assi L. (2001).** Flore de la Côte d'Ivoire: catalogue systématique, biogéographie et écologie I. *Boissiera*, 57: 1-396.
- Aké Assi L. (2002).** Flore de la Côte d'Ivoire: catalogue systématique, biogéographie et écologie II. *Boissiera*, 58: 1-401.
- Akinbisoye O.S., Oke S.O., Adebola S.I., Mokwenye A.I. (2014).** Influence of Taungya Agroforestry System on Diversity of Native Woody Species and Soil Physico-Chemical Properties in Nigeria. *International Journal of Scientific and Research Publications*, 4: 2250-3153.
- Ampofo E. A. (2006).** Soil moisture dynamics in coastal savanna soils in the tropics under different soil management practices, *Hydrological Sciences Journal*, 51:6, 1194-1202.
- Andary C., Doumbia B., Sauvan N., Olivier M., Garcia M. (2005).** *Anogeissus leiocarpus* (DC.) Guill. & Perr. Record from PROTA4U. Jansen, P.C.M. & Cardon, D. (Editors). PROTA (Plant Resources of Tropical Africa / Ressources végétales de l'Afrique tropicale), Wageningen, Netherlands retrieved from <http://www.prota4u.org/search.asp> on 15 November 2015.
- Anderson J.S., Ingram J.I.S. (1998).** Tropical Soil Biology and Fertility. A Handbook of Methods. 2nd Edition. Information Press, U.K. 221 p.
- Anderson J.R., Hardy E.E., Roach J.T., Whitmer R.E. (1976).** A landuse and land cover classification system for use with remote sensor data. Geological Survey Professional Paper 964. Washington, DC, US Geological Survey.
- Anyomi K.A., Kahle H.P., Spiecker H., Adu-Bredu S. (2007).** Climatic influences on stem radial growth of Teak (*Tectona grandis*) in Ghana. ITTO Report REF: 079107s. 20 pp.
- Arroyo L.A., Johansen K., Phinn S. (2010).** Integration of LiDAR and QuickBird imagery for mapping riparian biophysical parameters and land cover types in Australian tropical savannas. *Forest Ecology & Management*, 259: 598-606.
- Artigas J., García-Berthou E., Bauer D.E., Castro M.I., Cocherio J., Colautti D., Cortelezzi A., Donato J.C., Elozegi A., Feijoó C., Giorgi A., Gómez N., Leggeri L., Muñoz I., Rodrigues-Capítulo A., Romaní A.M., Sabater S. (2013).** Global pressures, specific responses: effects of nutrient enrichment in streams from different biomes. *Environmental Research Letters*, 8:014002.
- Asiedu E.K., Ampadu B., Bonsu M., Abunyewa A.K. (2013).** Hydrological and Physical Changes of Soils under Cocoa Plantations of Different Ages During the Dry Season in the Transition Zone of Ghana. *Journal of Natural Sciences Research*, 3:7.

- Avornyo V.K., Adjadeh T.A., Amatekpor J.K. (2013).** Morphological, Chemical and Physical Properties of Two Pan Soils in the Lower Volta Basin of Ghana. *West African Journal of Applied Ecology*, 21: 63–77.
- Azihou A.F., Glele Kakai R.L, Bellefontaine R., Sincin B.A. (2013).** Distribution of tree species along a gallery forest–savanna gradient: patterns, overlaps and ecological thresholds. *Journal of Tropical Ecology*, 29: 25-37.
- Bagan H., Kinoshita T., Yamagata Y. (2012).** Combination of AVNIR-2, PALSAR, and Polarimetric Parameters for Land Cover Classification. *IEEE Transactions on Geoscience and Remote Sensing*, 50:1318-1328.
- Baillie M.G.L., Pilcher J.R. (1973).** A simple cross dating program for tree-ring research. *Tree-Ring Bulletin*, 33:7–14.
- Balas N., Nicholson S.E., Klotter D. (2007).** The relationship of rainfall variability in West Central Africa to sea-surface temperature fluctuations. *International Journal of Climatology*, 27:1335–1349.
- Balme M., Lebel, T., Amani A. (2006).** Années sèches et années humides au Sahel: quo vadimus? *Journal of Hydrological Science*, J. 51: 254–271.
- Barbour M.M., Andrews A.J., Farquhar G.D. (2001).** Correlations between oxygen isotope ratios of wood constituents of *Quercus* and *Pinus* samples from around the world. *Australian Plant Physiology*, 28: 335-348.
- Battipaglia G., Jäggi M., Saurer M., Siegwolf R.T.W., Cotrufo M.F. (2008).** Climatic sensitivity of  $\delta^{18}\text{O}$  in the wood and cellulose of tree rings: Results from a mixed stand of *Acer pseudoplatanus* L. and *Fagus sylvatica* L. *Palaeogeography and Palaeoclimatology*, 261:193–202.
- Benhin J.K.A. (2006).** Agriculture and Deforestation in the Tropics: A Critical Theoretical and Empirical Review. *Ambio*, 35:9-16.
- BirdLife International (2014).** Important Bird Areas factsheet: Tankwidi Forest Reserve. Downloaded from <http://www.birdlife.org> on 12 February 2014.
- Black C.A. (1965).** Methods of Soil Analysis: Part I Physical and mineralogical properties. American Society of Agronomy, Madison, Wisconsin, USA.
- Boakye E.A., Gils H.V., Osei E.M. Jnr., Asare V.N.A. (2012).** Does forest restoration using taungya foster tree species diversity? A case of the Afram Headwaters Forest Reserve in Ghana. *African Journal of Ecology*, 50:319-325.

- Bonan G.B. (2008).** Forests and Climate Change: Forcings, Feedbacks, and the Climate Benefits of Forests. *Science*, 320: 1444–1449.
- Bonsu M. (1991).** Effect of liming on maize production and erosion on an acid soil in South-Western Ghana. *Tropical Agriculture*, 63:271-273.
- Borella S., Leuenberger M., Saurer M., Siegwolf R.T.W. (1998).** Reducing uncertainties in  $\delta^{13}\text{C}$  analysis of tree rings: Pooling, milling and cellulose extraction. *Journal Geophysical Research*, 103:19519–19526.
- Bouyouco G.J. (1962).** Hydrometer method improved for making particle size analyses of soil. *Agronomy Journal*, 52:464-465.
- Bradstreet R. B. (1965).** The Kjeldahl Method for Organic Nitrogen. New York, NY: Academic Press Incorporated.
- Bray R.H., Kurtz L.T. (1945).** Determination of total organic and available forms of phosphorus in soils. *Soil Science*, 59:39-45.
- Brienen R.J.W., Wanek W., Hietz P. (2011).** Stable carbon isotopes in tree rings indicate improved water use efficiency and drought responses of a tropical dry forest tree species. *TREES*, 25:103–113
- Bunn A.G., (2008).** A dendrochronology program library in R (dplR). *Dendrochronologia*, 26: 576 115–124.
- Bunn A.G., (2010).** Statistical and visual cross-dating in R using the dplR library.
- Caldararu S., Purves D.W., Palmer P.I. (2014).** Phenology as a strategy for carbon optimality: a global model. *Biogeosciences*, 11: 763–778.
- Callo-Concha D., Gaiser T., Ewert F. (2012).** Farming and cropping systems in the West African Sudanian Savanna. WASCAL research area: Northern Ghana, Southwest Burkina Faso and Northern Benin. ZEF Working Paper 100. Bonn.
- Canadell J.G., Raupach M.R., Houghton R.A. (2009).** Anthropogenic CO<sub>2</sub> Emissions in Africa. *Biogeosciences*, 6:463–468.
- Ceperley N., Montagnini F., Natta A. (2010).** Significance of sacred sites for riparian forest conservation in Central Benin. *Bois Et Forêts Des Tropiques*, 303:5-23.
- Chai S.L., Tanner E., McLaren K. (2009).** High rates of forest clearance and fragmentation pre- and post-National Park establishment: The case of a Jamaican montane rainforest. *Biodiversity Conservation*, 142:2484–2492.

- Cook E.R., Briffa K.R., Shiyatov S., Mazepa A., Jones P.D. (1990).** Data analysis. In: Cook, E.R., Kairiukstis, L.A. (Eds.), *Methods of Dendrochronology: Applications in the Environmental Sciences*. Kluwer Academic Publishers, 97–162 p.
- Cudjoe S.N. (2006).** Population dynamics and natural resources in the Volta in the Volta River Basin of Ghana. *Ghana Journal of Development Studies*, 3: 0855-6768.
- Dawoe E.K., Oppong S.K., Quashie-Sam J.S. (2014).** Effect of land-use conversion from forest to cocoa agroforest on soil characteristics and quality of a Ferric Lixisol in lowland humid Ghana. *Agroforestry System*, 88:87–99.
- D’Arrigo R.D., Wilson R., Deser C., Wiles G., Cook E., Villalba R., Tudhope A., Cole J., Linsley B. (2005).** Tropical –North Pacific climate linkages over the past four centuries. *Journal of Climatology*, 23, 1902-2578.
- Deser C., Phillips A., Hurrell J. (2004).** Pacific interdecadal climate variability: Linkages between the tropics and North Pacific during boreal winter since 1900. *Journal of Climatology*, 17, 3109–3124.
- de Condappa D., Lemoalle J. (2009).** Water atlas of the Volta Basin-Atlas de l’eau dans le bassin de la Volta. Challenge Program on Water and Food and Institut de Recherche pour le Développement, Colombo, Marseille, 96p.
- de Chazal J., Rounsevell M.D.A (2009).** Land-use and climate change within assessments of biodiversity change: A review . *Global Environmental Change*, 19: 306–315
- Denman K.L., Brasseur G., Chidthaisong A., Ciais P., Cox P.M., Dickinson R.E., Hauglustaine D., Heinze C., Holland E., Jacob D., Lohmann U., Ramachandran S., da Silva Dias P.L., Wofsy S.C., Zhang, X. (2007).** Couplings Between Changes in the Climate System and Biogeochemistry, In: S. Solomon, D. Qin, M. Manning, Z. Chen, M. Marquis, K.B. Averyt, M. Tignor, H.L. Miller (Eds.), *Climate Change 2007: The Physical Science Basis. Contribution of Working Group I to the Fourth Assessment Report of the Intergovernmental Panel on Climate Change*, Cambridge University Press, Cambridge, UK, 499–588p.
- Dybzinski R., Fargione J. E., Zak D. R., Fornara D., Tilman D. (2008).** Soil fertility increases with plant species diversity in a long-term biodiversity experiment. *Oecologia*, 158:85–93.
- Eckstein D., Bauch J. (1969).** Beitrag zur Rationalisierung eines dendrochronologischen Verfahrens und zur Analyse seiner Aussagesicherheit. *Forstwissenschaftliches Centralblatt*, 88:230-250.
- Ecowas/Swac ( 2008).** Climate and Climate Change, Atlas on Regional Integration in West Africa Environment Series, ECOWAS and SWAC/OECD, Abuja and Paris.

- Edusah S.E. (2011).** The impact of forest reserves on livelihoods of fringe communities in Ghana. *Journal of Science and Technology*, 31:1.
- Egyir I.S., Ofori K., Antwi G., Ntiama-Baidu Y. (2015).** Adaptive Capacity and Coping Strategies in the Face of Climate Change: A Comparative Study of Communities around Two Protected Areas in the Coastal Savanna and Transitional Zones of Ghana. *Journal of Sustainable Development*, 8:1.
- Eilu G., Obua J., Tumuhairwe J.K., Nkwine, C. (2003).** Traditional farming and plant species diversity in agricultural landscapes of south-western Uganda. *Agriculture, Ecosystems and Environment*, 99:125–134.
- Enanga, E.M., Shivoga, W.A., Maina-Gichaba, C., Creed, I.F. (2011).** Observing Changes in Riparian Buffer Strip Soil Properties Related to Land Use Activities in the River Njoro. Watershed, Kenya. *Water Air and Soil Pollution*, 218:587-601.
- FAO (2007).** State of the World's Forests 2007, Technical Report, Food and Agricultural Organization of the United Nations (FAO), Rome, 144p.
- Farquhar G.D., Lloyd, J. (1993).** Carbon and oxygen isotope effects in the exchange of carbon dioxide between terrestrial plants and the atmosphere. In *Stable Isotopes and Plant Carbon-Water Relations* (J. R. Ehleringer, A. E. Hall and G. D. Farquhar, eds), Academic Press, San Diego. 47-70p.
- Fichtler E., Helle, G., Worbes M. (2010).** Stable-carbon isotope time series from tropical tree rings indicate a precipitation signal. *TREES*, 66:35–4.
- Fichtler E., Trouet V., Beeckman H., Coppin P., Worbes M. (2004).** Climatic signals in tree rings of *Burkea africana* and *Pterocarpus angolensis* from semiarid forests in Namibia. *TREES*, 18:442–451.
- Fischer J., Stott J., Zerger A., Warren G., Sherren K., Forrester R.I. (2009).** Reversing a tree regeneration crisis in an endangered ecoregion. *Proceedings of the National Academy of Sciences*, 106:10386–10391.
- Fischlin A., Midgley G.F., Price J.T., Leemans R., Gopal B., Turley C., Rounsevell M.D.A., Dube O.P., Tarazona J., Velichko A.A. (2007).** Ecosystems, their Properties, Goods, and Services, In: M.L. Parry, O.F. Canziani, J.P. Palutikof, P.J. van der Linden, C.E. Hanson (Eds.), *Climate Change 2007: Impacts, Adaptation and Vulnerability. Contribution of Working Group II to the Fourth Assessment Report of the Intergovernmental Panel on Climate Change*, Cambridge University Press, Cambridge, 211–272p.

- Ford P.L. (2002).** Grasslands and savannas. In *Encyclopedia of Life Support Systems*, UNESCO. 20p.
- Gärtner H., Schweingruber F.H. (2013).** Microscopic Preparation Techniques for Plant Stem Analysis. Verlag Dr. Kessel, Remagen. 78p.
- Gebrekirstos A., Bräuning A., Sass-Klassen U., Mbow C. (2014).** Opportunities and applications of dendrochronology in Africa. *Sustainability Challenges*, 6:48-53.
- Gebrekirstos A., Brauning A., Van Noordwijk M., & Mitlohner R. (2011).** Understanding past, present, and future climate changes from East to West Africa. *Agricultural Innovations for Sustainable Development*, 3:77–86.
- Gebrekirstos A., Mitlohner R., Teketay D., Worbes M. (2008).** Climate–growth relationships of the dominant tree species from semi-arid savanna woodland in Ethiopia. *TREES*, 22:631–641.
- Gebrekirstos A., Mitlohner R., van Noordwijk M., Brauning A. (2012).** Tracing responses to climate variability from stable isotopes in tree rings of *Anogeissus leiocarpus* and *Sclerocarya birrea* from the Sahel zone, Burkina Faso. *TRACE*, 10:6–12.
- Geist H.J., Lambin E.F. (2002).** Proximate Causes and Underlying Driving Forces of Tropical Deforestation. *BioScience*, 52:143–150.
- Gérard J., Louppe D. (2011).** *Azelia africana* Sm. ex Pers. Record from PROTA4U. Lemmens, R.H.M.J., Louppe, D. & Oteng-Amoako, A.A. (Editors). PROTA (Plant Resources of Tropical Africa / Ressources végétales de l’Afrique tropicale), Wageningen, Netherlands retrieved from <http://www.prota4u.org/search.asp> on 15 November 2015.
- Global Carbon Project (2015).** [www.globalcarbonproject.org/](http://www.globalcarbonproject.org/).
- Goetze D., Horsch B., Porembski S. (2006).** Dynamics of forest-savanna mosaics in north-eastern Ivory Coast from 1954 to 2002. *Journal of Biogeography*, 33: 653-664.
- Government of Ghana (2011).** Ghana riparian buffer zone policy for managing freshwater bodies. Ministry of Water Resources, Works and Housing.
- Gullison R.E., Frumhoff P.C., Canadell J.G., Field C.B., Nepstad D.C., Hayhoe K., Avissar R., Curran L.M., Friedlingstein P., Jones C.D., Nobre C. (2007).** Tropical Forests and Climate Policy. *Science*, 316: 985–986.
- Gray C.L. (2014).** Riparian Reserves in Oil Palm Plantations: Biodiversity, Ecological Processes and Ecosystem Services. (PhD Thesis), Brasenose College and the Department of Zoology, University of Oxford, United Kingdom.

- Gray C.L., Slade E.M., Mann D.J., Lewis O.T. (2014).** Do riparian reserves support dung beetle biodiversity and ecosystem services in oil palm-dominated tropical landscapes? *Ecology and Evolution*, 4:1049-1060.
- Hartmann D.L., Klein Tank A.M.G., Rusticucci M., Alexander L.V., Brönnimann S., Charabi Y., Dentener F.J., Dlugokencky E.J., Easterling D.R., Kaplan A., Soden B.J., Thorne P.W., Wild M., Zhai P.M. (2013).** Observations: Atmosphere and Surface. In: Climate Change 2013: The Physical Science Basis. Contribution of Working Group I to the Fifth Assessment Report of the Intergovernmental Panel on Climate Change [Stocker, T.F., D. Qin, G.-K. Plattner, M. Tignor, S.K. Allen, J. Boschung, A. Nauels, Y. Xia, V. Bex and P.M. Midgley (eds.)]. Cambridge University Press, Cambridge, United Kingdom and New York, NY, USA.
- Hasselquist N.J., Allen M.F., Santiago L.S. (2010).** Water relations of evergreen and drought-deciduous trees along a seasonally dry tropical forest chronosequence. *Oecologia*, 164, 881-890.
- Hawthorne W.D. (1990).** Field guide to the forest trees of Ghana. Chatham: Natural Resources Institute, for the Overseas Development Administration, London. Ghana
- Hawthorne W.D., Jongkind C.H. (2006).** Woody plants of Western African forests. A guide to the forest trees, shrubs and lianes from Senegal to Ghana. Kew: Royal Botanic Gardens, 1023pp.
- Holl K.D. (1999).** Factors limiting tropical rain forest regeneration in abandoned pasture: seed rain, seed germination, microclimate, and soil. *Biotropica*, 31: 229–242.
- IPCC (2007).** Fourth Assessment Report: Climate Change 2007 (AR4). Intergovernmental Panel on Climate Change.
- IPCC (2013).** Fourth Assessment Report: Climate Change 2013 (AR5). Intergovernmental Panel on Climate Change.
- Irvine F.R. (1961).** Woody plants of Ghana. With special reference to their uses. London: Oxford University Press.
- IUCN (2015).** IUCN Protected Areas Categories System. Download from [http://www.iucn.org/about/work/programmes/gpap\\_home/gpap\\_quality/gpap\\_pacategories/](http://www.iucn.org/about/work/programmes/gpap_home/gpap_quality/gpap_pacategories/) on 4 May 2015.
- Jaccard P. (1908).** Nouvelles Recherches Sur La Distribution Florale. *Bulletin de la Société vaudoise des Sciences Naturelles*, 44: 223-270.

- Jackson P.C., Cavelier J., Goldstein G., Meinzer F.C., Holbrook N.M. (1995).** Partitioning of water resources among plants of a lowland tropical forest. *Oecologia*, 101:197–203.
- Jetz W., Wilcove D.S., Dobson A.P. (2007).** Projected Impacts of climate and land-use change on the global diversity of birds. *PLoS Biology*, 5: e157.
- Johansen K., Arroyo L.A., Armston J., Phinn S., Witte C. (2010).** Mapping riparian condition indicators in a sub-tropical savanna environment from discrete return LiDAR data using object-based image analysis. *Ecological Indicators*, 10: 796-807.
- Kayranli B., Scholz M., Mustafa A., Hedmark A. (2012).** Carbon storage and fluxes within freshwater wetlands: A critical review. *Wetlands*, 30: 111-124.
- Keay R.W.J., Hepper F.N. (eds). (1954-1972).** Flora of West Tropical Africa, by Hutchinson, J. and Dalziel, J.M., 2nd edition Vol. I (828p.), Vol. II (544p.), Vol. III. Millbank, London, 574p.
- Krepkowski J., Brauning A., Gebrekirstos A., Strobl, S. (2010).** Cambial growth dynamics and climatic control of different tree life forms in tropical mountain forest in Ethiopia. *TREES*, 25:59–70.
- Krepkowski J., Gebrekirstos A., Shibistova O., Brauning A. (2013).** Stable carbon isotope labeling reveals different carry-over effects between functional types of tropical trees in an Ethiopian mountain forest. *New Phytologist*, 199:441-51.
- Kyerematen R., Owusu E.H., Acquah-Lampsey D., Anderson R.S., Ntiamoah-Baidu Y. (2014).** Species Composition and Diversity of Insects of the Kogyae Strict Nature Reserve in Ghana. *Open Journal of Ecology*, 4:1061-1079.
- Laumer W., Andreu L., Helle G., Schleser G.H., Wieloch T., Wissel H. (2009).** A novel approach for the homogenization of cellulose to use micro-amounts for stable isotope analyses. *Rapid Communications in Mass Spectrometry*, 23: 1934–1940.
- Lillesand T.M., Kiefer R.W., Chipman J.W. (2004).** Remote Sensing and Image Interpretation. (4 ed.). New York: Wiley and Sons.
- Lykke A.M. (1998).** Assessment of species composition change in savanna vegetation by means of woody plants' size class distributions and local information. *Biodiversity and Conservation*, 7:1261–1275.
- Magurran A.E. (2004).** Measuring Biological diversity. Blackwell Publishing, Malden, Oxford and Victoria. 256pp.
- Manning A.D., Fischer J., Lindenmayer D.B. (2006).** Scattered trees are keystone structures - implications for conservation. *Biological Conservation*, 132:311–321.

- Mantyka-pringle C.S., Martin T.G., Rhodes J.R. (2012).** Interactions between climate and habitat loss effects on biodiversity: a systematic review and meta-analysis. *Global Change Biology*, 18: 1239-1252.
- McCarroll D., Loader N.J. (2004).** Stable isotopes in tree rings. *Quaternary Science Reviews*, 23:771–801.
- McCracken D.I., Cole L.J., Harrison W., Robertson D. (2012).** Improving the Farmland Biodiversity Value of Riparian Buffer Strips: Conflicts and Compromises. *Journal Environmental Quality*, 41:355–363.
- Mclean E.O. (1982).** Soil pH and lime requirement. In: Page AL, Miller RH, Keeney DR (eds). *Methods of Soil Analysis. Part 2.* 2nd ed. Agron. Monogr.9. ASA and SSSA. Madison, WI. 199-224p.
- Meinzer F.C., Andrade J.L., Goldstein G., Holbrook N.M., Cavelier J., Wright S.J. (1999).** Partitioning of soil water among canopy trees in a seasonally dry tropical forest. *Oecologia*, 121:293–301.
- Meyer J.L., Strayer D.L., Wallace J.B., Eggert S.L., Helfman G.S., Leonard N.E. (2007).** The contribution of headwater streams to biodiversity in river networks. *Journal of the American Water Resources Association*, 43: 86-103.
- Millennium Ecosystem Assessment (MA) (2005).** Ecosystems and Human Well-Being: Biodiversity Synthesis. Washington, DC: World Resources Institute.
- Mittelbach G.G., Steiner C.F., Scheiner S.M. (2001).** What is the observed relationship between species richness and productivity? *Ecology*, 82:238–2396.
- Morandin L.A., Winston M.L (2006).** Pollinators provide economic incentive to preserve natural land in agroecosystems. *Agriculture, Ecosystem Environment*, 116: 289–292.
- Morelli F. (2013).** Quantifying Effects of Spatial Heterogeneity of Farmlands on Bird Species Richness by Means of Similarity Index Pairwise. *International Journal of Biodiversity Conservation*, 914837:9.
- Nadeau M.B., Sullivan T.P. (2015).** Relationships between Plant Biodiversity and Soil Fertility in a Mature Tropical Forest, Costa Rica. *International Journal of Forestry Research*, 732946:13.
- Naiman R.J., Decamps H. (1997).** The Ecology of Interfaces: Riparian Zones. *Annual Review of Ecology and Systematics*, 28:621–658.
- Naiman R.J., Decamps H., Pollock M. (1993).** The Role of Riparian Corridors in Maintaining Regional Biodiversity. *Ecological Applications*, 3:209–212.

- Natta A.K. (2003).** Ecological assessment of riparian forests in Benin: Phytodiversity, phytosociology and spatial distribution of tree species (Ph.D. thesis), University of Wageningen, Wageningen, The Netherlands.
- Natta A.K., Porembski S. (2003).** Ouémé and Comoé: forest-savanna border relationships in two riparian ecosystems in West Africa. *Botanische Jahrbücher Systematics*, 124: 383-396.
- Natta A.K., Sinsin B., van der Maesen L.J.G. (2002).** Riparian forests, a unique but endangered ecosystem in Benin. *Botanische Jahrbücher Systematics*, 124: 59-69.
- Niles J.H., Allen M.F., Santiago L.S. (2010).** Water relations of evergreen and drought-deciduous trees along a seasonally dry tropical forest chronosequence. *Oecologia*, 164, 881-890. .
- Nirmal Kumar J.I., Kumar R.N., Bhoi R. K., Sajish P. R. (2010).** Tree species diversity and soil nutrient status in three sites of tropical dry deciduous forest of western India. *Tropical Ecology*, 51: 273–279.
- Oberhuber W., Hammerle A., Kofler W. (2015).** Tree water status and growth of saplings and mature Norway spruce (*Picea abies*) at a dry distribution limit. *Frontiers in Plant Sciences*, 6: 703.
- Okiror P., Chono J., Nyamukuru A., Lwanga J.S., Sasira P., Diogo P. (2012).** Variation in Woody Species Abundance and Distribution in and around Kibale National Park, Uganda. *International Scholarly Research Network Forestry*, 490461.
- Oliver T.H., Morecroft, M.D. (2014).** Interactions between climate change and land use change on biodiversity: attribution problems, risks, and opportunities. *Wiley Interdisciplinary Reviews: Climate Change*, 5: 317–335.
- Palm C.A., Swift M.J., Woomer P.L. (1996).** Soil biological dynamics in slash-and-burn agriculture. *Agriculture, Ecosystem and Environment*, 58:61–74.
- Potapov P., Laestadius L., Yaroshenko A., Turubanova S. (2009).** Measuring and assessing forest degradation. Global mapping and monitoring the extent of forest alteration: The intact forest landscapes method: Food and Agriculture Organization of the United Nations (FAO), Forest Resource Working Paper, 166.
- Poorter L., Markesteijn L. (2008).** Seedling traits determine drought-tolerance of tropical tree species. *Biotropica*, 40: 321-331.
- Puyravaud J.P. (2003).** Standardizing the calculation of the annual rate of deforestation. *Forest Ecology and Management*, 177: 593–596.

- Qin C., Yang B., Bräuning A., Griebinger J., Wernicke J. (2015).** Drought signals in tree-ring stable oxygen isotope series of Qilian juniper from the arid northeastern Tibetan Plateau. *Global and Planetary Change*, 125: 48–59.
- Rawata J.S., Kumarb M. (2015).** Monitoring land use/cover change using remote sensing and GIS techniques: A case study of Hawalbagh block, district Almora, Uttarakhand, India. *The Egyptian Journal of Remote Sensing and Space Science*, 18:77-84.
- Rayner N.A., Parker D.E., Horton E.B., Folland C.K., Alexander L.V., Rowell D.P., Kent E.C., Kaplan A. (2003).** Global analyses of sea surface temperature, sea ice, and night marine air temperature since the late nineteenth century. *Journal of Geophysical Research*, 108:14, 4407.
- Reddy K.R. Delaune R.D. (2008).** Biogeochemistry of Wetlands: Science and Applications. CRC Press., Boca Raton, Florida, 774p.
- Richardson K., Steffen W., Schellnhuber H.J., Alcamo J., Barker T., Kammen D., Leemans, R., Liverman D., Monasinghe M., Osman-Elasha B., Stern N., Waever O. (2009).** Climate Change: Global Risks Challenges and Decisions, Synthesis Report, University of Copenhagen, 39p.
- Rinn F. (2012).** TSAPWin Scientific: Time series analysis and presentation for dendrochronology and related applications. RINNTECH, D-69124 Heidelberg, Germany.
- Ruelland D., Levavasseur F., Tribotte A. (2010).** Patterns and dynamics of land-cover changes since the 1960s over three experimental areas in Mali. *International Journal of Applied Earth Observation and Geoinformation*, 12:S11-S17.
- Royal Netherlands Meteorological Institute (2015).** KNMI Climate Explorer. <http://climexp.knmi.nl>.
- Ruiz-Robledo J., Villar R. (2005).** Relative growth rate and biomass allocation in ten woody species with different leaf longevity using phylogenetic independent contrasts (PICs). *Plant Biology*, 7: 484-494
- Rykken J.J., Moldenke A.R., Olson D.H. (2007).** Headwater riparian forest-floor invertebrate communities associated with alternative forest management practices. *Ecological applications*, 17:1168–1183.
- Salifu T., Agyare, W.A. (2012).** Distinguishing land use types surface albedo and normalized difference vegetation index derived from the SEBAL Model for the Atankwidi and Afram Sub-catchments in Ghana. *Journal of Engineering & Applied Sciences*, 7: 1819-6608.

- Sarmiento G., Monasterio M. (1983).** Life forms and phenology. In: Tropical Savannas (ed Bourliere F), Elsevier, Amsterdam, 79–108 pp.
- Sambare O., Bognounou F., Wittig R., Thiombiano, A. (2011).** Woody species composition, diversity and structure of riparian forests of four watercourses types in Burkina Faso. *Journal of Forestry Research*, 22: 145–158.
- Scherer-Lorenzen M., Korner, C., Schulze E.D. (eds.). (2005).** Forest diversity and function: temperate and boreal systems. Springer, Berlin.
- Schetter T.A., Root K.V. (2011).** Assessing an imperiled Oak savanna landscape in Northwestern Ohio using Landsat Data. *Natural Areas Journal*, 31:118-130.
- Schifman L.A., Stella J.C., Teece M., Volk, T.A. (2012).** Plant growth and water stress response of hybrid willow (*Salix* spp.) among sites and years in central New York. *Biomass & Bioenergy*, 36: 316-326.
- Schongart J., Orthmann B., Hennenberg K.J., Porembski S., Worbes M. (2006).** Climate-growth relationships of tropical tree species in West Africa and their potential for climate reconstruction. *Global Change Biology*, 12: 1130-1150.
- Schweingruber F.H. (1988).** Tree rings. Basics and applications of dendrochronology. Reidel, Dordrecht.
- Schweingruber F.H., Borner A., Schulze E.D. (eds) (2006).** Atlas of woody plant stems. Springer, Berlin.
- Seavy N.E., Gardali T., Golet G.H., Griggs F.T., Howell C.A., Kelsey R., Small S.L., Viers J.H., Weigand J.F. (2009).** Why Climate Change Makes Riparian Restoration More Important than Ever: Recommendations for Practice and Research. *Ecological Restoration*, 27:1522-4740.
- Seghieri J., Do F.C., Devineau J., Fournier A. (2012).** Phenology of Woody Species Along the Climatic Gradient in West Tropical Africa. Phenology and Climate Change, Dr. Xiaoyang Zhang (Ed.). Retrieved from <http://www.intechopen.com/books/phenology-and-climate-change/phenology-of-woody-species-along-the-climatic-gradient-in-west-tropical-africa-> on 16 October 2015.
- Shannon C.E. (1948).** A mathematical theory of communication, Part 1. *Bell System Technical Journal*, 27:379–423.
- Sidorova O.V., Siegwolf R.T.W., Saurer M., Naurzbaev M.M., Vaganov E.A. (2008).** Isotopic composition ( $d^{13}C$ ,  $d^{18}O$ ) in wood and cellulose of Siberian larch trees for early Medieval and recent periods. *Journal of Geophysical Research*, 113:0148-0227.

- Simpson E.H. (1949).** Measurement of diversity. *Nature*, 163, 688.
- Singer M.B., Stella J.C., Dufour S., Piégay H., Wilson R.J.S., Johnstone, L. (2013).** Contrasting water-uptake and growth responses to drought in co-occurring riparian tree species. *Ecohydrology*, 6: 402-412.
- Smith J.B., Schneider S.H., Oppenheimer M., Yohe G.W., Hare W., Mastrandrea M.D., Patwardhan A., Burton I., Corfee-Morlot J., Magadza C.H.D., Fussel H.M., Pittock A.B., Rahman A., Suarez A., van Ypersele J.P. (2009).** Assessing Dangerous Climate Change Through an Update of the Intergovernmental Panel on Climate Change (IPCC) “Reasons for Concern”. Proceedings of the National Academy of Sciences, 1–5p.
- Spracklen D., Yaron G., Singh T., Righelato R., Sweetman T. (2008).** The Root of the Matter: Carbon Sequestration in Forests and Peatlands, Policy Exchange, London, UK, 36p.
- Surasinghe T.D., Baldwin R.F. (2015).** Importance of Riparian Forest Buffers in Conservation of Stream Biodiversity: Responses to Land Uses by Stream-Associated Salamanders across Two Southeastern Temperate Ecoregions. *Journal of Herpetology*, 49:83-94.
- Stern N. (2008).** The Economics of Climate Change: The Stern Review, Cambridge University Press, Cambridge, UK, 1st edit., 692p.
- Stokes M.A., Smiley T.L. (1968).** An Introduction to Tree-Ring Dating. University of Chicago Press, Chicago, IL.
- Schweiger E.W., Ashton I.W., Muhlfeld C.C., Jones L.A., Bahls L.L. (2011).** The distribution and abundance of a nuisance native alga, *Didymosphenia geminata*, in streams of Glacier National Park: Climate drivers and management implications. *Parks Journal*, 28:2.
- Thompson I., Mackey B., McNulty S., Mosseler, A. (2009).** Forest resilience, biodiversity, and climate change. A synthesis of the biodiversity/resilience/stability relationship in forest ecosystems. Technical Series No. 43, Secretariat of the Convention on Biological Diversity. Montreal, Canada
- Tilman D. (1982).** Resource Competition and Community Structure, Princeton University Press, Princeton, NJ, USA.
- Tom-Dery D., Hinneh P., Asante W.J. (2013).** Biodiversity in Kenikeni Forest Reserve of Northern Ghana. *African Journal of Agricultural Research*, 8:5896-5904.
- Tomlinson K.W., Poorter L., Bongers F., Borghetti F., Jacobs L., van Langevelde, F. (2014).** Relative growth rate variation of evergreen and deciduous savanna tree species is driven by different traits. *Annals of Botany*, 114: 315–324.

- Torrence C., Compo G.P. (1998).** A practical guide to wavelet analysis. *Bulletin of the American Meteorological Society*, 79(1), 61–78.
- Traoré S., Ouattara K., Ilstedt U., Schmidt M., Thiombiano A., Malmer A., Nyberg G. (2015).** Effect of land degradation on carbon and nitrogen pools in two soil types of a semi-arid landscape in West Africa. *Geoderma*, 241–242:330–338
- Traoré L., Ouédraogo A., Thiombiano A. (2012).** To What Extent Do Protected Areas Determine the Conservation of Native Flora? A Case Study in the Sudanian Zone of Burkina Faso. *International Scholarly Research Notices Botany*, 168196:10.
- Trouet V., Esper J., Beeckman H. (2010).** Climate/growth relationships of *Brachystegia spiciformis* from the Miombo woodland in south central Africa'. *Dendrochronologia*, 28: 161-171.
- Torrence C., Compo G.P. (1998).** A practical guide to wavelet analysis. *Bulletin of the American Meteorological Society*, 79: 61–78.
- UNEP-GEF Volta Project (2013).** Volta Basin Transboundary Diagnostic Analysis. UNEP/GEF/Volta/RR 4/2013.
- UNEP-GEF (2012).** Volta River Basin, West Africa.
- University of East Anglia Climatic Research Unit; Jones, P.D.; Harris, I. (2008).** Climatic Research Unit (CRU) time-series datasets of variations in climate with variations in other phenomena. NCAS British Atmospheric Data Centre, retrieved from <http://catalogue.ceda.ac.uk/uuid/3f8944800cc48e1cbc29a5ee12d8542d> on 13 July, 2015.
- University of Oxford (2014).** The virtual field herbarium image database retrieved from <http://herbaria.plants.ox.ac.uk/vfh/> on 15 June 2014.
- United States Geological Survey National Center for Earth Resources Observation and Science (2014).** Landsat satellite images, retrieved from GLOVIS data portal <http://glovis.usgs.gov/> on 20 January 2014.
- Van Laar A., Akça A. (2007).** Forest Mensuration. Springer, the Netherlands.
- Volta Basin Authority (2000).** Land cover in the Volta Basin area. Retrieved from <http://131.220.109.2/geonetwork/srv/en/main.home> on 21 November, 2014.
- Vieilledent G., Vaudry R., Andriamanohisoa S.F.D., Rakotonarivo O.S., Randrianasolo H.Z., Razafindrabe H.N., Bidaud Rakotoarivony C., Ebeling J., Rasamoelina M. (2012).** A universal approach to estimate biomass and carbon stock in tropical forests using generic allometric models. *Ecological Applications*, 22: 572-583.

- Warren R., Price J., de la Nava Santos S., Fischlin A., Midgley G. (2011).** Increasing impacts of climate change upon ecosystems with increasing global mean temperature rise. *Climatic Change*, 106: 141-177.
- White F. (1983).** The vegetation of Africa, a descriptive memoir to accompany the UNESCO/AETFAT/UNSO. UNESCO, Natural Resources Research, Vol. 20: 1-356.
- Wieloch T., Helle G., Heinrich I., Voigt M., Schyma P. (2011).** A novel device for batchwise isolation of  $\alpha$ -cellulose from small-amount wholewood samples. *Dendrochronologia*, 29: 115e117.
- Wigley T.M.L., Briffa K.R., Jones P.D. (1984).** On the average value of correlated time series, with applications in dendroclimatology and hydrometeorology. *Journal of Applied Meteorology and Climatology*, 23:201–213.
- Wilcox B.A. (1995).** Tropical forest resources and biodiversity the risks of forest loss and degradation. *Unasylva*, 46:43-49.
- Wildlife Department of Ghana (1994).** Kogyae Strict Nature Reserve Development and Management Plan. <http://gem.tropicalforests.ox.ac.uk/sites/kogyae>
- Worbes M. (2002).** One hundred years of tree ring research in the tropics—a brief history and an outlook to future challenges. *Dendrochronologia*, 20:217–231.
- Young-Mathews A., Culman S.W., Sanchez-Moreno S., O’Geen A.T., Ferris H., Hollander A.D., Jackson L.E. (2010).** Plant-soil biodiversity relationships and nutrient retention in agricultural riparian zones of the Sacramento Valley, California. *Agroforestry System*, 80:41–60.
- Zak D.R., Holmes W.E., White D.C., Peacock A.D., Tilman D. (2003).** Plant diversity, soil microbial communities and ecosystem function: are there any links? *Ecology*, 84:2042–2050.

# ANNEXES

## 1. Lists of woody plants in Afram and Tankwidi riparian forests

### A. Afram Riparian Forests

Species	Family	LF	Chorotype	Protected	
				Area	Farmland
<i>Acacia macrostachya</i> Reichenb. ex DC.	Fabaceae	Mph	S		11
<i>Afzelia africana</i> Smith ex Pers.	Fabaceae	mPh	S	12	5
<i>Albizia adianthifolia</i> (Schumach.) W. Wight	Fabaceae	mPh	GC	23	7
<i>Albizia glaberrima</i> (Schum. & Thonn.) Benth.	Fabaceae	Mph	GC	19	
<i>Albizia ferruginea</i> (Guill. & Perr.) Benth.	Fabaceae	mPh	GC	4	9
<i>Albizia zygia</i> (DC.) J. F. Macbr.	Fabaceae	mPh	SG	7	
<i>Alchornea cordifolia</i> (Schum. & Thonn.) Müll. Arg.	Euphorbiaceae	mph	GC	10	
<i>Allophylus africanus</i> P.Beauv.	Sapindaceae	mph	Pt	2	
<i>Anogeissus leiocarpus</i> (DC.) Guill. & Perr. syn. <i>A. leiocarpus</i> (DC.) Guill. & Perr.	Combretaceae	mPh	S	16	15
<i>Antiaris toxicaria</i> Lesch. var <i>africana</i> A. Chev. syn. <i>A. africana</i> Engl.	Moraceae	MPh	GC	45	26
<i>Anthocleista nobilis</i> G.Don	Gentianaceae	mPh	SG/GC		6
<i>Azadirachta indica</i> A. Juss.	Meliaceae	mPh	Pal		6
<i>Baphia pubescens</i> (Hook. F.)	Fabaceae	mph	GC	27	15
<i>Bridelia ferruginea</i> Benth.	Euphorbiaceae	mph	SG	1	
<i>Blighia unijugata</i> Baker	Sapindaceae	mph	GC	10	4
<i>Bombax buonopozense</i> P.Beauv	Bombacaceae	MPh	GC	8	

<i>Canthium vulgare</i> (K. Schum.) Bullock. F.R.	Rubiaceae	mph	Pt		10
<i>Ceiba pentandra</i> (L.) Gaertn.	Bombacaceae	MPh	Pt	41	15
<i>Christiana africana</i> DC.	Tiliaceae	mPh	Pt	19	13
<i>Cissus doeringii</i> (Gilg & Brandt) Desc.	Vitaceae	He	SG	2	
<i>Cleistopholis patens</i> (Benth.) Engl. & Diels	Annonaceae	mPh	GC	2	
<i>Cola cordifolia</i> (Cav.) R.Br.	Sterculiaceae	mPh	GC	12	
<i>Cola gigantea</i> A. Chev.	Sterculiaceae	mPh	GC	3	15
<i>Cynometra megalophylla</i> Harms	Fabaceae	mPh	GC	54	38
<i>Dalbergia afzeliana</i> G.Don	Fabaceae	LmPh	GC	3	
<i>Daniellia oliveri</i> (Rolfe) Hutch. & Dalz.	Fabaceae	mPh	SZ	3	10
<i>Dialium guineense</i> Willd.	Fabaceae	mPh	GC	17	15
<i>Diospyros mespiliformis</i> Hochst. ex A. DC.	Ebenaceae	mPh	SZ	26	19
<i>Elaeis guineensis</i> Jacq.	Arecaceae	mPh	GC	14	13
<i>Ficus exasperata</i> Vahl	Moraceae	mPh	GC	9	2
<i>Ficus vogeliana</i> (Miq.) Miq.	Moraceae	mPh	GC	3	6
<i>Hallea ledermannii</i> (K. Krause) B. Verdcourt	Rubiaceae	mph	GC	1	
<i>Holarrhena floribunda</i> (G. Don) Dur. & Schinz	Apocynaceae	mph	SG	10	
<i>Hymenostegia afzelii</i> (Oliv.)Harms	Fabaceae	mPh	GC	5	1
<i>Khaya senegalensis</i> (Desv.) A. Juss.	Meliaceae	mPh	S	5	3
<i>Lecaniodiscus cupanioides</i> Planch.	Sapindaceae	mph	GC	7	4
<i>Lonchocarpus sericeus</i> (Poir.) H. B. & K.	Fabaceae	Mph	SG	3	7
<i>Milicia exelsa</i> (Welw.) Berg syn. <i>Chlorophora excelsa</i> (Welw.) benth.		mPh	GC		
	Moraceae			5	

<i>Manilkara obovata</i> (Sabine & G. Don) syn. <i>M. multinervis</i> (Baker) Dubard	Sapotaceae	mPh	GC	4	
<i>Mitragyna inermis</i> (Willd.) O. Kuntze	Rubiaceae	Mph	S	88	49
<i>Morinda lucida</i> Benth	Rubiaceae	Mph	Pt	3	
<i>Motandra guineensis</i> (Thonning) A. DC.	Apocynaceae	Lmph	SG	2	2
<i>Napoleonaea vogelii</i> Hook. & Planch. syn. <i>N. leonensis</i> Hutch. & Dalz.	Lecythidaceae	mph	GC	5	
<i>Nauclea diderrichii</i> (De Wild. & T.Durand)	Rubiaceae	mph	At	5	
<i>Nesogordonia papaverifera</i> (A. Chev.) R. Capuron (Kotibé)	Sterculiaceae	mph	GC	7	3
<i>Newbouldia laevis</i> (P. Beauv.) Seem. ex Bureau	Bignoniaceae	mph	GC	7	
<i>Olex subscorpioidea</i> Oliv. var. <i>subscorpioidea</i>	Olacaceae	mph	GC	14	3
<i>Pancovia pedicellaris</i> (Radlk. & Gilg)	Sapindaceae	mph	GC	4	
<i>Pentaclethra macrophylla</i> Benth	Fabaceae	mPh	GC	7	
<i>Pterocarpus santalinoides</i> DC.	Fabaceae	mph	SG	98	35
<i>Raphia hookeri</i> Mann & Wendl.	Arecaceae	mph	GC		3
<i>Ricinodendron heudelotii</i> (Baill.) Pierre ex Pax	Euphorbiaceae	mPh	GC	8	4
<i>Sarcocephalus latifolius</i> (Smith) Bruce syn. <i>Nauclea latifolia</i> Smith	Rubiaceae	mph	At	2	
<i>Spondias mombin</i> L.	Anacardiaceae	mPh	Pt	23	11
<i>Sterculia tragacantha</i> Lindl.	Sterculiaceae	mPh	SG	32	6
<i>Synsepalum brevipes</i> (Baker) Pennington syn. <i>Pachystela brevipes</i> (Baker) Engl.	Sapotaceae	mPh	GC	4	
<i>Terminalia glaucescens</i> Planch. ex Benth	Combretaceae	mph	SG	1	

<i>Terminalia superba</i> Engl. & Diels	Combretaceae	mPh	GC	14	1
<i>Tetrapleura tetraptera</i> (Schum. & Thonn.)Taub.	Fabaceae	mPh	GC	7	5
<i>Trichilia prieuriana</i> A. Juss.	Meliaceae	mph	GC	16	5
<i>Triplochiton scleroxylon</i> K.Schum.	Malvaceae	MPh	GC	8	6
<i>Vitex doniana</i> Sweet	Verbenaceae	mph	SZ	18	7
<i>Zanthoxylum zanthoxyloides</i> (Lam.) Zepernick & Timber	Rutaceae	mph	SG	12	

---

LF: Life form follows Raunkiaer (1934), Schnell (1971), and Keay & Hepper (1954-1972): MPh: megaphanerophyte (> 30 m tall), mPh: mesophanerophyte (8-30 m), mph: microphanerophyte (2-8 m), nph: nanophanerophyte (0.5-2 m), HC: Hemicryptophyte, Ep: Epiphyte.  
 Chor.: Chorology: GC: Guineo-Congolian, S: Sudanian, SG: Sudano/Guinean transition, SZ: Sudano-Zambezian, At: Tropical Africa, Pt: Pantropical, PAL: Paleotropical

## B. Tankwidi riparian forests

Species	Family	LF	Chorotype	Protected	
				Area	Farmland
<i>Acacia nilotica</i> (L.) Delile	Fabaceae	mPh	S	2	
<i>Acacia polyacantha</i> Willd.	Facaceae	mPh	SZ	17	
<i>Acacia gourmaensis</i> A. Chev.	Facaceae	mph	S	2	
<i>Acacia sieberiana</i> DC.	Facaceae	mph	SZ	18	16
<i>Adansonia digitata</i> L.	Bombacaceae	mPh	SZ	5	5
<i>Afzelia africana</i> Smith ex Pers.	Fabaceae	mPh	S	10	
<i>Anogeissus leiocarpus</i> Guill. & Perr.	Combretaceae	mPh	S	89	33
<i>Annona senegalensis</i> Pers.	Annonaceae	nph	SZ	4	
<i>Azadirachta indica</i> A. Juss.	Meliaceae	mPh	Pal	7	6
<i>Balanites aegyptiaca</i> (L.) Del.	Balanitaceae	mph	SZ	9	3
<i>Bombax costatum</i> Pellegr. & Vuill.	Bombacaceae	mph	S	1	
<i>Calotropis procera</i> (Aiton) W. T. Aiton	Apocynaceae	mph	SG	4	
<i>Combretum ghasalense</i> Engl. & Diels	Combretaceae	mph	S	4	
<i>Combretum nigricans</i> Lepr. ex Guill. & Perr	Combretaceae	mph	S	21	
<i>Daniellia oliveri</i> (Rolfe) Hutch. & Dalz.	Fabaceae	mPh	SZ	24	8
<i>Dichrostachys glomerata</i> (Forssk.) Chiov	Fabaceae	mph	S	6	
<i>Diospyros mespiliformis</i> Hochst. ex A. DC.	Ebenaceae	mPh	SZ	7	9
<i>Entada africana</i> Guill. & Perr.	Fabaceae	Mph	SZ	8	
<i>Ficus sycomorus</i> L.	Moraceae	Mph	SZ	4	28

<i>Ficus lepriurii</i> (Miquel) C.C. Berg	Moraceae	mphEp	GC	2	
<i>Gardenia aqualla</i> Stapf & Hutch.	Rubiaceae	Mph	SZ	16	2
<i>Gardenia erubescens</i> Stapf & Hutch.	Rubiaceae	Nph	S	2	
<i>Khaya senegalensis</i> A. Juss.	Meliaceae	mPh	S	3	
<i>Lannea acida</i> A. Rich.	Anacardiaceae	mPh	S	10	
<i>Lannea microcarpa</i> Engl. & K. Krause	Anacardiaceae	mPh	SZ	20	5
<i>Maytenus senegalensis</i> (Lam.) Exell	Celastraceae	nph	SZ	2	
<i>Mitragyna inermis</i> (Willd.) O. Kuntze	Rubiaceae	Mph	S	84	37
<i>Nauclea latifolia</i> Sm.	Rubiaceae	mph	At	6	2
<i>Parkia biglobosa</i> (Jacq.) R. Br. ex G. Don f.	Fabaceae	mPh	S	3	12
<i>Pericopsis laxiflora</i> (Benth.) van. Meeuwen	Fabaceae	mph	S	8	
<i>Piliostigma thonningii</i> (Schumach.) milne-Redh.	Fabaceae	mph	SG	4	
<i>Pseudocedrela kotschyi</i> (Schweinf.) Harms	Meliaceae	mph	S	2	
<i>Pterocarpus erinaceus</i> Poir subsp. lucens	Fabaceae	mPh	S	38	15
<i>Sclerocarya birrea</i> (A. Rich.) Hochst.	Anacardiaceae	mph	S	5	2
<i>Stereospermum kunthianum</i> Cham. var. kunthianum	Bignoniaceae	mph	SZ	2	1
<i>Tamarindus indica</i> L.	Fabaceae	mPh	Pt	2	1
<i>Terminalia macroptera</i> Guill. & Perr.	Combretaceae	mph	S	2	
<i>Vitellaria paradoxa</i> C. F. Gaertn. subsp. paradoxa	Sapotaceae	mPh	S	35	19
<i>Vitex doniana</i> Sweet	Verbenaceae	mph	SZ	38	21
<i>Ximenia americana</i> L.	Olcaceae	nph	Pt	6	

LF: Life form follows Raunkiaer (1934), Schnell (1971), and Keay & Hepper (1954-1972): MPh: megaphanerophyte (> 30 m tall), mPh: mesophanerophyte (8-30 m), mph: microphanerophyte (2-8 m), nph: nanophanerophyte (0.5-2 m), HC: Hemicryptophyte, Ep: Epiphyte.

Chor.: Chorology: GC: Guineo-Congolian, S: Sudanian, SG: Sudano/Guinean transition, SZ: Sudano-Zambezian, At: Tropical Africa, Pt: Pantropical, PAL: Paleotropical

# **PUBLICATION**